UNIVERSITY OF AMSTERDAM

UvA-DARE (Digital Academic Repository)

Search for direct production of electroweakinos in final states with missing transverse momentum and a Higgs boson decaying into photons in pp collisions at √s = 13 TeV with the ATLAS detector

The ATLAS Collaboration

DOI
10.1007/JHEP10(2020)005

Publication date
2020

Document Version
Final published version

Published in
Journal of High Energy Physics

License
CC BY

Link to publication

Citation for published version (APA):
The ATLAS Collaboration (2020). Search for direct production of electroweakinos in final states with missing transverse momentum and a Higgs boson decaying into photons in pp collisions at $\sqrt{s}$ = 13 TeV with the ATLAS detector. *Journal of High Energy Physics*, *2020*(10), Article 005. https://doi.org/10.1007/JHEP10(2020)005

General rights
It is not permitted to download or to forward/distribute the text or part of it without the consent of the author(s) and/or copyright holder(s), other than for strictly personal, individual use, unless the work is under an open content license (like Creative Commons).

Disclaimer/Complaints regulations
If you believe that digital publication of certain material infringes any of your rights or (privacy) interests, please let the Library know, stating your reasons. In case of a legitimate complaint, the Library will make the material inaccessible and/or remove it from the website. Please Ask the Library: https://uba.uva.nl/en/contact, or a letter to: Library of the University of Amsterdam, Secretariat, P.O. Box 19185, 1000 GD Amsterdam, The Netherlands. You will be contacted as soon as possible.

UvA-DARE is a service provided by the library of the University of Amsterdam (https://dare.uva.nl)

Download date:13 Sept 2026

Published for SISSA by Springer

Received: *April 24, 2020*
Accepted: *September 1, 2020*
Published: *October 1, 2020*

Search for direct production of electroweakinos in final states with missing transverse momentum and a Higgs boson decaying into photons in pp collisions at $\sqrt{s} = 13$ TeV with the ATLAS detector

The ATLAS collaboration

E-mail: atlas.publications@cern.ch

Abstract: A search for a chargino-neutralino pair decaying via the 125 GeV Higgs boson into photons is presented. The study is based on the data collected between 2015 and 2018 with the ATLAS detector at the LHC, corresponding to an integrated luminosity of 139 fb^{-1} of pp collisions at a centre-of-mass energy of 13 TeV. No significant excess over the expected background is observed. Upper limits at 95% confidence level for a massless $\tilde{\chi}_1^0$ are set on several electroweakino production cross-sections and the visible cross-section for beyond the Standard Model processes. In the context of simplified supersymmetric models, 95% confidence-level limits of up to 310 GeV in $m(\tilde{\chi}_1^{\pm}/\tilde{\chi}_2^0)$, where $m(\tilde{\chi}_1^0) = 0.5$ GeV, are set. Limits at 95% confidence level are also set on the $\tilde{\chi}_1^{\pm}\tilde{\chi}_2^0$ cross-section in the mass plane of $m(\tilde{\chi}_1^{\pm}/\tilde{\chi}_2^0)$ and $m(\tilde{\chi}_1^0)$, and on scenarios with gravitino as the lightest supersymmetric particle. Upper limits at the 95% confidence-level are set on the higgsino production cross-section. Higgsino masses below 380 GeV are excluded for the case of the higgsino fully decaying into a Higgs boson and a gravitino.

Keywords: Hadron-Hadron scattering (experiments)

ArXiv ePrint: 2004.10894

Open Access, Copyright CERN,
for the benefit of the ATLAS Collaboration.
Article funded by SCOAP^3.

https://doi.org/10.1007/JHEP10(2020)005

JHEP10(2020)005

Contents

1 Introduction **1**

2 ATLAS detector **3**

3 Data and simulation samples **4**

4 Event reconstruction **6**

5 Event selection **9**
5.1 Baseline selection 9
5.2 Follow-up selection 10

6 Signal and background parameterisation **10**

7 Systematic uncertainties **11**

8 Results **14**
8.1 Limits on the visible cross-section 15
8.2 Interpretation of the wino-like $\tilde{\chi}_1^{\pm}\tilde{\chi}_2^0 \to W^{\pm}\tilde{\chi}_1^0 h\tilde{\chi}_1^0$ model 16
8.3 Interpretation of the higgsino-like $h\tilde{G}h\tilde{G}$ model 17

9 Conclusion **18**

The ATLAS collaboration **29**

JHEP10(2020)005

1 Introduction

Theoretical and experimental arguments suggest that the Standard Model (SM) is an effective theory valid up to a certain energy scale. The SM Higgs boson, denoted by h, is observed by the ATLAS and CMS collaborations [1–4]. The Higgs boson mass is strongly sensitive to quantum corrections from physics at very high energy scales and demands a high level of fine-tuning, known as the hierarchy problem [5–8]. Supersymmetry (SUSY) [9–14] resolves the hierarchy problem by introducing, for each known particle state, a new partner (superpartner) that shares the same mass and internal quantum numbers with the exception of spin if supersymmetry is unbroken. However, these superpartners have not been observed, so SUSY must be a broken symmetry and the mass scale of the supersymmetric particles is as yet undetermined. The possibility of a supersymmetric dark matter candidate [15, 16] is closely related to the conservation of R-parity [17]. Under the R-parity conservation hypothesis, the lightest supersymmetric particle (LSP) is stable. If the LSP is weakly interacting, it may provide a viable dark matter candidate. The nature

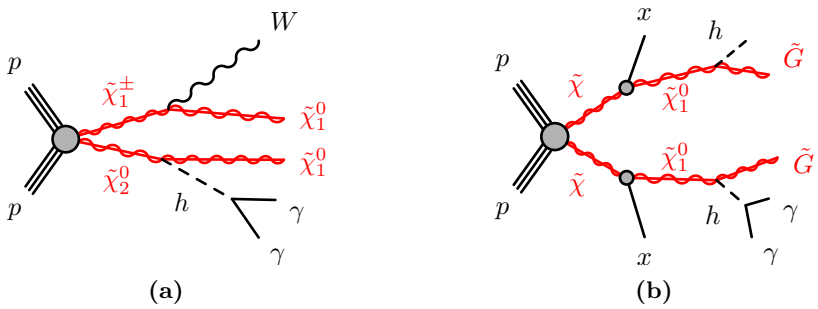

Figure 1. Signal diagrams illustrating (a) $\tilde{\chi}_1^{\pm}\tilde{\chi}_2^0$ production, and (b) a higgsino production mode from a GMSB model: $\tilde{\chi}_1^0 \to h\tilde{G}$. For $\tilde{\chi}_1^{\pm}\tilde{\chi}_2^0$ production, the lightest chargino ($\tilde{\chi}_1^{\pm}$) and next-to-lightest neutralino ($\tilde{\chi}_2^0$) are nearly mass degenerate. In the higgsino models, the two lightest neutralinos, $\tilde{\chi}_1^0$ and $\tilde{\chi}_2^0$, and the lightest chargino $\tilde{\chi}_1^{\pm}$ are approximately mass degenerate, and the $\tilde{\chi}_1^0$ is the lightest of the four nearly degenerate higgsino states, x is the particle with low momentum from the promptly decay of $\tilde{\chi}_1^{\pm}$ and $\tilde{\chi}_2^0$.

of the LSP is defined by the mechanism that spontaneously breaks supersymmetry and the parameters of the chosen theoretical framework.

In the SUSY scenarios considered as a first benchmark in this paper, the LSP is the lightest of the neutralinos $\tilde{\chi}_j^0$ ($j = 1, 2, 3, 4$) that, together with the charginos $\tilde{\chi}_i^{\pm}$ ($i = 1, 2$), represent the mass eigenstates formed from the mixture of the γ, W, Z and Higgs bosons' superpartners (the winos, binos and higgsinos). The neutralinos and charginos are collectively referred to as *electroweakinos*. Specifically, the electroweakino mass eigenstates are designated in order of increasing mass. Naturalness considerations [18, 19] suggest that the lightest of the charginos and neutralinos have masses near the electroweak scale. Their direct production may be the dominant mechanism at the Large Hadron Collider (LHC) if the superpartners of the gluons and quarks are heavier than a few TeV. In SUSY models where the heaviest (pseudoscalar, charged) minimal supersymmetric Standard Model (MSSM) Higgs bosons and the superpartners of the leptons have masses larger than those of the lightest chargino and next-to-lightest neutralino, the former might decay into the $\tilde{\chi}_1^0$ and a W boson ($\tilde{\chi}_1^{\pm} \to W\tilde{\chi}_1^0$), while the latter could decay into the $\tilde{\chi}_1^0$ and the lightest MSSM Higgs boson or Z boson ($\tilde{\chi}_2^0 \to h/Z\tilde{\chi}_1^0$) [17, 20, 21]. The decay via the Higgs boson is dominant for many choices of parameters as long as the mass-splitting between the two lightest neutralinos is larger than the Higgs boson mass and the higgsinos are heavier than the winos. SUSY models of this kind could provide a possible explanation for the discrepancy between measurements of the muon's anomalous magnetic moment $g - 2$ and SM predictions [22–25].

This paper presents a search in proton-proton (pp) collisions produced at the LHC at a centre-of-mass energy $\sqrt{s} = 13\,\text{TeV}$ for the direct pair production of electroweakinos that promptly decay into the LSP, producing at least one Higgs boson, decaying into two photons in each event. The primary model, for which the search is optimised, involves the production of a chargino in association with a next-to-lightest neutralino, which promptly decay as $\tilde{\chi}_1^{\pm} \to W\tilde{\chi}_1^0$ and $\tilde{\chi}_2^0 \to h\tilde{\chi}_1^0$ respectively (see figure 1a), the $\tilde{\chi}_1^0$ in the final state

JHEP10(2020)005

leading to a signature of missing transverse momentum, whose magnitude is denoted by $E_{\mathrm{T}}^{\mathrm{miss}}$. A simplified SUSY model [26, 27] is considered for the optimisation of the search and the interpretation of results. The $\tilde{\chi}_1^{\pm} \to W\tilde{\chi}_1^0$ and $\tilde{\chi}_2^0 \to h\tilde{\chi}_1^0$ decays are each assumed to have a 100% branching fraction. The Higgs boson branching fractions are assumed to be the same as in the SM [28]. The result from the CMS experiment using an integrated luminosity of 77.5 fb^{-1} of pp collision data is given in ref. [29]. Although the branching fraction of the SM Higgs boson decaying into a pair of photons is small, the diphoton system presented in this paper falls in a narrower mass range around the Higgs boson mass than in refs. [30, 31] where the SM Higgs boson decay into a pair of b-quarks. With the diphoton trigger, this channel is more sensitive in the low $E_{\mathrm{T}}^{\mathrm{miss}}$ region than the channel with the SM Higgs boson decaying into a pair of b-quarks, which relies on the high $E_{\mathrm{T}}^{\mathrm{miss}}$ trigger. In addition, a prior search from ATLAS [32] for this process making use of 36.1 fb^{-1} of pp collision data, based purely on leptonic decays of the W boson, observed a small excess of events above the SM prediction. This prior search is also updated to the full Run 2 data, and referred to as 'follow-up' analysis.

The analysis optimised for the search for $\tilde{\chi}_1^{\pm}$ $\tilde{\chi}_2^0$ production is also used to search for a gauge-mediated supersymmetry breaking (GMSB) [33–35] scenario featuring direct production of pairs of higgsinos [36–38], collectively denoted by $\tilde{\chi}\tilde{\chi}$. In this model, the two lightest neutralinos, $\tilde{\chi}_1^0$ and $\tilde{\chi}_2^0$, and the lightest chargino $\tilde{\chi}_1^{\pm}$ are approximately mass degenerate, and the $\tilde{\chi}_1^0$ is the lightest of the four nearly degenerate higgsino states. The masses are assumed to be related by $m(\tilde{\chi}_1^{\pm}) = m(\tilde{\chi}_2^0) = m(\tilde{\chi}_1^0) + 1\,\mathrm{GeV}$. The effective cross-section for higgsino production is a combination of the cross-sections for $\tilde{\chi}_1^0$ $\tilde{\chi}_2^0$, $\tilde{\chi}_1^0$ $\tilde{\chi}_1^{\pm}$, $\tilde{\chi}_2^0$ $\tilde{\chi}_1^{\pm}$, and $\tilde{\chi}_1^{\pm}$ $\tilde{\chi}_1^{\mp}$ production. In the GMSB scenarios considered (figure 1b), a 100% branching fraction for $\tilde{\chi}_1^0 \to h\tilde{G}$ is assumed, where $\tilde{G}$ indicates the gravitino (the superpartner of the graviton). This scenario is denoted by $h\tilde{G}h\tilde{G}$ in the following. In this scenario, $\tilde{G}$ in the final state is stable, weakly interacting, and nearly massless, which leads to an $E_{\mathrm{T}}^{\mathrm{miss}}$ signature.

The general strategy of the analysis is to search for beyond the Standard Model (BSM) events by using a simultaneous signal-plus-background fit to the full $m_{\gamma\gamma}$ spectrum for different categories. The paper is organised as follows. Section 2 presents a brief description of the ATLAS detector. Section 3 introduces the data, the signal and background Monte Carlo (MC) simulation samples used. Section 4 outlines the event reconstruction, while section 5 explains the optimisation of the event selection and categorisation. Section 6 discusses the signal and background modelling. Section 7 summarises the experimental and theoretical systematic uncertainties that affect the results. Section 8 describes the results and their interpretations, and conclusions are drawn in section 9.

2 ATLAS detector

The ATLAS detector [39] is a multipurpose particle detector with a forward-backward symmetric cylindrical geometry and nearly 4π coverage in solid angle.[1] The inner tracking

[1] ATLAS uses a right-handed coordinate system with its origin at the nominal interaction point in the centre of the detector. The positive x-axis is defined by the direction from the interaction point to the

JHEP10(2020)005

detector (ID) consists of pixel and microstrip silicon detectors covering the pseudorapidity region $|\eta| < 2.5$, surrounded by a transition radiation tracker that enhances electron identification in the region $|\eta| < 2.0$. A new inner pixel layer, the insertable B-layer [40, 41], was added at a mean radius of 3.3 cm during the period between Run 1 and Run 2 of the LHC. The inner detector is surrounded by a thin superconducting solenoid providing an axial 2 T magnetic field and by a lead/liquid-argon electromagnetic (EM) sampling calorimeter covering $|\eta| < 3.2$, with a fine-granularity region up to $|\eta| = 2.5$. A steel/scintillator-tile hadronic sampling calorimeter provides coverage in the central pseudorapidity range ($|\eta| < 1.7$). The endcap and forward regions ($1.5 < |\eta| < 4.9$) of the hadronic calorimeter are made of liquid-argon active layers with either copper or tungsten as the absorber material. A muon spectrometer with an air-core toroid magnet system surrounds the calorimeters. Three layers of high-precision tracking chambers provide coverage in the range $|\eta| < 2.7$, while dedicated fast chambers allow triggering in the region $|\eta| < 2.4$. The ATLAS trigger system consists of a hardware-based first-level trigger followed by a software-based high-level trigger [42].

3 Data and simulation samples

The analysis uses pp collision data with a bunch crossing interval of 25 ns, collected from 2015 to 2018 at $\sqrt{s} = 13$ TeV. Only events that were recorded in stable beam conditions, when relevant detector components were functioning properly, are considered. A diphoton trigger [43] was used to collect the events by requiring two reconstructed photon candidates with transverse energies (E_{T}) of at least 35 GeV and 25 GeV for the E_{T}-ordered leading and subleading photons respectively. The trigger efficiency relative to the offline-reconstructed photons was 99%. The data sample corresponds to an integrated luminosity of $139.0 \pm 2.4\,\mathrm{fb}^{-1}$. There are, on average, 25 to 38 interactions in the same bunch crossing (in-time pile-up) in the data sample.

The MC simulation of signal and background processes is used to optimise the selection criteria, estimate uncertainties and study the shapes of the signal and background diphoton invariant mass ($m_{\gamma\gamma}$) distributions. Signal events were generated with up to two additional partons in the matrix element using MadGraph_aMC@NLO 2.6.2 [44] at leading order (LO) in quantum chromodynamics (QCD) using the NNPDF3.0LO [45] parton distribution function (PDF) set and CKKW-L merging scheme. Parton showering and hadronisation were handled by the Pythia 8.230 [46] event generator with the A14 [47] set of tuned parameters (tune), using the NNPDF2.3LO PDF set [48]. MC samples for the $\tilde{\chi}_1^{\pm}\tilde{\chi}_2^0$ production were generated assuming $m(\tilde{\chi}_1^{\pm}) = m(\tilde{\chi}_2^0)$ for a range of values of $m(\tilde{\chi}_1^0)$. As shown in figure 2a, the transverse momentum (p_{T}) distribution of the $\tilde{\chi}_1^0\tilde{\chi}_1^0$ system is broader for higher values of the difference $m(\tilde{\chi}_1^{\pm}/\tilde{\chi}_2^0) - m(\tilde{\chi}_1^0)$. The p_{T} distributions of

centre of the LHC ring, with the positive y-axis pointing upwards, while the beam direction defines the z-axis. Cylindrical coordinates (r, ϕ) are used in the transverse plane, ϕ being the azimuthal angle around the z-axis. The pseudorapidity η is defined in terms of the polar angle θ by $\eta = -\ln\tan(\theta/2)$. Rapidity is defined as $y = 0.5\ln[(E + p_z)/(E - p_z)]$ where E denotes the energy and p_z is the component of the momentum along the beam direction. The angular distance ΔR is defined as $\sqrt{(\Delta y)^2 + (\Delta\phi)^2}$.

JHEP10(2020)005

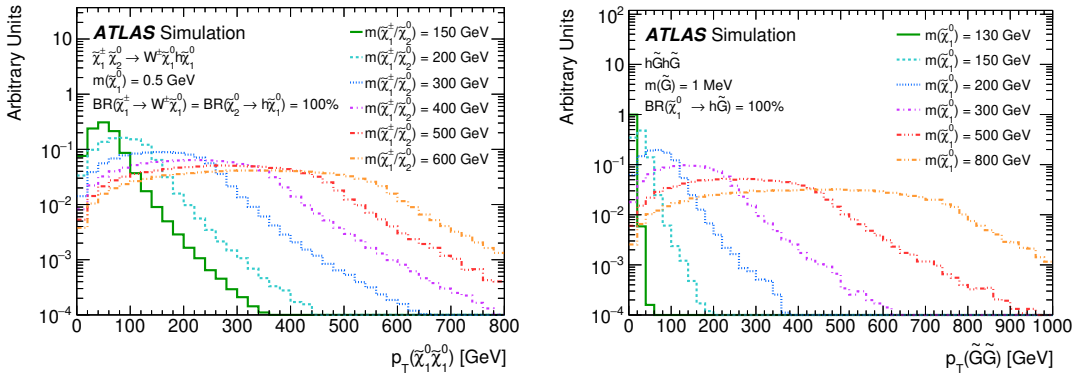

Figure 2. The p_{T} distribution of (a) the $\tilde{\chi}_1^0\tilde{\chi}_1^0$ in $W^{\pm}\tilde{\chi}_1^0 h\tilde{\chi}_1^0$ production and (b) $\tilde{G}\tilde{G}$ in $h\tilde{G}h\tilde{G}$ production.

the $\tilde{G}\tilde{G}$ system for the higgsino production of $h\tilde{G}h\tilde{G}$ are presented in figure 2b. The MC samples include $\tilde{\chi}_1^0\ \tilde{\chi}_2^0$, $\tilde{\chi}_1^0\ \tilde{\chi}_1^{\pm}$, $\tilde{\chi}_2^0\ \tilde{\chi}_1^{\pm}$, and $\tilde{\chi}_1^{\pm}\ \tilde{\chi}_1^{\mp}$ production. The kinematic distributions depend strongly on the mass of the $\tilde{\chi}_1^0$, where the mass of the $\tilde{G}$ is assumed to be 1 MeV.

Signal cross-sections were calculated to NLO in the strong coupling constant, α_{S}, adding the resummation of soft gluon emission at next-to-leading-logarithm accuracy (NLO+NLL) [49–53]. The nominal cross-section and its uncertainty are taken from an envelope of cross-section predictions using different PDF sets and factorisation and renormalisation scales, as described in ref. [54].

The dominant backgrounds are resonant SM $h \to \gamma\gamma$ processes, and non-resonant processes that include $\gamma\gamma$, γ+jets, $V\gamma$ (V=W, Z) and $V\gamma\gamma$ production. Both the shape and normalisation of the total non-resonant background are obtained directly from data, as described in section 6. Simulation events for the total non-resonant background are used in figure 3 and for the choice of background analytic parametrisation as described in section 6. For the production of the resonant SM Higgs boson, events from the Wh and Zh processes were generated with Pythia 8.186 with the A14 tune and the NNPDF2.3LO PDF set. The gluon-gluon fusion (ggF) and vector-boson fusion (VBF) samples were generated with Powheg-Box v2 [55–59] interfaced to Pythia 8.186 with the AZNLO [60] tune and the CT10 PDF set [61]. Samples of $t\bar{t}h$ events were generated with MadGraph_aMC@NLO 2.2.3 interfaced to Pythia 8.186 with the NNPDF3.0LO PDF set. Samples of $b\bar{b}h$ events were generated with MadGraph_aMC@NLO 2.2.3 interfaced to Pythia 8.186 with the A14 tune and the NNPDF2.3LO PDF set. The non-resonant diphoton processes with associated jets were generated using Sherpa 2.2.4 [62]. Matrix elements (ME) were calculated with up to three partons at LO and merged with the Sherpa 2.2.4 parton shower (PS) [63] using the ME+PS@LO prescription [64]. The CT10 PDF set was used in conjunction with a dedicated parton-shower tuning developed by the authors of Sherpa 2.2.4. The $V\gamma$ and $V\gamma\gamma$ samples were generated using Sherpa 2.2.4 with the CT10 PDF set.

The cross-sections for the SM Higgs boson processes were calculated at next-to-leading order (NLO) in electroweak theory and next-to-next-to-leading order (NNLO) in QCD for the VBF, Zh and Wh samples [28, 65–71] and next-to-next-to-next-to-leading order plus

JHEP10(2020)005

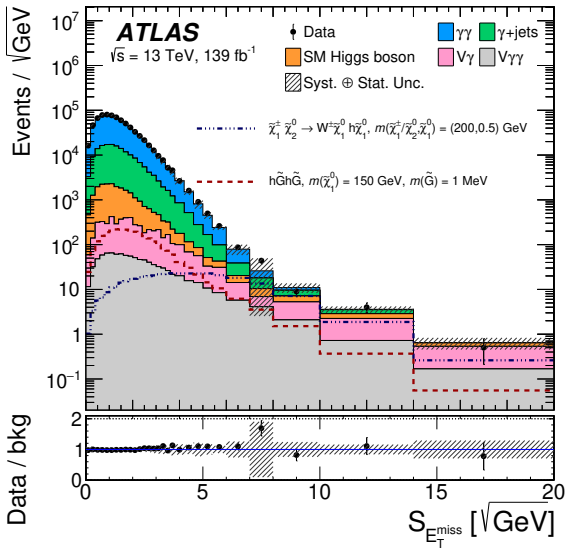

Figure 3. The distribution of $S_{E_{\mathrm{T}}^{\mathrm{miss}}}$ after the selection of diphoton candidates with $120 < m_{\gamma\gamma} < 130\,\mathrm{GeV}$. Expected distributions are shown for the $\tilde{\chi}_1^{\pm}\tilde{\chi}_2^0 \to W^{\pm}\tilde{\chi}_1^0 h\tilde{\chi}_1^0$ signal with $m(\tilde{\chi}_1^{\pm}/\tilde{\chi}_2^0) = 200\,\mathrm{GeV}$ and $m(\tilde{\chi}_1^0) = 0.5\,\mathrm{GeV}$, and the $h\tilde{G}h\tilde{G}$ signal with $m(\tilde{\chi}_1^0) = 150\,\mathrm{GeV}$ and $m(\tilde{G}) = 1\,\mathrm{MeV}$. These overlaid signal points are representative of the model kinematics. The sum in quadrature of the MC statistical and experimental systematic uncertainties in the total background is shown as the hatched bands, while the theoretical uncertainties in the background normalisation are not included. The $tt\gamma$ and $tt\gamma\gamma$ processes have a negligible contribution and are not represented. Overflow events are included in the rightmost bin. The lower panel shows the ratio of the data to the background, called "bkg".

next-to-next-to-leading logarithm (N^{3}LO+NNLL) in QCD for the ggF sample [28, 72–75]. The $t\bar{t}h$ cross-section was calculated with NLO accuracy in QCD with NLO electroweak corrections [76–79]. The $b\bar{b}h$ cross-section was obtained by matching the five-flavor scheme cross section accurate to NNLO in QCD with the four-flavor scheme cross section accurate to NLO in QCD [80–82]. The SM Higgs boson mass was set to 125.09 GeV [3] and its branching fraction to decay into two photons was 0.227% [28].

Different pile-up conditions from same and neighbouring bunch crossings as a function of the instantaneous luminosity were simulated by overlaying minimum-bias events, generated with Pythia 8.186 with the MSTW2008LO PDF set [83] and the A3 [84] tune, onto all hard-process events. Differences between the simulated and observed distributions of the number of interactions per bunch crossing were corrected for by applying weights to simulated events. Detector effects were simulated using a full simulation [85] performed using GEANT4 [86] for the signals, SM Higgs boson processes, $V\gamma$ and $V\gamma\gamma$ backgrounds. The diphoton continuum background and some of the signal samples were simulated using a fast simulation of the calorimeter based on AtlFastII [85].

4 Event reconstruction

Photons are reconstructed in the region $|\eta| < 2.37$, excluding the EM calorimeter transition region $1.37 < |\eta| < 1.52$, from clusters of energy deposits in the EM calorimeters. Clusters

JHEP10(2020)005

without a matching track or reconstructed conversion vertex in the ID are classified as unconverted photons. Those with a matching reconstructed conversion vertex or with a matching track, consistent with originating from a photon conversion, are classified as converted photons. The reconstruction efficiency is 99% for photons and the conversion reconstruction efficiency is 70% [87]. The photon energy is calibrated using a multivariate regression algorithm trained with fully reconstructed MC samples and then corrected using data-driven techniques [87]. The overall energy scale in data and the difference in the constant term on the resolution between data and simulation are estimated from using a sample with Z boson decays into electrons [87]. The photon direction is estimated using either EM calorimeter longitudinal segmentation (if unconverted) or the conversion vertex position (if converted), together with constraints from the pp collision point.

To reduce the misidentification of hadronic jets containing a high-p_{T} neutral hadron (e.g. π^0) decaying into two photons, 'Tight' identification criteria [87] are applied. The photon identification is based on the lateral profile of the energy deposits in the first and second layers of the EM calorimeter, and on the shower leakage fraction in the hadronic calorimeter. The selection requirements are tuned for converted and unconverted photon candidates, separately. The identification efficiency for unconverted and converted photons ranges from 85% to 99% between 30 GeV and 250 GeV [87]. Corrections are applied to the EM shower-shape variables for simulated photons, to account for small differences between data and simulation.

To further suppress hadronic backgrounds, requirements on two photon isolation variables are applied. The first variable, $E_{\mathrm{T}}^{\mathrm{iso}}$, calculates the sum of the transverse energies deposited in topological clusters [88] in the calorimeter within a cone of size $\Delta R = 0.2$ around each photon. The photon cluster energy and an estimate of the energy deposited by the photon outside its associated cluster are also subtracted from this sum. To reduce underlying-event and pile-up effects, $E_{\mathrm{T}}^{\mathrm{iso}}$ is further corrected using the method described in refs. [89–91]. The second variable expresses track-based isolation, defined as the scalar sum of the transverse momenta of all tracks with $p_{\mathrm{T}} > 1$ GeV and consistent with originating from the primary vertex (PV) within a cone of size $\Delta R = 0.2$ around each photon. The isolation efficiency for photons, which is mostly independent of their kinematic variables, is about 90%.

Events are required to have at least one PV, defined as a vertex associated with at least two tracks with $p_{\mathrm{T}} > 0.5$ GeV. In each event, the PV most likely to be the origin of the diphoton, selected from the PV candidates using a neural network [92], is required to be consistent with the PV with the highest sum of squared transverse momenta of associated tracks. The neural network algorithm selects a diphoton vertex within 0.3 mm of the true $h \to \gamma\gamma$ production vertex in 79% of simulated gluon-gluon fusion events. For the other Higgs production modes this fraction ranges from 84% to 97%, increasing with jet activity or the presence of charged leptons [92].

Electrons are reconstructed from energy deposits measured in the EM calorimeter that are matched to tracks from ID [87]. They are required to satisfy $|\eta| < 2.47$, excluding the EM calorimeter transition region $1.37 < |\eta| < 1.52$, and to have $p_{\mathrm{T}} > 10$ GeV. The electrons are identified using a likelihood-based algorithm that uses track and shower-shape variables.

JHEP10(2020)005

The 'MediumLLH' criteria are applied, providing an identification efficiency varying from 85% to 95% as a function of E_{T} [87]. Loose calorimeter and track isolation requirements are applied to electrons. The efficiency of the isolation requirements is 98% [93].

Muons are reconstructed from high-quality track segments in the muon spectrometer. In the region $|\eta| < 2.5$, they must be matched to ID tracks. They are required to have $p_{\mathrm{T}} > 10\,\mathrm{GeV}$ and $|\eta| < 2.7$. The muon 'medium' criteria are applied with a 96% [94] identification efficiency. The muon candidates must also satisfy loose calorimeter and track isolation criteria. The combined isolation efficiency varies from 95% to 99% as a function of p_{T} from 25 GeV to 60 GeV [94].

The significance of the track's transverse impact parameter relative to the PV is required to be $|d_0|/\sigma_{d_0} < 5$ (3) for electrons (muons). The longitudinal impact parameter z_0 must satisfy $|z_0| \sin\theta < 0.5$ mm for electrons and muons.

Jets are reconstructed from three-dimensional topological clusters using the anti-k_t algorithm [95, 96] with a radius parameter of $R = 0.4$. The jets are required to have $p_{\mathrm{T}} > 20\,\mathrm{GeV}$ and $|\eta| < 4.5$ for the $E_{\mathrm{T}}^{\mathrm{miss}}$ calculation and $p_{\mathrm{T}} > 25\,\mathrm{GeV}$ and $|\eta| < 4.4$ for the event selection. Jets with $|\eta| < 2.4$ and $p_{\mathrm{T}} < 60\,\mathrm{GeV}$ must satisfy the jet vertex tagger (JVT) selection [97], in which a jet is identified as originating from the PV depending on a likelihood value calculated from the track information. In addition, quality criteria are applied to the jets, and events with jets consistent with noise in the calorimeter or non-collision backgrounds are rejected [98].

Reconstruction ambiguities between photons, electrons, muons, and jets are resolved using an 'overlap removal' procedure among all the objects in the following order. First, electrons, muons, and jets found within $\Delta R = 0.4$ of a photon are removed. Next, jets found within $\Delta R = 0.2$ of an electron are removed. Lastly, electrons and muons within $\Delta R = 0.4$ of the remaining jets are removed. A different overlap removal strategy was used in the previous study [32] and the selection is discussed in section 5.2. It was motivated by the prioritisation of electrons, as opposed to photons. The results show no significant difference in sensitivity between these two strategies.

Jets containing a b-hadron are identified using the MV2c10 [99, 100] multivariate discriminant built with information from track impact parameters and the presence of reconstructed secondary vertices, which applies a multi-vertex fitter to reconstruct the hadron decay chain $b \to c$. A value of the discriminating variable is chosen such that it provides a b-tagging efficiency of 70% in simulated $t\bar{t}$ events. The rejection for c-jets and jets originating from gluons or light (u, d, s) quarks are 8.9 and 300 [99], respectively. An additional energy correction is applied to b-jets to account for the presence of muons in the jet [99].

The $E_{\mathrm{T}}^{\mathrm{miss}}$ is calculated as the magnitude of the negative vectorial sum of the transverse momenta of calibrated photons, electrons, muons and jets associated with the PV. The transverse momenta of all remaining tracks that originate from the PV but are not already used in the $E_{\mathrm{T}}^{\mathrm{miss}}$ calculation are summed and taken into account in the $E_{\mathrm{T}}^{\mathrm{miss}}$ calculation. This term is defined as the track-based soft term [101]. In this way, the $E_{\mathrm{T}}^{\mathrm{miss}}$ is adjusted for the best calibration of the jets and the other identified physics objects above, while maintaining pileup independence in the soft term.

JHEP10(2020)005

5 Event selection

5.1 Baseline selection

Each event is first required to contain at least two photons with $p_{\mathrm{T}} > 22\,\mathrm{GeV}$. The photons are ordered by their p_{T}. The leading and subleading photons are then required to have $p_{\mathrm{T}}^{\gamma}/m_{\gamma\gamma} > 0.35$ and 0.25, respectively, where $m_{\gamma\gamma}$ is the invariant mass of the leading and subleading photon pair. The signal region is defined as $105 < m_{\gamma\gamma} < 160\,\mathrm{GeV}$, where $m_{\gamma\gamma}$ is calculated using the photon momentum vectors recomputed relative to the PV. The selected events are divided into 12 categories based on the number of leptons (N_ℓ), number of jets (N_j), the invariant mass of the two highest-p_{T} jets (m_{jj}), and the $E_{\mathrm{T}}^{\mathrm{miss}}$ significance $S_{E_{\mathrm{T}}^{\mathrm{miss}}} = E_{\mathrm{T}}^{\mathrm{miss}}/\sqrt{\sum E_{\mathrm{T}}}$. The total transverse energy $\sum E_{\mathrm{T}}$ is calculated from the scalar sum of the transverse momenta of the calibrated photons, electrons, muons and jets used in the $E_{\mathrm{T}}^{\mathrm{miss}}$ calculation described in section 4, as well as the tracks not associated with these but consistent with originating from the PV. Because both the $E_{\mathrm{T}}^{\mathrm{miss}}$ and $\sum E_{\mathrm{T}}$ resolutions increase linearly with the number of pileup events, $S_{E_{\mathrm{T}}^{\mathrm{miss}}}$ is more resilient to pileup than $E_{\mathrm{T}}^{\mathrm{miss}}$. No b-jet veto is applied in the baseline selection. The 12 categories are defined in table 1. The $\tilde{\chi}_1^{\pm}\,\tilde{\chi}_2^0$ signal sample with $m(\tilde{\chi}_1^{\pm}/\tilde{\chi}_2^0) = 150\,\mathrm{GeV}$ and $m(\tilde{\chi}_1^0) = 0.5\,\mathrm{GeV}$ is used to optimise the boundary of each category to maximise the significance when combining all 12 categories. This signal point has low $E_{\mathrm{T}}^{\mathrm{miss}}$, where the diphoton channel is expected to have a better sensitivity than the channel with the SM Higgs boson decaying into a pair of b-quarks [30, 31]. The 'Leptonic' and 'Hadronic' categories are used to accommodate the most clearly identifiable leptonic and hadronic decays of the W boson, while the 'Rest' category retains all additional signal topologies. The signal $\tilde{\chi}_1^{\pm}\tilde{\chi}_2^0 \to W^{\pm}\tilde{\chi}_1^0 h\tilde{\chi}_1^0$ has the highest expected significance in the Leptonic categories, and the $h\tilde{G}h\tilde{G}$ signals have the highest expected significance in the Rest categories. Because the different signal models and mass points have different p_{T} distributions as shown in figure 2, and since p_{T} and $S_{E_{\mathrm{T}}^{\mathrm{miss}}}$ distributions are highly correlated, each region is divided into $S_{E_{\mathrm{T}}^{\mathrm{miss}}}$ bins to improve the sensitivity. The regions do not change significantly if a different mass point is used for optimisation.

Figure 3 shows the distribution of $S_{E_{\mathrm{T}}^{\mathrm{miss}}}$ after the selection of diphoton candidates with $120 < m_{\gamma\gamma} < 130\,\mathrm{GeV}$, where signal dominates. The shapes and normalisations of the $V\gamma$ and $V\gamma\gamma$ contributions are obtained from the MC simulation. The shape of the $\gamma\gamma$ contribution is obtained from the MC simulation while the normalisation is fixed to the yields in the sidebands ($105 < m_{\gamma\gamma} \leq 120\,\mathrm{GeV}$, $130 \leq m_{\gamma\gamma} < 160\,\mathrm{GeV}$) of the data multiplied by the diphoton purity among all the backgrounds. The diphoton purity is measured in the data, using a two-dimensional sideband technique by counting the number of events in which one or both photons satisfy or fail to satisfy the identification or isolation requirements [102]. The diphoton purity varies from 65% to 93% for different categories. The shape of the γ+jets contribution is obtained using the data distribution in a control region where the event selection is the same as for the signal region but one of the photons fails to satisfy the identification criteria, after subtracting the contamination from $\gamma\gamma$, $V\gamma$ and $V\gamma\gamma$ using MC simulation. Its normalisation is fixed to the γ+jets purity and varies from 34% to 7% of the total yield in different categories.

JHEP10(2020)005

Channels	Names	Selection
Leptonic	Category 1	$0 < S_{E_{\mathrm{T}}^{\mathrm{miss}}} \leq 2,\ N_\ell \geq 1$
	Category 2	$2 < S_{E_{\mathrm{T}}^{\mathrm{miss}}} \leq 4,\ N_\ell \geq 1$
	Category 3	$4 < S_{E_{\mathrm{T}}^{\mathrm{miss}}} \leq 6,\ N_\ell \geq 1$
	Category 4	$S_{E_{\mathrm{T}}^{\mathrm{miss}}} > 6,\ N_\ell \geq 1$
Hadronic	Category 5	$5 < S_{E_{\mathrm{T}}^{\mathrm{miss}}} \leq 6,\ N_\ell = 0,\ N_j \geq 2,\ m_{jj} \in [40, 120]$ GeV
	Category 6	$6 < S_{E_{\mathrm{T}}^{\mathrm{miss}}} \leq 7,\ N_\ell = 0,\ N_j \geq 2,\ m_{jj} \in [40, 120]$ GeV
	Category 7	$7 < S_{E_{\mathrm{T}}^{\mathrm{miss}}} \leq 8,\ N_\ell = 0,\ N_j \geq 2,\ m_{jj} \in [40, 120]$ GeV
	Category 8	$S_{E_{\mathrm{T}}^{\mathrm{miss}}} > 8,\ N_\ell = 0,\ N_j \geq 2,\ m_{jj} \in [40, 120]$ GeV
Rest	Category 9	$6 < S_{E_{\mathrm{T}}^{\mathrm{miss}}} \leq 7,\ N_\ell = 0,\ N_j < 2$ or $(N_j \geq 2,\ m_{jj} \notin [40, 120]$ GeV$)$
	Category 10	$7 < S_{E_{\mathrm{T}}^{\mathrm{miss}}} \leq 8,\ N_\ell = 0,\ N_j < 2$ or $(N_j \geq 2,\ m_{jj} \notin [40, 120]$ GeV$)$
	Category 11	$8 < S_{E_{\mathrm{T}}^{\mathrm{miss}}} \leq 9,\ N_\ell = 0,\ N_j < 2$ or $(N_j \geq 2,\ m_{jj} \notin [40, 120]$ GeV$)$
	Category 12	$S_{E_{\mathrm{T}}^{\mathrm{miss}}} > 9,\ N_\ell = 0,\ N_j < 2$ or $(N_j \geq 2,\ m_{jj} \notin [40, 120]$ GeV$)$

Table 1. Criteria used in the categorisation.

5.2 Follow-up selection

To check the small excess of events observed in the previous search from ATLAS using 36.1 fb^{-1} of pp collision data [32], two signal regions ('SR1L$\gamma\gamma$-a' and 'SR1L$\gamma\gamma$-b') defined in the previous search are reused in this analysis. Events are required to have exactly one lepton with $p_{\mathrm{T}} > 25$ GeV and exactly two photons with $p_{\mathrm{T}} > 40$ (30) GeV for the leading (subleading) photon. The invariant mass of the two photons is required to be $105 < m_{\gamma\gamma} < 160$ GeV, with $E_{\mathrm{T}}^{\mathrm{miss}} > 40$ GeV. The difference in azimuthal angle in the transverse plane between the diphoton system and the lepton plus $E_{\mathrm{T}}^{\mathrm{miss}}$ vector is required to be greater than 2.25 radians. To reduce contributions from $t\bar{t}h$, a b-jet veto is used in both the signal regions.

To further reduce contributions from SM backgrounds, the transverse mass m_{T}^{W} [32] of the lepton and $E_{\mathrm{T}}^{\mathrm{miss}}$, and the three-body transverse mass $m_{\mathrm{T}}^{W\gamma i}$ [32] of the lepton, $E_{\mathrm{T}}^{\mathrm{miss}}$ and the i^{th} photon ordered by p_{T} are used to define the two orthogonal signal regions. For both signal regions, events are required to have $m_{\mathrm{T}}^{W\gamma 1} > 150$ GeV and $m_{\mathrm{T}}^{W\gamma 2} > 80$ GeV. The first signal region, 'SR1L$\gamma\gamma$-a', selects events with $m_{\mathrm{T}}^{W} > 110$ GeV and $m_{\mathrm{T}}^{W\gamma 2} > 140$ GeV while the events that fail to satisfy these requirements define the second signal region ('SR1L$\gamma\gamma$-b').

6 Signal and background parameterisation

The signals and the SM Higgs boson background mass distributions are described independently using double-sided Crystal Ball functions (as defined in ref. [103]). The parameter values for the functions are extracted by fitting the diphoton invariant mass distributions of the MC simulation for each category. The expected normalisations are calculated from

JHEP10(2020)005

the theoretical cross-sections multiplied by the acceptance and efficiency from the MC simulation.

The normalisation and shape of the non-resonant background are extracted by fitting the diphoton invariant mass distribution in data for each category. Following the method used in the measurement of the SM Higgs boson decaying into two photons [104], several candidate analytic functions are chosen for the non-resonant background parameterisation: the exponential functions of different-order polynomials, Bernstein polynomials of different order, and an adapted dijet function [105]. The potential bias, denoted by $\Delta N_{\text{bkg}}^{\text{non-res}}$, from the functional form modelling the continuum background in each category is estimated. It is defined as the maximal signal yield extracted from the fit to a continuum-background-only diphoton invariant mass distribution. This distribution is taken from MC simulations and is normalised to the integrated luminosity of $139\,\text{fb}^{-1}$, with small statistical uncertainty, using a signal-plus-background model. The Higgs boson mass varies from 115 GeV to 135 GeV [104]. This is to ensure the bias from choosing different background models is conservatively estimated. For categories 2 to 12, the functional form with $\Delta N_{\text{bkg}}^{\text{non-res}}$ less than 20% of the statistical uncertainty in data and with the fewest free parameters is chosen as the nominal background function. In the case of Category 1, with large MC statistical uncertainty, none of the functional forms satisfies the criterion on the fraction of the statistical uncertainty in data, thus the functional form with the smallest $\Delta N_{\text{bkg}}^{\text{non-res}}$ is chosen. The $\Delta N_{\text{bkg}}^{\text{non-res}}$ value of the chosen functional form is taken as the non-resonant background modelling uncertainty in each category and is shown in table 2.

7 Systematic uncertainties

Uncertainties from experimental and theoretical sources that affect the signal efficiency and the SM Higgs boson background yield are estimated from the MC simultation. The non-resonant background is obtained directly from the fit to the data. The only systematic uncertainty in the non-resonant background is the potential bias in $\Delta N_{\text{bkg}}^{\text{non-res}}$ from the choice of background modelling. A summary of the experimental and theoretical uncertainties in the yield from the SM Higgs boson background processes, non-resonant background, and signal production is shown in table 3.

The uncertainty in the combined 2015–2018 integrated luminosity is 1.7% [106], obtained using the LUCID-2 detector [107] for the primary luminosity measurements.

The efficiency of the diphoton trigger used to select events is evaluated in MC simulation using a trigger matching technique and in data using a bootstrap method [43]. The uncertainty in the trigger efficiency for events with $105 < m_{\gamma\gamma} < 160\,\text{GeV}$ is found to be 0.4%.

The uncertainty in the vertex selection efficiency is assessed by comparing the efficiency of finding photon-pointing vertices in $Z \to e^+e^-$ events in data with that in MC simulation [108]. The resulting uncertainty is found to be negligible in the inclusive photon selection.

The systematic uncertainties due to the photon energy scale and resolution are obtained from ref. [87]. The uncertainty in the energy scale has an effect below 1% on the

JHEP10(2020)005

Category	Function	$\Delta N_{\text{bkg}}^{\text{non-res}}$	$\Delta N_{\text{bkg}}^{\text{non-res}}/N_{\text{bkg}}^{\text{non-res.}}$ [%]
1	$(1-x^{1/3})^{b}\cdot x^{a}$	5.5	2.4
2	$\sum_{j=0}^{3} C_3^j x^j (1-x)^{3-j} b_{j,3}$	1.8	2.4
3	$\exp(a\cdot x)$	0.6	3.6
4	$\exp(a\cdot x)$	0.3	3.7
5	$\exp(a\cdot x)$	1.6	2.8
6	$\exp(a\cdot x)$	0.5	3.3
7	$\exp(a\cdot x)$	0.3	5.1
8	$\exp(a\cdot x)$	0.2	4.6
9	$\exp(a\cdot x)$	1.5	2.3
10	$\exp(a\cdot x)$	0.6	2.5
11	$\exp(a\cdot x)$	0.4	5.6
12	$\exp(a\cdot x)$	0.4	3.0

Table 2. The analytic functions used to model the non-resonant background, the extracted signals from the background-only fits ($\Delta N_{\text{bkg}}^{\text{non-res}}$) to the MC and the relative uncertainty in the non-resonant background within $120 < m_{\gamma\gamma} < 130\,\text{GeV}$ ($\Delta N_{\text{bkg}}^{\text{non-res}}/N_{\text{bkg}}^{\text{non-res.}}$) for each category. The variable x is defined as $m_{\gamma\gamma}/\sqrt{s}$ while a and b are parameters of the background functions. The C_3^j are binomial coefficients and the $b_{j,3}$ are the fitted parameters for the third order Bernstein polynomial parameterization.

normalisation of the signals and the SM Higgs boson background in the p_{T} range of the photons used in the analysis. The uncertainty in the energy resolution has an effect below 2% on the normalisation of the signals and the SM Higgs boson background. The uncertainties affecting the signal and the SM Higgs boson background mass distributions due to the photon energy scale and resolution are also evaluated. The uncertainties vary from below 1% to 20% for different categories and for different SM Higgs boson production processes. Overall, they amount to less than 3% of the total SM Higgs boson background.

Uncertainties in photon identification and isolation efficiencies are estimated [87], and their impact on the number of events in each category is quantified. The photon identification uncertainty varies in the range 1%–3% for the SM Higgs boson background and 1%–2% for the signals in all categories. The uncertainty in the photon calorimeter isolation efficiency is calculated from efficiency differences between applying and not applying corrections derived from inclusive photon events to the isolation variables in simulation. The measurements of the efficiency correction factors using inclusive photon events are used to derive the uncertainty in the photon track isolation efficiency. The photon isolation efficiency uncertainty is found to be in the range 1%–3% for the SM Higgs boson background and 1%–2% for the signals.

Migration of events among categories occurs if the energies of identified particles, jets and the $E_{\text{T}}^{\text{miss}}$, are varied within their uncertainties. The uncertainties in the jet energy scale, resolution [109] and jet vertex tagger are propagated to the $E_{\text{T}}^{\text{miss}}$ calculation. In

JHEP10(2020)005

Source	Signals [%]	Backgrounds [%]	
		SM Higgs boson	Non-resonant background
Experimental			
Luminosity		1.7	—
Jets (scale, resolution, JVT)	0.2–3.3	0.9–31	—
Electron/Photon (scale, resolution)	0.3–1.5	0.6–2.7	—
Photon (identification, isolation, trigger)	2.2–2.6	2.8–4.3	—
Electron (identification isolation)	0.0–0.5	0.0–0.6	—
Muon (identification, isolation, scale, resolution)	< 0.6	< 0.3	—
$E_{\mathrm{T}}^{\mathrm{miss}}$ reconstruction (jets, soft term)	< 0.7	0.4–14	—
Pile-up reweighting	0.3–1.8	1.3–1.5	—
Non-resonant background modelling		—	2–6
Theoretical			
Factorisation and renormalisation scale	< 1	4.1–6.5	—
PDF+α_{S}	< 6.6	3.3–6.4	—
Multiple parton-parton interactions		< 1	—
$\mathcal{B}(H \to \gamma\gamma)$		1.73	—

Table 3. Breakdown of the dominant systematic uncertainties. The uncertainties (in %) in the yield of signals, the background from the SM Higgs boson processes and non-resonant background are shown. All production modes of the SM Higgs boson are considered together. A "—" indicates that the systematic uncertainty is not applicable to the corresponding sample. If a given source has a different impact on the various categories, the given range corresponds to the smallest and largest impacts among categories or among the different signal models used in the analysis. In addition, the potential bias coming from non-resonant background modelling is shown relative to the background in the signal region $120 < m_{\gamma\gamma} < 130\,\mathrm{GeV}$.

addition, the uncertainties in the scale and resolution of the $E_{\mathrm{T}}^{\mathrm{miss}}$ soft term are estimated by using the method described in ref. [101]. The overall jet and $E_{\mathrm{T}}^{\mathrm{miss}}$ uncertainties in the SM Higgs boson processes vary from 1.0% to 34% for each category and for different SM Higgs boson production processes. Overall, they amount to 0.4%–14% for the total SM Higgs boson background. For the signal processes, the overall jet and $E_{\mathrm{T}}^{\mathrm{miss}}$ uncertainties range from 0.2% to 3.3%. An uncertainty in the pile-up modelling in MC simulation is accounted for. This results in an uncertainty of 0.3%–1.8% in the signal yield and 1.3%–1.5% in the SM Higgs boson yield. The uncertainties related to the b-tagging of jets are typically less than 1.5% in the SM Higgs boson yield used in the 'follow-up' analysis.

The predicted cross-sections of the SM Higgs boson and signal processes are affected by uncertainties due to missing higher-order terms in perturbative QCD. These uncertainties are estimated by varying the factorisation and renormalisation scales up and down from their nominal values by a factor of two, recalculating the cross-section in each case, and taking the largest deviation from the nominal cross-section as the uncertainty. The acceptance uncertainty related to the renormalisation and factorisation scales is less than

JHEP10(2020)005

1% for the signal and 3.7%–5.9% for the SM Higgs boson processes [28]. The normalisation uncertainty of the SM Higgs boson processes is 1.7% to 2.8%. For the signal processes, the effect of PDF and α_S uncertainties in the acceptance times selection efficiency is below 6.6%. It is estimated by using the recommendations of PDF4LHC [28]. Both the intra-PDF and inter-PDF uncertainties are extracted. Intra-PDF uncertainties are obtained by varying the parameters of the NNPDF3.0LO PDF set, while inter-PDF uncertainties are estimated by using alternative PDF sets (CT14 [110] at LO and MMHT2014 [111] at LO). The final inter-PDF uncertainty is the maximum deviation among all the variations from the central value obtained using the NNPDF3.0LO PDF set. In the case of the SM Higgs boson processes, the acceptance effect of α_S and the choice of PDFs ranges from 2.1% to 2.9%, and its normalisation effect is 2.5% to 5.7%. The uncertainty in the branching fraction of $h \to \gamma\gamma$ is 1.73% [28]. The uncertainty in the effect of multiple parton-parton interactions is estimated by switching them on and off in Pythia in the production of the ggF SM Higgs boson and signal samples. The resulting uncertainty in the number of events in this sample conservatively reaches 1% for all the categories.

8 Results

The results are derived from an unbinned likelihood fit to the $m_{\gamma\gamma}$ distributions in the range $105 < m_{\gamma\gamma} < 160\,\text{GeV}$ in each category simultaneously. The impact of the SM Higgs boson mass uncertainty is negligible. The signal strength and the background shape parameters are free parameters. The SM Higgs boson yields are taken from the SM predictions as discussed in section 3. The systematic uncertainty in each nuisance parameter is taken into account by multiplying the likelihood by a Gaussian penalty function centred on the nominal value of this parameter with a width set to its uncertainty. The nominal value of each SM Higgs boson background nuisance parameter (including its yield) is taken from the simulation normalised to the SM theoretical predictions.

Figures 4, 5 and 6 show the $m_{\gamma\gamma}$ distribution as well as the analytical signal-plus-background fits, for all 12 signal categories. The total background contains the non-resonant background and the predicted SM Higgs boson contribution. The fit results combining the $\tilde{\chi}_1^{\pm}\tilde{\chi}_2^0 \to W^{\pm}\tilde{\chi}_1^0 h\tilde{\chi}_1^0$ signal with $m(\tilde{\chi}_1^{\pm}/\tilde{\chi}_2^0) = 200\,\text{GeV}$ and $m(\tilde{\chi}_1^0) = 0.5\,\text{GeV}$, SM Higgs boson and non-resonant background are shown as the solid curves. A small excess of around two standard deviations is seen in Category 4, however it is consistent with a statistical fluctuation of the SM prediction.

The event yields in the range $120 < m_{\gamma\gamma} < 130\,\text{GeV}$ for data, the signal models, the SM Higgs boson background and non-resonant background in the 12 categories are shown in table 4. The signal samples shown correspond to the $\tilde{\chi}_1^{\pm}\tilde{\chi}_2^0 \to W^{\pm}\tilde{\chi}_1^0 h\tilde{\chi}_1^0$ signal with $m(\tilde{\chi}_1^{\pm}/\tilde{\chi}_2^0) = 200\,\text{GeV}$ and $m(\tilde{\chi}_1^0) = 0.5\,\text{GeV}$, and the $h\tilde{G}h\tilde{G}$ signal with $m(\tilde{\chi}_1^0) = 150\,\text{GeV}$ and $m(\tilde{G}) = 1\,\text{MeV}$. The yields for the non-resonant background and the SM Higgs boson are obtained from a simultaneous background-only fit to the full $m_{\gamma\gamma}$ spectrum for the 12 categories. For the 'Leptonic' categories, the Wh process is the largest SM Higgs boson process and occupies 38%–55% of total events. The $t\bar{t}h$ events dominate in the 'Hadronic' categories, which account for 36%–41% of total SM Higgs boson process events. In the

JHEP10(2020)005

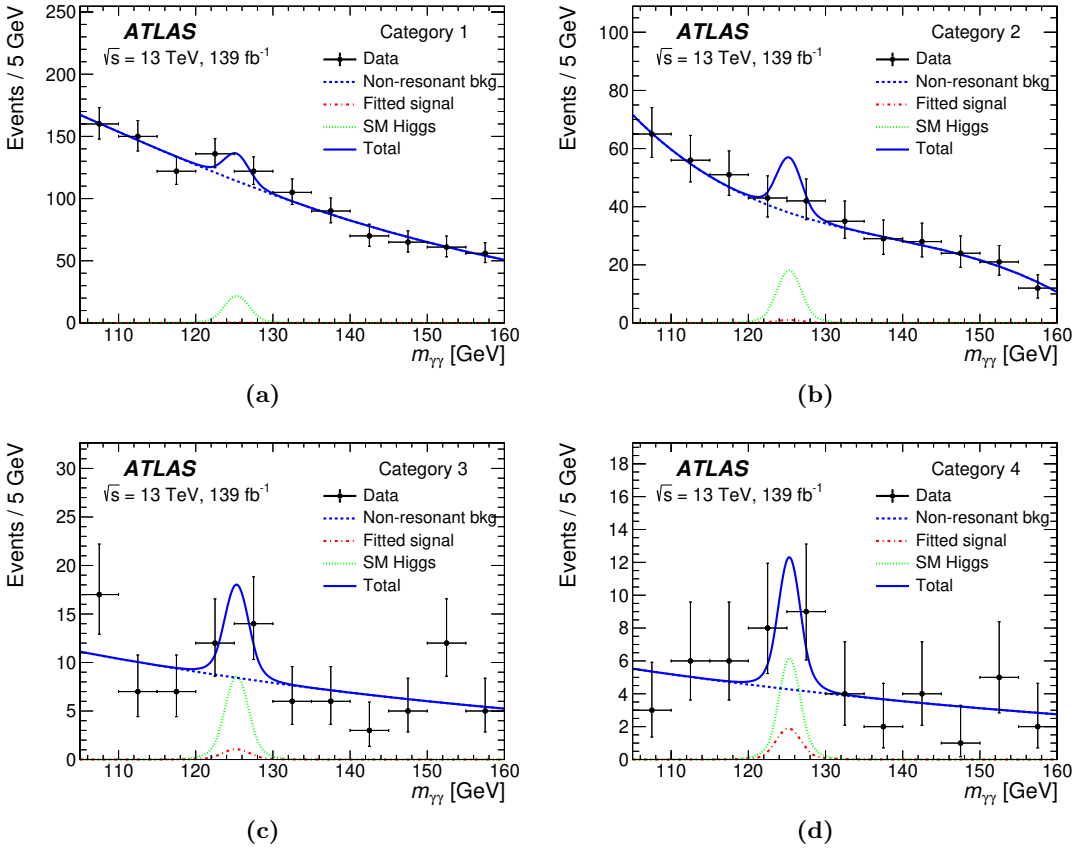

Figure 4. Diphoton invariant mass spectra and the corresponding fitted signal and background in the Leptonic categories (a) 1, (b) 2, (c) 3, and (d) 4. The signal samples shown correspond to the $\tilde{\chi}_1^{\pm}\tilde{\chi}_2^0 \to W^{\pm}\tilde{\chi}_1^0 h\tilde{\chi}_1^0$ signal with $m(\tilde{\chi}_1^{\pm}/\tilde{\chi}_2^0) = 200\,\text{GeV}$ and $m(\tilde{\chi}_1^0) = 0.5\,\text{GeV}$. The non-resonant background (dashed curve), the SM Higgs boson (dotted curve), and the signal (dash-dotted curve) are obtained from a simultaneous signal-plus-background fit to the full $m_{\gamma\gamma}$ spectrum for the 12 categories. The total of these contributions is shown by the solid curves.

'Rest' categories, events from the Zh process dominates and holds 37%–58% of total SM Higgs boson contribution. The yields for the signals are estimated from the simulation and normalized to the NLO+NLL predicted cross-sections. The uncertainties correspond to the statistical and systematic uncertainties summed in quadrature. For all the categories, data and background predictions agree within the statistical and systematic uncertainties.

The independently fitted $m_{\gamma\gamma}$ distributions for the 'follow-up' signal regions are shown in figure 7. No significant excess of events is seen in either of the two regions. In 'SR1L$\gamma\gamma$-a', two events are observed with 3.1 ± 0.8 non-resonant background events and $0.5^{+0.2}_{-0.4}$ SM Higgs boson events expected in the range $120 < m_{\gamma\gamma} < 130\,\text{GeV}$. In the case of 'SR1L$\gamma\gamma$-b', 31 events are observed, whereas 16.6 ± 1.9 events from non-resonant background and $8.6^{+1.3}_{-2.1}$ events from the SM Higgs boson are expected in the range $120 < m_{\gamma\gamma} < 130\,\text{GeV}$.

8.1 Limits on the visible cross-section

The observed yields agree with the background predictions, as shown in table 4, and no significant excess of events is observed. Upper limits are set on the visible cross-section

JHEP10(2020)005

Category	Data	Total bkg.	Non-resonant bkg.	SM Higgs boson	$W^{\pm}\tilde{\chi}_1^0 h\tilde{\chi}_1^0$	$h\tilde{G}h\tilde{G}$
1	258	246 ± 7	230 ± 7	16.3 ± 1.4	2.8 ± 0.6	13 ± 6
2	85	93 ± 4	77 ± 4	15.6 ± 1.3	6.6 ± 1.5	16 ± 7
3	26	24.1 ± 2.0	17.1 ± 1.9	7.0 ± 0.6	6.9 ± 1.5	6.5 ± 2.7
4	17	12.8 ± 1.4	8.4 ± 1.3	4.4 ± 0.4	10.7 ± 2.4	3.8 ± 1.6
5	54	60 ± 4	57.9 ± 3.5	1.9 ± 0.6	7.2 ± 1.6	3.3 ± 1.4
6	11	16.1 ± 1.8	15.4 ± 1.8	0.74 ± 0.26	6.0 ± 1.3	1.6 ± 0.7
7	8	6.3 ± 1.1	5.9 ± 1.1	0.42 ± 0.10	4.3 ± 1.0	0.71 ± 0.34
8	4	5.2 ± 1.0	4.4 ± 1.0	0.80 ± 0.11	5.3 ± 1.2	0.76 ± 0.33
9	71	69 ± 4	65 ± 4	3.9 ± 0.8	9.1 ± 2.0	3.1 ± 1.3
10	29	26.3 ± 2.2	24.2 ± 2.2	2.1 ± 0.4	6.9 ± 1.5	1.8 ± 0.8
11	6	8.6 ± 1.2	7.2 ± 1.2	1.40 ± 0.22	4.6 ± 1.0	1.1 ± 0.5
12	22	16.6 ± 1.7	13.4 ± 1.7	3.15 ± 0.33	7.9 ± 1.8	1.7 ± 0.7

Table 4. Event yields in the range $120 < m_{\gamma\gamma} < 130\,\text{GeV}$ for data, the signal models, the SM Higgs boson background and non-resonant background in each analysis category, for an integrated luminosity of $139\,\text{fb}^{-1}$. The signal samples shown correspond to the $\tilde{\chi}_1^{\pm}\tilde{\chi}_2^0 \to W^{\pm}\tilde{\chi}_1^0 h\tilde{\chi}_1^0$ signal with $m(\tilde{\chi}_1^{\pm}/\tilde{\chi}_2^0) = 200\,\text{GeV}$ and $m(\tilde{\chi}_1^0) = 0.5\,\text{GeV}$, and the $h\tilde{G}h\tilde{G}$ signals with $m(\tilde{\chi}_1^0) = 150\,\text{GeV}$ and $m(\tilde{G}) = 1\,\text{MeV}$. The yields for the non-resonant background and SM Higgs boson are obtained from a simultaneous background-only fit to the full $m_{\gamma\gamma}$ spectrum for the 12 categories. The yields for the signals are estimated from the simulation. The uncertainties correspond to the statistical and systematic uncertainties summed in quadrature.

$\sigma_{\text{vis}}^{\text{BSM}} \equiv (\mathcal{A} \times \epsilon \times \sigma)^{\text{BSM}}$ for BSM physics processes producing $E_{\text{T}}^{\text{miss}}$ and an SM Higgs boson decaying into two photons, where $\mathcal{A}$ and ϵ are the acceptance and the efficiency for the signal, respectively. The limits are extracted by performing a fit to the non-resonant background and SM Higgs boson background, individually for each category, each time injecting a signal with the same mass distribution as the SM Higgs boson but with a free normalisation. Figure 8 shows the observed and expected 95% confidence level (CL) upper limits on $\sigma_{\text{vis}}^{\text{BSM}}$ for each of the 12 different categories, which are calculated using a one-sided profile-likelihood ratio and the CL_s formalism [112] with the asymptotic approximation described in ref. [113]. The statistical uncertainty is dominant for all categories.

8.2 Interpretation of the wino-like $\tilde{\chi}_1^{\pm}\tilde{\chi}_2^0 \to W^{\pm}\tilde{\chi}_1^0 h\tilde{\chi}_1^0$ model

Since no significant excess is observed, fit results are interpreted in terms of 95% CL exclusion limits on the production cross-section of the wino-like $\tilde{\chi}_1^{\pm}\tilde{\chi}_2^0 \to W^{\pm}\tilde{\chi}_1^0 h\tilde{\chi}_1^0$ model [26, 27]. Upper limits on the contribution of events from the considered processes are computed by using the modified frequentist CL_s approach based on asymptotic formulae [112, 113]. Figure 9 shows 95% CL exclusion limits on the production cross-section of $\tilde{\chi}_1^{\pm}\tilde{\chi}_2^0 \to W^{\pm}\tilde{\chi}_1^0 h\tilde{\chi}_1^0$ as a function of $m(\tilde{\chi}_1^{\pm}/\tilde{\chi}_2^0)$. The observed 95% CL upper limits on the production cross-section vary from 1.92 pb to 0.16 pb for $m(\tilde{\chi}_1^{\pm}/\tilde{\chi}_2^0)$ from 150 GeV to 600 GeV. The expected 95% CL upper limits range from 1.43 pb to 0.11 pb for the same range. A 95% CL lower limit of 310 GeV in $m(\tilde{\chi}_1^{\pm}/\tilde{\chi}_2^0)$, where $m(\tilde{\chi}_1^0) = 0.5\,\text{GeV}$, is set.

JHEP10(2020)005

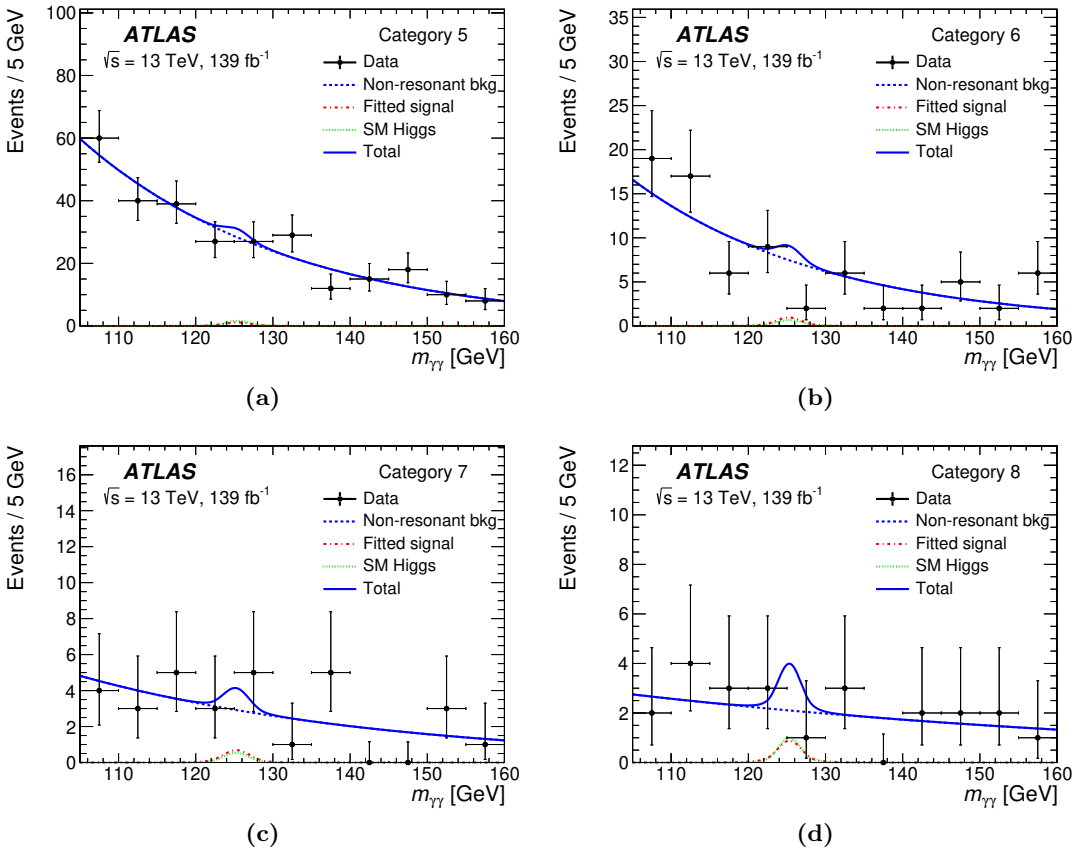

Figure 5. Diphoton invariant mass spectra and the corresponding fitted signal and background in the Hadronic categories (a) 5, (b) 6, (c) 7, and (d) 8. The signal samples shown correspond to the $\tilde{\chi}_1^{\pm}\tilde{\chi}_2^0 \to W^{\pm}\tilde{\chi}_1^0 h\tilde{\chi}_1^0$ signal with $m(\tilde{\chi}_1^{\pm}/\tilde{\chi}_2^0) = 200\,\text{GeV}$ and $m(\tilde{\chi}_1^0) = 0.5\,\text{GeV}$. The non-resonant background (dashed curve), the SM Higgs boson (dotted curve), and the signal (dash-dotted curve) are obtained from a simultaneous signal-plus-background fit to the full $m_{\gamma\gamma}$ spectrum for the 12 categories. The total of these contributions is shown by the solid curves.

The observed and expected exclusion contours at 95% CL for the $\tilde{\chi}_1^{\pm}\tilde{\chi}_2^0$ production in the $m(\tilde{\chi}_1^{\pm}/\tilde{\chi}_2^0)$–$m(\tilde{\chi}_1^0)$ plane are shown in figure 10.

8.3 Interpretation of the higgsino-like $h\tilde{G}h\tilde{G}$ model

As a second SUSY scenario, a GMSB model where the two lightest neutralinos and the lightest chargino are higgsinos is considered [36–38]. The $\tilde{\chi}_1^{\pm}$, $\tilde{\chi}_1^0$ and $\tilde{\chi}_2^0$ are almost mass degenerate in this model, with $\tilde{\chi}_1^0$ being the lightest of the three states. The LSP is a gravitino. In figure 11, the observed and expected 95% CL upper limits, with uncertainties, on the higgsino production cross-section in the $h\tilde{G}h\tilde{G}$ models for different $m(\tilde{\chi}_1^0)$ masses are presented. The levelling off of expected limits at low $m(\tilde{\chi}_1^0)$ masses is due to the acceptance times efficiency in this region. The theoretical prediction includes the $\tilde{\chi}_1^0\,\tilde{\chi}_2^0$, $\tilde{\chi}_1^0\,\tilde{\chi}_1^{\pm}$, $\tilde{\chi}_2^0\,\tilde{\chi}_1^{\pm}$, and $\tilde{\chi}_1^{\pm}\,\tilde{\chi}_1^{\mp}$ production modes, where $\tilde{\chi}_1^{\pm}$ and $\tilde{\chi}_2^0$ promptly decay into the $\tilde{\chi}_1^0$ and particles that have too low momentum to be detected. In the $h\tilde{G}h\tilde{G}$ model, higgsino masses below 380 GeV are excluded at 95% CL.

JHEP10(2020)005

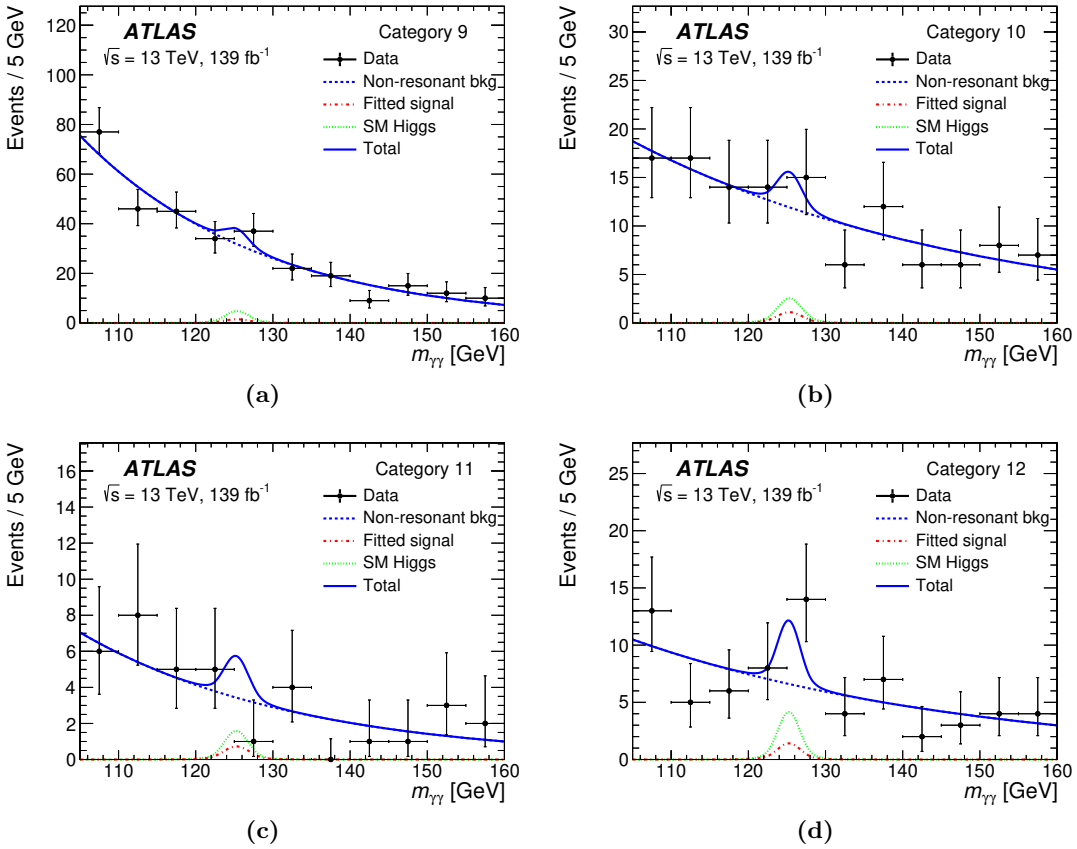

Figure 6. Diphoton invariant mass spectra and the corresponding fitted signal and background in the Rest categories (a) 9, (b) 10, (c) 11, and (d) 12. The signal samples shown correspond to the $\tilde{\chi}_1^{\pm}\tilde{\chi}_2^0 \to W^{\pm}\tilde{\chi}_1^0 h\tilde{\chi}_1^0$ signal with $m(\tilde{\chi}_1^{\pm}/\tilde{\chi}_2^0) = 200\,\text{GeV}$ and $m(\tilde{\chi}_1^0) = 0.5\,\text{GeV}$. The non-resonant background (dashed curve), the SM Higgs boson (dotted curve), and the signal (dash-dotted curve) are obtained from a simultaneous signal-plus-background fit to the full $m_{\gamma\gamma}$ spectrum for the 12 categories. The total of these contributions is shown by the solid curves.

9 Conclusion

A search for a chargino and a neutralino decaying via the 125 GeV Higgs boson into photons is presented. This study is based on the full data collected between 2015 and 2018 with the ATLAS detector at the LHC, corresponding to an integrated luminosity of $139\,\text{fb}^{-1}$ of pp collisions at a centre-of-mass energy of 13 TeV. No significant excess over the expected background is observed. Upper limits at 95% confidence level are set on the $\tilde{\chi}_1^{\pm}\tilde{\chi}_2^0$ and higgsino production cross-section, and the visible cross-section for beyond the Standard Model physics processes. For the $\tilde{\chi}_1^{\pm}\tilde{\chi}_2^0 \to W^{\pm}\tilde{\chi}_1^0 h\tilde{\chi}_1^0$ model, the observed 95% confidence-level upper limits on the production cross-section vary from 1.92 pb to 0.16 pb for $m(\tilde{\chi}_1^{\pm}/\tilde{\chi}_2^0)$ from 150 GeV to 600 GeV, where $m(\tilde{\chi}_1^0)$ is set to 0.5 GeV. The expected 95% confidence-level upper limits range from 1.43 pb to 0.11 pb for the same mass interval. A 95% confidence-level lower limit of 310 GeV in $m(\tilde{\chi}_1^{\pm}/\tilde{\chi}_2^0)$, where $m(\tilde{\chi}_1^0) = 0.5\,\text{GeV}$, is set. Upper limits at the 95% confidence-level are set on the higgsino production cross-section. Higgsino masses

JHEP10(2020)005

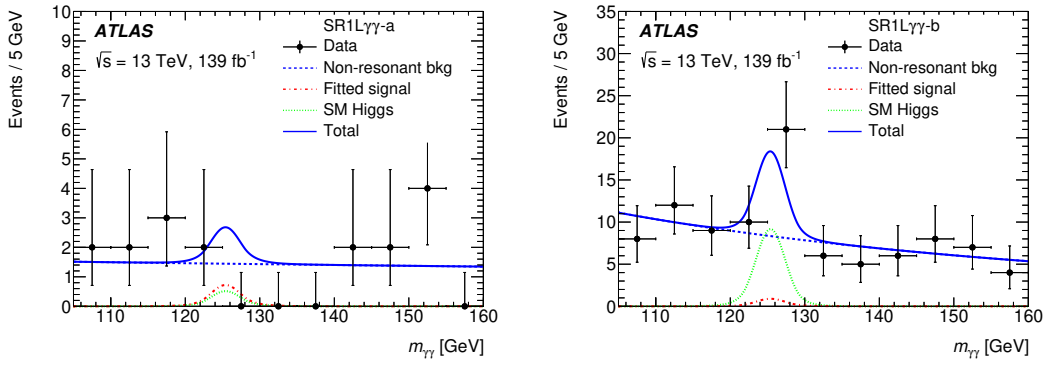

(a) (b)

Figure 7. Diphoton invariant mass spectra and the corresponding fitted signal and background in the signal regions (a) 'SR1L$\gamma\gamma$-a' and (b) 'SR1L$\gamma\gamma$-b'. The signal samples shown correspond to the $\tilde{\chi}_1^{\pm}\tilde{\chi}_2^0 \to W^{\pm}\tilde{\chi}_1^0 h\tilde{\chi}_1^0$ signal with $m(\tilde{\chi}_1^{\pm}/\tilde{\chi}_2^0) = 200\,\text{GeV}$ and $m(\tilde{\chi}_1^0) = 0.5\,\text{GeV}$. The non-resonant background (dashed curve), the SM Higgs boson (dotted curve), and the signal (dash-dotted curve) are obtained from a signal-plus-background fit to the full $m_{\gamma\gamma}$ spectrum in 'SR1L$\gamma\gamma$-a' (a) and 'SR1L$\gamma\gamma$-b' (b) separately. The total of these contributions is shown by the solid curves.

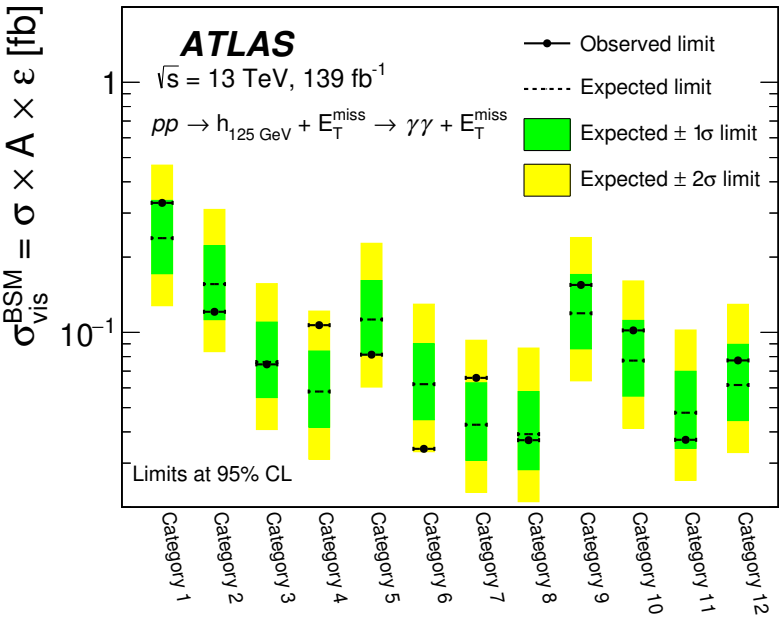

Figure 8. The 95% CL model-independent upper limits computed from individual fits in each of 12 categories on the visible cross-section $\sigma_{\text{vis}}^{\text{BSM}} = \sigma \times A \times \epsilon$ for any $pp \to h + E_{\text{T}}^{\text{miss}} \to \gamma\gamma + E_{\text{T}}^{\text{miss}}$ BSM processes.

JHEP10(2020)005

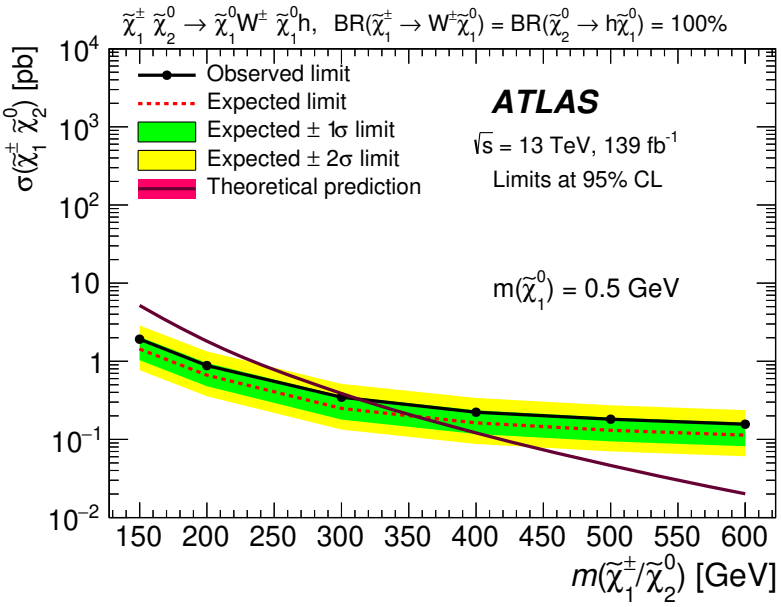

Figure 9. Expected and observed 95% CL exclusion upper limits on the production cross-section of $\tilde{\chi}_1^\pm \tilde{\chi}_2^0 \to W^\pm \tilde{\chi}_1^0 h \tilde{\chi}_1^0$ as a function of $m(\tilde{\chi}_1^\pm/\tilde{\chi}_2^0)$.

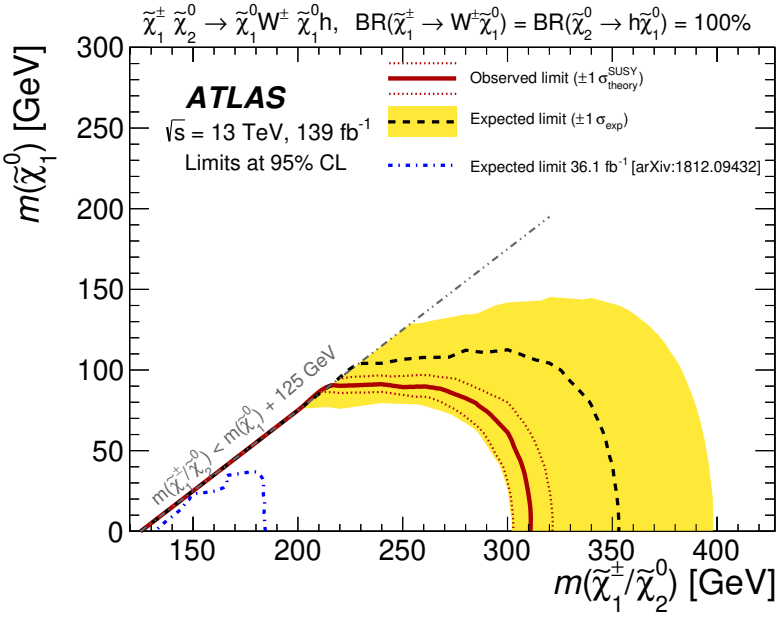

Figure 10. The observed (solid line) and expected (dashed lines) exclusion limit contours at 95% CL for the $\tilde{\chi}_1^\pm \tilde{\chi}_2^0$ production in the $m(\tilde{\chi}_1^\pm/\tilde{\chi}_2^0)$–$m(\tilde{\chi}_1^0)$ plane. The dotted lines represent the $\pm 1\sigma$ theoretical uncertainty for the observed limit. The $\pm 1\sigma$ expected exclusion limit contour is shown as the shaded band. The expected limit for the 36.1 fb^{-1} analysis [32] is also shown for comparison in the dash-dotted line.

JHEP10(2020)005

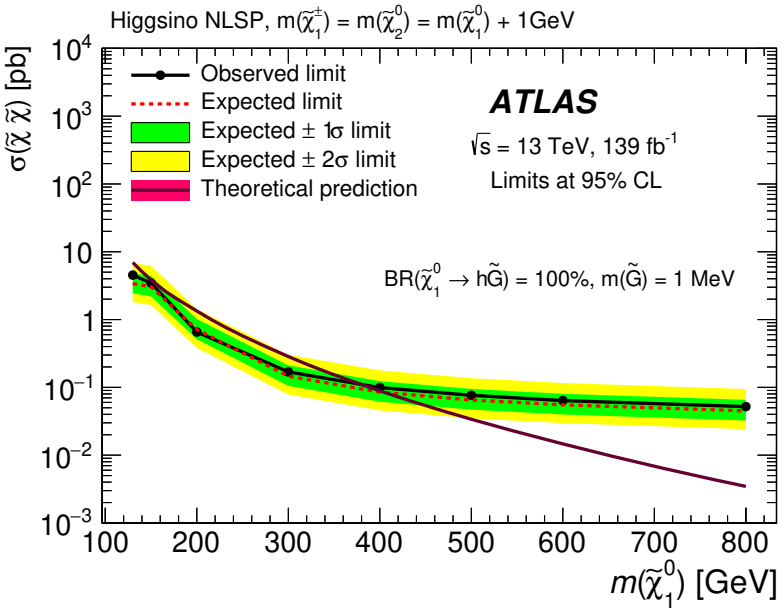

Figure 11. Expected and observed 95% CL exclusion upper limits on the higgsino production ($\tilde{\chi}\tilde{\chi} \equiv \tilde{\chi}_1^0\tilde{\chi}_2^0, \tilde{\chi}_1^0\tilde{\chi}_1^\pm, \tilde{\chi}_2^0\tilde{\chi}_1^\pm, \tilde{\chi}_1^\pm\tilde{\chi}_1^\mp$) cross-section for the $h\tilde{G}h\tilde{G}$ signal model. As a function of the higgsino mass. The theoretical prediction includes the $\tilde{\chi}_1^0\ \tilde{\chi}_2^0$, $\tilde{\chi}_1^0\ \tilde{\chi}_1^\pm$, $\tilde{\chi}_2^0\ \tilde{\chi}_1^\pm$, and $\tilde{\chi}_1^\pm\ \tilde{\chi}_1^\mp$ production modes, where $\tilde{\chi}_1^\pm$ and $\tilde{\chi}_2^0$ promptly decay into the $\tilde{\chi}_1^0$ and particles that have too low momentum to be detected.

below 380 GeV are excluded for the case of the higgsino fully decaying into a Higgs boson and a gravitino.

Acknowledgments

We thank CERN for the very successful operation of the LHC, as well as the support staff from our institutions without whom ATLAS could not be operated efficiently.

We acknowledge the support of ANPCyT, Argentina; YerPhI, Armenia; ARC, Australia; BMWFW and FWF, Austria; ANAS, Azerbaijan; SSTC, Belarus; CNPq and FAPESP, Brazil; NSERC, NRC and CFI, Canada; CERN; CONICYT, Chile; CAS, MOST and NSFC, China; COLCIENCIAS, Colombia; MSMT CR, MPO CR and VSC CR, Czech Republic; DNRF and DNSRC, Denmark; IN2P3-CNRS and CEA-DRF/IRFU, France; SRNSFG, Georgia; BMBF, HGF and MPG, Germany; GSRT, Greece; RGC and Hong Kong SAR, China; ISF and Benoziyo Center, Israel; INFN, Italy; MEXT and JSPS, Japan; CNRST, Morocco; NWO, Netherlands; RCN, Norway; MNiSW and NCN, Poland; FCT, Portugal; MNE/IFA, Romania; MES of Russia and NRC KI, Russia Federation; JINR; MESTD, Serbia; MSSR, Slovakia; ARRS and MIZŠ, Slovenia; DST/NRF, South Africa; MINECO, Spain; SRC and Wallenberg Foundation, Sweden; SERI, SNSF and Cantons of Bern and Geneva, Switzerland; MOST, Taiwan; TAEK, Turkey; STFC, United Kingdom; DOE and NSF, United States of America. In addition, individual groups and members have received support from BCKDF, CANARIE, Compute Canada and CRC, Canada; ERC,

JHEP10(2020)005

ERDF, Horizon 2020, Marie Skłodowska-Curie Actions and COST, European Union; Investissements d'Avenir Labex, Investissements d'Avenir Idex and ANR, France; DFG and AvH Foundation, Germany; Herakleitos, Thales and Aristeia programmes co-financed by EU-ESF and the Greek NSRF, Greece; BSF-NSF and GIF, Israel; CERCA Programme Generalitat de Catalunya and PROMETEO Programme Generalitat Valenciana, Spain; Göran Gustafssons Stiftelse, Sweden; The Royal Society and Leverhulme Trust, United Kingdom.

The crucial computing support from all WLCG partners is acknowledged gratefully, in particular from CERN, the ATLAS Tier-1 facilities at TRIUMF (Canada), NDGF (Denmark, Norway, Sweden), CC-IN2P3 (France), KIT/GridKA (Germany), INFN-CNAF (Italy), NL-T1 (Netherlands), PIC (Spain), ASGC (Taiwan), RAL (U.K.) and BNL (U.S.A.), the Tier-2 facilities worldwide and large non-WLCG resource providers. Major contributors of computing resources are listed in ref. [114].

Open Access. This article is distributed under the terms of the Creative Commons Attribution License (CC-BY 4.0), which permits any use, distribution and reproduction in any medium, provided the original author(s) and source are credited.

JHEP10(2020)005

References

[1] ATLAS collaboration, *Observation of a new particle in the search for the Standard Model Higgs boson with the ATLAS detector at the LHC*, *Phys. Lett. B* **716** (2012) 1 [arXiv:1207.7214] [INSPIRE].

[2] CMS collaboration, *Observation of a New Boson at a Mass of* 125 *GeV with the CMS Experiment at the LHC*, *Phys. Lett. B* **716** (2012) 30 [arXiv:1207.7235] [INSPIRE].

[3] ATLAS and CMS collaborations, *Combined Measurement of the Higgs Boson Mass in pp Collisions at* $\sqrt{s} = 7$ *and* 8 *TeV with the ATLAS and CMS Experiments*, *Phys. Rev. Lett.* **114** (2015) 191803 [arXiv:1503.07589] [INSPIRE].

[4] ATLAS and CMS collaborations, *Measurements of the Higgs boson production and decay rates and constraints on its couplings from a combined ATLAS and CMS analysis of the LHC pp collision data at* $\sqrt{s} = 7$ *and* 8 *TeV*, *JHEP* **08** (2016) 045 [arXiv:1606.02266] [INSPIRE].

[5] N. Sakai, *Naturalness in Supersymmetric Guts*, *Z. Phys. C* **11** (1981) 153 [INSPIRE].

[6] S. Dimopoulos, S. Raby and F. Wilczek, *Supersymmetry and the Scale of Unification*, *Phys. Rev. D* **24** (1981) 1681 [INSPIRE].

[7] L.E. Ibáñez and G.G. Ross, *Low-Energy Predictions in Supersymmetric Grand Unified Theories*, *Phys. Lett. B* **105** (1981) 439 [INSPIRE].

[8] S. Dimopoulos and H. Georgi, *Softly broken supersymmetry and* SU(5), *Nucl. Phys. B* **193** (1981) 150 [INSPIRE].

[9] Y. Golfand and E.P. Likhtman, *Extension of the Algebra of Poincaré Group Generators and Violation of p Invariance*, *JETP Lett.* **13** (1971) 323 [INSPIRE].

[10] D.V. Volkov and V.P. Akulov, *Is the Neutrino a Goldstone Particle?*, *Phys. Lett. B* **46** (1973) 109 [INSPIRE].

[11] J. Wess and B. Zumino, *Supergauge Transformations in Four-Dimensions*, *Nucl. Phys. B* **70** (1974) 39 [INSPIRE].

[12] J. Wess and B. Zumino, *Supergauge Invariant Extension of Quantum Electrodynamics*, *Nucl. Phys. B* **78** (1974) 1 [INSPIRE].

[13] S. Ferrara and B. Zumino, *Supergauge invariant Yang-Mills theories*, *Nucl. Phys. B* **79** (1974) 413 [INSPIRE].

[14] A. Salam and J.A. Strathdee, *Supersymmetry and Nonabelian Gauges*, *Phys. Lett. B* **51** (1974) 353 [INSPIRE].

[15] H. Goldberg, *Constraint on the Photino Mass from Cosmology*, *Phys. Rev. Lett.* **50** (1983) 1419 [*Erratum ibid.* **103** (2009) 099905] [INSPIRE].

[16] J.R. Ellis, J.S. Hagelin, D.V. Nanopoulos, K.A. Olive and M. Srednicki, *Supersymmetric Relics from the Big Bang*, *Nucl. Phys. B* **238** (1984) 453 [INSPIRE].

[17] G.R. Farrar and P. Fayet, *Phenomenology of the Production, Decay, and Detection of New Hadronic States Associated with Supersymmetry*, *Phys. Lett. B* **76** (1978) 575 [INSPIRE].

[18] R. Barbieri and G.F. Giudice, *Upper Bounds on Supersymmetric Particle Masses*, *Nucl. Phys. B* **306** (1988) 63 [INSPIRE].

[19] B. de Carlos and J.A. Casas, *One loop analysis of the electroweak breaking in supersymmetric models and the fine tuning problem*, *Phys. Lett. B* **309** (1993) 320 [hep-ph/9303291] [INSPIRE].

[20] P. Fayet, *Supersymmetry and Weak, Electromagnetic and Strong Interactions*, *Phys. Lett. B* **64** (1976) 159 [INSPIRE].

[21] P. Fayet, *Spontaneously Broken Supersymmetric Theories of Weak, Electromagnetic and Strong Interactions*, *Phys. Lett. B* **69** (1977) 489 [INSPIRE].

[22] S.P. Das, M. Guchait and D.P. Roy, *Testing SUSY models for the muon $g-2$ anomaly via chargino-neutralino pair production at the LHC*, *Phys. Rev. D* **90** (2014) 055011 [arXiv:1406.6925] [INSPIRE].

[23] M.A. Ajaib, B. Dutta, T. Ghosh, I. Gogoladze and Q. Shafi, *Neutralinos and sleptons at the LHC in light of muon $(g-2)_\mu$*, *Phys. Rev. D* **92** (2015) 075033 [arXiv:1505.05896] [INSPIRE].

[24] M. Chakraborti, U. Chattopadhyay, A. Choudhury, A. Datta and S. Poddar, *Reduced LHC constraints for higgsino-like heavier electroweakinos*, *JHEP* **11** (2015) 050 [arXiv:1507.01395] [INSPIRE].

[25] M. Endo, K. Hamaguchi, S. Iwamoto and K. Yanagi, *Probing minimal SUSY scenarios in the light of muon $g-2$ and dark matter*, *JHEP* **06** (2017) 031 [arXiv:1704.05287] [INSPIRE].

[26] J. Alwall, P. Schuster and N. Toro, *Simplified Models for a First Characterization of New Physics at the LHC*, *Phys. Rev. D* **79** (2009) 075020 [arXiv:0810.3921] [INSPIRE].

[27] LHC New Physics Working Group, *Simplified Models for LHC New Physics Searches*, *J. Phys. G* **39** (2012) 105005 [arXiv:1105.2838] [INSPIRE].

[28] LHC Higgs Cross Section Working Group, *Handbook of LHC Higgs Cross Sections: 4. Deciphering the Nature of the Higgs Sector*, in *CERN Yellow Reports: Monographs* **2**, CERN, Geneva Switzerland (2017) [CERN-2017-002-M] [arXiv:1610.07922] [INSPIRE].

JHEP10(2020)005

[29] CMS collaboration, *Search for supersymmetry using Higgs boson to diphoton decays at* $\sqrt{s} = 13$ *TeV*, *JHEP* **11** (2019) 109 [arXiv:1908.08500] [INSPIRE].

[30] ATLAS collaboration, *Search for direct production of electroweakinos in final states with one lepton, missing transverse momentum and a Higgs boson decaying into two b-jets in pp collisions at* $\sqrt{s} = 13$ *TeV with the ATLAS detector*, *Eur. Phys. J. C* **80** (2020) 691 [arXiv:1909.09226] [INSPIRE].

[31] CMS collaboration, *Combined search for electroweak production of charginos and neutralinos in proton-proton collisions at* $\sqrt{s} = 13$ *TeV*, *JHEP* **03** (2018) 160 [arXiv:1801.03957] [INSPIRE].

[32] ATLAS collaboration, *Search for chargino and neutralino production in final states with a Higgs boson and missing transverse momentum at* $\sqrt{s} = 13$ *TeV with the ATLAS detector*, *Phys. Rev. D* **100** (2019) 012006 [arXiv:1812.09432] [INSPIRE].

[33] M. Dine and W. Fischler, *A Phenomenological Model of Particle Physics Based on Supersymmetry*, *Phys. Lett. B* **110** (1982) 227 [INSPIRE].

[34] L. Álvarez-Gaumé, M. Claudson and M.B. Wise, *Low-Energy Supersymmetry*, *Nucl. Phys. B* **207** (1982) 96 [INSPIRE].

[35] C.R. Nappi and B.A. Ovrut, *Supersymmetric Extension of the* SU(3) × SU(2) × U(1) *Model*, *Phys. Lett. B* **113** (1982) 175 [INSPIRE].

[36] CMS collaboration, *Searches for electroweak neutralino and chargino production in channels with Higgs, Z, and W bosons in pp collisions at* 8 *TeV*, *Phys. Rev. D* **90** (2014) 092007 [arXiv:1409.3168] [INSPIRE].

[37] K.T. Matchev and S.D. Thomas, *Higgs and Z boson signatures of supersymmetry*, *Phys. Rev. D* **62** (2000) 077702 [hep-ph/9908482] [INSPIRE].

[38] J.T. Ruderman and D. Shih, *General Neutralino NLSPs at the Early LHC*, *JHEP* **08** (2012) 159 [arXiv:1103.6083] [INSPIRE].

[39] ATLAS collaboration, *The ATLAS Experiment at the CERN Large Hadron Collider*, 2008 *JINST* **3** S08003 [INSPIRE].

[40] ATLAS collaboration, *ATLAS Insertable B-Layer Technical Design Report*, CERN-LHCC-2010-013 (2010) [ATLAS-TDR-19] [*Addendum* ATLAS-TDR-19-ADD-1 (2012)] [INSPIRE].

[41] ATLAS IBL collaboration, *Production and Integration of the ATLAS Insertable B-Layer*, 2018 *JINST* **13** T05008 [arXiv:1803.00844] [INSPIRE].

[42] ATLAS collaboration, *Performance of the ATLAS Trigger System in 2015*, *Eur. Phys. J. C* **77** (2017) 317 [arXiv:1611.09661] [INSPIRE].

[43] ATLAS collaboration, *Performance of electron and photon triggers in ATLAS during LHC Run 2*, *Eur. Phys. J. C* **80** (2020) 47 [arXiv:1909.00761] [INSPIRE].

[44] J. Alwall et al., *The automated computation of tree-level and next-to-leading order differential cross sections, and their matching to parton shower simulations*, *JHEP* **07** (2014) 079 [arXiv:1405.0301] [INSPIRE].

[45] NNPDF collaboration, *Parton distributions for the LHC Run II*, *JHEP* **04** (2015) 040 [arXiv:1410.8849] [INSPIRE].

[46] T. Sjöstrand, S. Mrenna and P.Z. Skands, *A Brief Introduction to PYTHIA 8.1*, *Comput. Phys. Commun.* **178** (2008) 852 [arXiv:0710.3820] [INSPIRE].

JHEP10(2020)005

[47] ATLAS collaboration, *ATLAS PYTHIA 8 tunes to 7 TeV datas*, ATL-PHYS-PUB-2014-021 (2014) [INSPIRE].

[48] NNPDF collaboration, *Parton distributions with LHC data*, *Nucl. Phys. B* **867** (2013) 244 [arXiv:1207.1303] [INSPIRE].

[49] J. Debove, B. Fuks and M. Klasen, *Threshold resummation for gaugino pair production at hadron colliders*, *Nucl. Phys. B* **842** (2011) 51 [arXiv:1005.2909] [INSPIRE].

[50] B. Fuks, M. Klasen, D.R. Lamprea and M. Rothering, *Gaugino production in proton-proton collisions at a center-of-mass energy of 8 TeV*, *JHEP* **10** (2012) 081 [arXiv:1207.2159] [INSPIRE].

[51] B. Fuks, M. Klasen, D.R. Lamprea and M. Rothering, *Precision predictions for electroweak superpartner production at hadron colliders with Resummino*, *Eur. Phys. J. C* **73** (2013) 2480 [arXiv:1304.0790] [INSPIRE].

[52] J. Fiaschi and M. Klasen, *Neutralino-chargino pair production at NLO + NLL with resummation-improved parton density functions for LHC Run II*, *Phys. Rev. D* **98** (2018) 055014 [arXiv:1805.11322] [INSPIRE].

[53] W. Beenakker, M. Klasen, M. Krämer, T. Plehn, M. Spira and P.M. Zerwas, *The Production of charginos/neutralinos and sleptons at hadron colliders*, *Phys. Rev. Lett.* **83** (1999) 3780 [*Erratum ibid.* **100** (2008) 029901] [hep-ph/9906298] [INSPIRE].

[54] C. Borschensky et al., *Squark and gluino production cross sections in pp collisions at* $\sqrt{s} = 13$, 14, 33 *and* 100 *TeV*, *Eur. Phys. J. C* **74** (2014) 3174 [arXiv:1407.5066] [INSPIRE].

[55] P. Nason, *A New method for combining NLO QCD with shower Monte Carlo algorithms*, *JHEP* **11** (2004) 040 [hep-ph/0409146] [INSPIRE].

[56] S. Alioli, P. Nason, C. Oleari and E. Re, *NLO Higgs boson production via gluon fusion matched with shower in POWHEG*, *JHEP* **04** (2009) 002 [arXiv:0812.0578] [INSPIRE].

[57] S. Frixione, P. Nason and C. Oleari, *Matching NLO QCD computations with Parton Shower simulations: the POWHEG method*, *JHEP* **11** (2007) 070 [arXiv:0709.2092] [INSPIRE].

[58] P. Nason and C. Oleari, *NLO Higgs boson production via vector-boson fusion matched with shower in POWHEG*, *JHEP* **02** (2010) 037 [arXiv:0911.5299] [INSPIRE].

[59] S. Alioli, P. Nason, C. Oleari and E. Re, *A general framework for implementing NLO calculations in shower Monte Carlo programs: the POWHEG BOX*, *JHEP* **06** (2010) 043 [arXiv:1002.2581] [INSPIRE].

[60] ATLAS collaboration, *Measurement of the* Z/γ^* *boson transverse momentum distribution in pp collisions at* $\sqrt{s} = 7$ *TeV with the ATLAS detector*, *JHEP* **09** (2014) 145 [arXiv:1406.3660] [INSPIRE].

[61] H.-L. Lai et al., *New parton distributions for collider physics*, *Phys. Rev. D* **82** (2010) 074024 [arXiv:1007.2241] [INSPIRE].

[62] T. Gleisberg et al., *Event generation with SHERPA 1.1*, *JHEP* **02** (2009) 007 [arXiv:0811.4622] [INSPIRE].

[63] S. Schumann and F. Krauss, *A Parton shower algorithm based on Catani-Seymour dipole factorisation*, *JHEP* **03** (2008) 038 [arXiv:0709.1027] [INSPIRE].

[64] S. Höche, F. Krauss, S. Schumann and F. Siegert, *QCD matrix elements and truncated showers*, *JHEP* **05** (2009) 053 [arXiv:0903.1219] [INSPIRE].

JHEP10(2020)005

[65] M. Ciccolini, A. Denner and S. Dittmaier, *Strong and electroweak corrections to the production of Higgs + 2jets via weak interactions at the LHC*, *Phys. Rev. Lett.* **99** (2007) 161803 [arXiv:0707.0381] [INSPIRE].

[66] M. Ciccolini, A. Denner and S. Dittmaier, *Electroweak and QCD corrections to Higgs production via vector-boson fusion at the LHC*, *Phys. Rev. D* **77** (2008) 013002 [arXiv:0710.4749] [INSPIRE].

[67] P. Bolzoni, F. Maltoni, S.-O. Moch and M. Zaro, *Higgs production via vector-boson fusion at NNLO in QCD*, *Phys. Rev. Lett.* **105** (2010) 011801 [arXiv:1003.4451] [INSPIRE].

[68] K. Mimasu, V. Sanz and C. Williams, *Higher Order QCD predictions for Associated Higgs production with anomalous couplings to gauge bosons*, *JHEP* **08** (2016) 039 [arXiv:1512.02572] [INSPIRE].

[69] O. Brein, A. Djouadi and R. Harlander, *NNLO QCD corrections to the Higgs-strahlung processes at hadron colliders*, *Phys. Lett. B* **579** (2004) 149 [hep-ph/0307206] [INSPIRE].

[70] L. Altenkamp, S. Dittmaier, R.V. Harlander, H. Rzehak and T.J.E. Zirke, *Gluon-induced Higgs-strahlung at next-to-leading order QCD*, *JHEP* **02** (2013) 078 [arXiv:1211.5015] [INSPIRE].

[71] A. Denner, S. Dittmaier, S. Kallweit and A. Muck, *Electroweak corrections to Higgs-strahlung off W/Z bosons at the Tevatron and the LHC with HAWK*, *JHEP* **03** (2012) 075 [arXiv:1112.5142] [INSPIRE].

[72] C. Anastasiou, C. Duhr, F. Dulat, F. Herzog and B. Mistlberger, *Higgs Boson Gluon-Fusion Production in QCD at Three Loops*, *Phys. Rev. Lett.* **114** (2015) 212001 [arXiv:1503.06056] [INSPIRE].

[73] C. Anastasiou et al., *High precision determination of the gluon fusion Higgs boson cross-section at the LHC*, *JHEP* **05** (2016) 058 [arXiv:1602.00695] [INSPIRE].

[74] S. Actis, G. Passarino, C. Sturm and S. Uccirati, *NLO Electroweak Corrections to Higgs Boson Production at Hadron Colliders*, *Phys. Lett. B* **670** (2008) 12 [arXiv:0809.1301] [INSPIRE].

[75] C. Anastasiou, R. Boughezal and F. Petriello, *Mixed QCD-electroweak corrections to Higgs boson production in gluon fusion*, *JHEP* **04** (2009) 003 [arXiv:0811.3458] [INSPIRE].

[76] W. Beenakker, S. Dittmaier, M. Krämer, B. Plumper, M. Spira and P.M. Zerwas, *NLO QCD corrections to $t\bar{t}H$ production in hadron collisions*, *Nucl. Phys. B* **653** (2003) 151 [hep-ph/0211352] [INSPIRE].

[77] S. Dawson, C.B. Jackson, L.H. Orr, L. Reina and D. Wackeroth, *Associated Higgs production with top quarks at the large hadron collider: NLO QCD corrections*, *Phys. Rev. D* **68** (2003) 034022 [hep-ph/0305087] [INSPIRE].

[78] Y. Zhang, W.-G. Ma, R.-Y. Zhang, C. Chen and L. Guo, *QCD NLO and EW NLO corrections to $t\bar{t}H$ production with top quark decays at hadron collider*, *Phys. Lett. B* **738** (2014) 1 [arXiv:1407.1110] [INSPIRE].

[79] S. Frixione, V. Hirschi, D. Pagani, H.S. Shao and M. Zaro, *Electroweak and QCD corrections to top-pair hadroproduction in association with heavy bosons*, *JHEP* **06** (2015) 184 [arXiv:1504.03446] [INSPIRE].

[80] S. Dawson, C.B. Jackson, L. Reina and D. Wackeroth, *Exclusive Higgs boson production with bottom quarks at hadron colliders*, *Phys. Rev. D* **69** (2004) 074027 [hep-ph/0311067] [INSPIRE].

JHEP10(2020)005

[81] S. Dittmaier, M. Krämer and M. Spira, *Higgs radiation off bottom quarks at the Tevatron and the CERN LHC*, *Phys. Rev. D* **70** (2004) 074010 [hep-ph/0309204] [INSPIRE].

[82] R. Harlander, M. Krämer and M. Schumacher, *Bottom-quark associated Higgs-boson production: reconciling the four- and five-flavour scheme approach*, arXiv:1112.3478 [INSPIRE].

[83] A.D. Martin, W.J. Stirling, R.S. Thorne and G. Watt, *Parton distributions for the LHC*, *Eur. Phys. J. C* **63** (2009) 189 [arXiv:0901.0002] [INSPIRE].

[84] ATLAS collaboration, *The PYTHIA 8 A3 tune description of ATLAS minimum bias and inelastic measurements incorporating the Donnachie-Landshoff diffractive model*, ATL-PHYS-PUB-2016-017 (2016) [INSPIRE].

[85] ATLAS collaboration, *The ATLAS Simulation Infrastructure*, *Eur. Phys. J. C* **70** (2010) 823 [arXiv:1005.4568] [INSPIRE].

[86] GEANT4 collaboration, *GEANT4 — a simulation toolkit*, *Nucl. Instrum. Meth. A* **506** (2003) 250 [INSPIRE].

[87] ATLAS collaboration, *Electron and photon performance measurements with the ATLAS detector using the 2015–2017 LHC proton-proton collision data*, 2019 *JINST* **14** P12006 [arXiv:1908.00005] [INSPIRE].

[88] ATLAS collaboration, *Topological cell clustering in the ATLAS calorimeters and its performance in LHC Run 1*, *Eur. Phys. J. C* **77** (2017) 490 [arXiv:1603.02934] [INSPIRE].

[89] ATLAS collaboration, *Measurement of the inclusive isolated prompt photon cross section in pp collisions at $\sqrt{s} = 7$ TeV with the ATLAS detector*, *Phys. Rev. D* **83** (2011) 052005 [arXiv:1012.4389] [INSPIRE].

[90] M. Cacciari, G.P. Salam and G. Soyez, *The Catchment Area of Jets*, *JHEP* **04** (2008) 005 [arXiv:0802.1188] [INSPIRE].

[91] M. Cacciari, G.P. Salam and S. Sapeta, *On the characterisation of the underlying event*, *JHEP* **04** (2010) 065 [arXiv:0912.4926] [INSPIRE].

[92] ATLAS collaboration, *Measurements of Higgs boson properties in the diphoton decay channel with 36 fb^{-1} of pp collision data at $\sqrt{s} = 13$ TeV with the ATLAS detector*, *Phys. Rev. D* **98** (2018) 052005 [arXiv:1802.04146] [INSPIRE].

[93] ATLAS collaboration, *Measurements of fiducial and differential cross sections for Higgs boson production in the diphoton decay channel at $\sqrt{s} = 8$ TeV with ATLAS*, *JHEP* **09** (2014) 112 [arXiv:1407.4222] [INSPIRE].

[94] ATLAS collaboration, *Muon reconstruction performance of the ATLAS detector in proton-proton collision data at $\sqrt{s} = 13$ TeV*, *Eur. Phys. J. C* **76** (2016) 292 [arXiv:1603.05598] [INSPIRE].

[95] M. Cacciari, G.P. Salam and G. Soyez, *The anti-k_t jet clustering algorithm*, *JHEP* **04** (2008) 063 [arXiv:0802.1189] [INSPIRE].

[96] M. Cacciari, G.P. Salam and G. Soyez, *FastJet User Manual*, *Eur. Phys. J. C* **72** (2012) 1896 [arXiv:1111.6097] [INSPIRE].

[97] ATLAS collaboration, *Tagging and suppression of pileup jets*, ATL-PHYS-PUB-2014-001 (2014) [INSPIRE].

[98] ATLAS collaboration, *Selection of jets produced in 13 TeV proton-proton collisions with the ATLAS detector*, ATLAS-CONF-2015-029 (2015) [INSPIRE].

JHEP10(2020)005

[99] ATLAS collaboration, *ATLAS b-jet identification performance and efficiency measurement with $t\bar{t}$ events in pp collisions at $\sqrt{s} = 13$ TeV*, *Eur. Phys. J. C* **79** (2019) 970 [arXiv:1907.05120] [INSPIRE].

[100] ATLAS collaboration, *Optimisation and performance studies of the ATLAS b-tagging algorithms for the 2017–18 LHC run*, ATL-PHYS-PUB-2017-013 (2017) [INSPIRE].

[101] ATLAS collaboration, *Performance of missing transverse momentum reconstruction with the ATLAS detector using proton-proton collisions at $\sqrt{s} = 13$ TeV*, *Eur. Phys. J. C* **78** (2018) 903 [arXiv:1802.08168] [INSPIRE].

[102] ATLAS collaboration, *Measurement of isolated-photon pair production in pp collisions at $\sqrt{s} = 7$ TeV with the ATLAS detector*, *JHEP* **01** (2013) 086 [arXiv:1211.1913] [INSPIRE].

[103] ATLAS collaboration, *Search for Scalar Diphoton Resonances in the Mass Range 65–600 GeV with the ATLAS Detector in pp Collision Data at $\sqrt{s} = 8$ TeV*, *Phys. Rev. Lett.* **113** (2014) 171801 [arXiv:1407.6583] [INSPIRE].

[104] ATLAS collaboration, *Measurement of Higgs boson production in the diphoton decay channel in pp collisions at center-of-mass energies of 7 and 8 TeV with the ATLAS detector*, *Phys. Rev. D* **90** (2014) 112015 [arXiv:1408.7084] [INSPIRE].

[105] CDF collaboration, *Search for new particles decaying into dijets in proton-antiproton collisions at $\sqrt{s} = 1.96$ TeV*, *Phys. Rev. D* **79** (2009) 112002 [arXiv:0812.4036] [INSPIRE].

[106] ATLAS collaboration, *Luminosity determination in pp collisions at $\sqrt{s} = 13$ TeV using the ATLAS detector at the LHC*, ATLAS-CONF-2019-021 (2019) [INSPIRE].

[107] G. Avoni et al., *The new LUCID-2 detector for luminosity measurement and monitoring in ATLAS*, 2018 *JINST* **13** P07017 [INSPIRE].

[108] ATLAS collaboration, *Search for resonances in diphoton events at $\sqrt{s} = 13$ TeV with the ATLAS detector*, *JHEP* **09** (2016) 001 [arXiv:1606.03833] [INSPIRE].

[109] ATLAS collaboration, *Jet energy scale measurements and their systematic uncertainties in proton-proton collisions at $\sqrt{s} = 13$ TeV with the ATLAS detector*, *Phys. Rev. D* **96** (2017) 072002 [arXiv:1703.09665] [INSPIRE].

[110] S. Dulat et al., *New parton distribution functions from a global analysis of quantum chromodynamics*, *Phys. Rev. D* **93** (2016) 033006 [arXiv:1506.07443] [INSPIRE].

[111] L.A. Harland-Lang, A.D. Martin, P. Motylinski and R.S. Thorne, *Parton distributions in the LHC era: MMHT 2014 PDFs*, *Eur. Phys. J. C* **75** (2015) 204 [arXiv:1412.3989] [INSPIRE].

[112] A.L. Read, *Presentation of search results: The CL_s technique*, *J. Phys. G* **28** (2002) 2693 [INSPIRE].

[113] G. Cowan, K. Cranmer, E. Gross and O. Vitells, *Asymptotic formulae for likelihood-based tests of new physics*, *Eur. Phys. J. C* **71** (2011) 1554 [*Erratum ibid.* **73** (2013) 2501] [arXiv:1007.1727] [INSPIRE].

[114] ATLAS collaboration, *ATLAS Computing Acknowledgements*, ATL-GEN-PUB-2016-002 (2016).

JHEP10(2020)005

The ATLAS collaboration

G. Aad[102], B. Abbott[129], D.C. Abbott[103], A. Abed Abud[71a,71b], K. Abeling[53], D.K. Abhayasinghe[94], S.H. Abidi[167], O.S. AbouZeid[40], N.L. Abraham[156], H. Abramowicz[161], H. Abreu[160], Y. Abulaiti[6], B.S. Acharya[67a,67b,o], B. Achkar[53], S. Adachi[163], L. Adam[100], C. Adam Bourdarios[5], L. Adamczyk[84a], L. Adamek[167], J. Adelman[121], M. Adersberger[114], A. Adiguzel[12c,ak], S. Adorni[54], T. Adye[144], A.A. Affolder[146], Y. Afik[160], C. Agapopoulou[65], M.N. Agaras[38], A. Aggarwal[119], C. Agheorghiesei[27c], J.A. Aguilar-Saavedra[140f,140a,aj], F. Ahmadov[80], W.S. Ahmed[104], X. Ai[18], G. Aielli[74a,74b], S. Akatsuka[86], T.P.A. Åkesson[97], E. Akilli[54], A.V. Akimov[111], K. Al Khoury[65], G.L. Alberghi[23b,23a], J. Albert[176], M.J. Alconada Verzini[161], S. Alderweireldt[36], M. Aleksa[36], I.N. Aleksandrov[80], C. Alexa[27b], D. Alexandre[19], T. Alexopoulos[10], A. Alfonsi[120], F. Alfonsi[23b,23a], M. Alhroob[129], B. Ali[142], G. Alimonti[69a], J. Alison[37], S.P. Alkire[148], C. Allaire[65], B.M.M. Allbrooke[156], B.W. Allen[132], P.P. Allport[21], A. Aloisio[70a,70b], A. Alonso[40], F. Alonso[89], C. Alpigiani[148], A.A. Alshehri[57], M. Alvarez Estevez[99], D. Álvarez Piqueras[174], M.G. Alviggi[70a,70b], Y. Amaral Coutinho[81b], A. Ambler[104], L. Ambroz[135], C. Amelung[26], D. Amidei[106], S.P. Amor Dos Santos[140a], S. Amoroso[46], C.S. Amrouche[54], F. An[79], C. Anastopoulos[149], N. Andari[145], T. Andeen[11], C.F. Anders[61b], J.K. Anders[20], A. Andreazza[69a,69b], V. Andrei[61a], C.R. Anelli[176], S. Angelidakis[38], A. Angerami[39], A.V. Anisenkov[122b,122a], A. Annovi[72a], C. Antel[61a], M.T. Anthony[149], M. Antonelli[51], D.J.A. Antrim[171], F. Anulli[73a], M. Aoki[82], J.A. Aparisi Pozo[174], L. Aperio Bella[15a], G. Arabidze[107], J.P. Araque[140a], V. Araujo Ferraz[81b], R. Araujo Pereira[81b], C. Arcangeletti[51], A.T.H. Arce[49], F.A. Arduh[89], J-F. Arguin[110], S. Argyropoulos[78], J.-H. Arling[46], A.J. Armbruster[36], A. Armstrong[171], O. Arnaez[167], H. Arnold[120], Z.P. Arrubarrena Tame[114], A. Artamonov[124,*], G. Artoni[135], S. Artz[100], S. Asai[163], N. Asbah[59], E.M. Asimakopoulou[172], L. Asquith[156], J. Assahsah[35d], K. Assamagan[29], R. Astalos[28a], R.J. Atkin[33a], M. Atkinson[173], N.B. Atlay[19], H. Atmani[65], K. Augsten[142], G. Avolio[36], R. Avramidou[60a], M.K. Ayoub[15a], A.M. Azoulay[168b], G. Azuelos[110,ax], H. Bachacou[145], K. Bachas[68a,68b], M. Backes[135], F. Backman[45a,45b], P. Bagnaia[73a,73b], M. Bahmani[85], H. Bahrasemani[152], A.J. Bailey[174], V.R. Bailey[173], J.T. Baines[144], M. Bajic[40], C. Bakalis[10], O.K. Baker[183], P.J. Bakker[120], D. Bakshi Gupta[8], S. Balaji[157], E.M. Baldin[122b,122a], P. Balek[180], F. Balli[145], W.K. Balunas[135], J. Balz[100], E. Banas[85], A. Bandyopadhyay[24], Sw. Banerjee[181,j], A.A.E. Bannoura[182], L. Barak[161], W.M. Barbe[38], E.L. Barberio[105], D. Barberis[55b,55a], M. Barbero[102], G. Barbour[95], T. Barillari[115], M-S. Barisits[36], J. Barkeloo[132], T. Barklow[153], R. Barnea[160], S.L. Barnes[60c], B.M. Barnett[144], R.M. Barnett[18], Z. Barnovska-Blenessy[60a], A. Baroncelli[60a], G. Barone[29], A.J. Barr[135], L. Barranco Navarro[45a,45b], F. Barreiro[99], J. Barreiro Guimarães da Costa[15a], S. Barsov[138], R. Bartoldus[153], G. Bartolini[102], A.E. Barton[90], P. Bartos[28a], A. Basalaev[46], A. Bassalat[65,ar], M.J. Basso[167], R.L. Bates[57], S. Batlamous[35e], J.R. Batley[32], B. Batool[151], M. Battaglia[146], M. Bauce[73a,73b], F. Bauer[145], K.T. Bauer[171], H.S. Bawa[31,m], J.B. Beacham[49], T. Beau[136], P.H. Beauchemin[170], F. Becherer[52], P. Bechtle[24], H.C. Beck[53], H.P. Beck[20,s], K. Becker[52], M. Becker[100], C. Becot[46], A. Beddall[12d], A.J. Beddall[12a], V.A. Bednyakov[80], M. Bedognetti[120], C.P. Bee[155], T.A. Beermann[77], M. Begalli[81b], M. Begel[29], A. Behera[155], J.K. Behr[46], F. Beisiegel[24], A.S. Bell[95], G. Bella[161], L. Bellagamba[23b], A. Bellerive[34], P. Bellos[9], K. Beloborodov[122b,122a], K. Belotskiy[112], N.L. Belyaev[112], D. Benchekroun[35a], N. Benekos[10], Y. Benhammou[161], D.P. Benjamin[6], M. Benoit[54], J.R. Bensinger[26], S. Bentvelsen[120], L. Beresford[135], M. Beretta[51], D. Berge[46], E. Bergeaas Kuutmann[172], N. Berger[5], B. Bergmann[142], L.J. Bergsten[26], J. Beringer[18], S. Berlendis[7], N.R. Bernard[103], G. Bernardi[136], C. Bernius[153], F.U. Bernlochner[24], T. Berry[94], P. Berta[100], C. Bertella[15a], I.A. Bertram[90],

JHEP10(2020)005

O. Bessidskaia Bylund[182], N. Besson[145], A. Bethani[101], S. Bethke[115], A. Betti[24], A.J. Bevan[93], J. Beyer[115], D.S. Bhattacharya[177], R. Bi[139], R.M. Bianchi[139], O. Biebel[114], D. Biedermann[19], R. Bielski[36], K. Bierwagen[100], N.V. Biesuz[72a,72b], M. Biglietti[75a], T.R.V. Billoud[110], M. Bindi[53], A. Bingul[12d], C. Bini[73a,73b], S. Biondi[23b,23a], M. Birman[180], T. Bisanz[53], J.P. Biswal[161], D. Biswas[181,j], A. Bitadze[101], C. Bittrich[48], K. Bjørke[134], K.M. Black[25], T. Blazek[28a], I. Bloch[46], C. Blocker[26], A. Blue[57], U. Blumenschein[93], G.J. Bobbink[120], V.S. Bobrovnikov[122b,122a], S.S. Bocchetta[97], A. Bocci[49], D. Boerner[46], D. Bogavac[14], A.G. Bogdanchikov[122b,122a], C. Bohm[45a], V. Boisvert[94], P. Bokan[53,172,53], T. Bold[84a], A.S. Boldyrev[113], A.E. Bolz[61b], M. Bomben[136], M. Bona[93], J.S. Bonilla[132], M. Boonekamp[145], H.M. Borecka-Bielska[91], A. Borisov[123], G. Borissov[90], J. Bortfeldt[36], D. Bortoletto[135], D. Boscherini[23b], M. Bosman[14], J.D. Bossio Sola[104], K. Bouaouda[35a], J. Boudreau[139], E.V. Bouhova-Thacker[90], D. Boumediene[38], S.K. Boutle[57], A. Boveia[127], J. Boyd[36], D. Boye[33c,as], I.R. Boyko[80], A.J. Bozson[94], J. Bracinik[21], N. Brahimi[102], G. Brandt[182], O. Brandt[32], F. Braren[46], B. Brau[103], J.E. Brau[132], W.D. Breaden Madden[57], K. Brendlinger[46], L. Brenner[46], R. Brenner[172], S. Bressler[180], B. Brickwedde[100], D.L. Briglin[21], D. Britton[57], D. Britzger[115], I. Brock[24], R. Brock[107], G. Brooijmans[39], W.K. Brooks[147d], E. Brost[121], J.H Broughton[21], P.A. Bruckman de Renstrom[85], D. Bruncko[28b], A. Bruni[23b], G. Bruni[23b], L.S. Bruni[120], S. Bruno[74a,74b], B.H. Brunt[32], M. Bruschi[23b], N. Bruscino[139], P. Bryant[37], L. Bryngemark[97], T. Buanes[17], Q. Buat[36], P. Buchholz[151], A.G. Buckley[57], I.A. Budagov[80], M.K. Bugge[134], F. Bührer[52], O. Bulekov[112], T.J. Burch[121], S. Burdin[91], C.D. Burgard[120], A.M. Burger[130], B. Burghgrave[8], J.T.P. Burr[46], C.D. Burton[11], J.C. Burzynski[103], V. Büscher[100], E. Buschmann[53], P.J. Bussey[57], J.M. Butler[25], C.M. Buttar[57], J.M. Butterworth[95], P. Butti[36], W. Buttinger[36], A. Buzatu[158], A.R. Buzykaev[122b,122a], G. Cabras[23b,23a], S. Cabrera Urbán[174], D. Caforio[56], H. Cai[173], V.M.M. Cairo[153], O. Cakir[4a], N. Calace[36], P. Calafiura[18], A. Calandri[102], G. Calderini[136], P. Calfayan[66], G. Callea[57], L.P. Caloba[81b], S. Calvente Lopez[99], D. Calvet[38], S. Calvet[38], T.P. Calvet[155], M. Calvetti[72a,72b], R. Camacho Toro[136], S. Camarda[36], D. Camarero Munoz[99], P. Camarri[74a,74b], D. Cameron[134], R. Caminal Armadans[103], C. Camincher[36], S. Campana[36], M. Campanelli[95], A. Camplani[40], A. Campoverde[151], V. Canale[70a,70b], A. Canesse[104], M. Cano Bret[60c], J. Cantero[130], T. Cao[161], Y. Cao[173], M.D.M. Capeans Garrido[36], M. Capua[41b,41a], R. Cardarelli[74a], F. Cardillo[149], G. Carducci[41b,41a], I. Carli[143], T. Carli[36], G. Carlino[70a], B.T. Carlson[139], L. Carminati[69a,69b], R.M.D. Carney[45a,45b], S. Caron[119], E. Carquin[147d], S. Carrá[46], J.W.S. Carter[167], M.P. Casado[14,e], A.F. Casha[167], D.W. Casper[171], R. Castelijn[120], F.L. Castillo[174], V. Castillo Gimenez[174], N.F. Castro[140a,140e], A. Catinaccio[36], J.R. Catmore[134], A. Cattai[36], J. Caudron[24], V. Cavaliere[29], E. Cavallaro[14], M. Cavalli-Sforza[14], V. Cavasinni[72a,72b], E. Celebi[12b], F. Ceradini[75a,75b], L. Cerda Alberich[174], K. Cerny[131], A.S. Cerqueira[81a], A. Cerri[156], L. Cerrito[74a,74b], F. Cerutti[18], A. Cervelli[23b,23a], S.A. Cetin[12b], Z. Chadi[35a], D. Chakraborty[121], S.K. Chan[59], W.S. Chan[120], W.Y. Chan[91], J.D. Chapman[32], B. Chargeishvili[159b], D.G. Charlton[21], T.P. Charman[93], C.C. Chau[34], S. Che[127], S. Chekanov[6], S.V. Chekulaev[168a], G.A. Chelkov[80,ap], M.A. Chelstowska[36], B. Chen[79], C. Chen[60a], C.H. Chen[79], H. Chen[29], J. Chen[60a], J. Chen[39], S. Chen[137], S.J. Chen[15c], X. Chen[15b,aw], Y. Chen[83], Y-H. Chen[46], H.C. Cheng[63a], H.J. Cheng[15a], A. Cheplakov[80], E. Cheremushkina[123], R. Cherkaoui El Moursli[35e], E. Cheu[7], K. Cheung[64], T.J.A. Chevalérias[145], L. Chevalier[145], V. Chiarella[51], G. Chiarelli[72a], G. Chiodini[68a], A.S. Chisholm[21], A. Chitan[27b], I. Chiu[163], Y.H. Chiu[176], M.V. Chizhov[80], K. Choi[66], A.R. Chomont[73a,73b], S. Chouridou[162], Y.S. Chow[120], M.C. Chu[63a], X. Chu[15a,15d], J. Chudoba[141], A.J. Chuinard[104], J.J. Chwastowski[85], L. Chytka[131], D. Cieri[115], K.M. Ciesla[85], D. Cinca[47], V. Cindro[92], I.A. Cioară[27b], A. Ciocio[18], F. Cirotto[70a,70b], Z.H. Citron[180,k], M. Citterio[69a], D.A. Ciubotaru[27b], B.M. Ciungu[167], A. Clark[54], M.R. Clark[39], P.J. Clark[50], C. Clement[45a,45b], Y. Coadou[102], M. Cobal[67a,67c], A. Coccaro[55b], J. Cochran[79],

JHEP10(2020)005

H. Cohen[161], A.E.C. Coimbra[36], L. Colasurdo[119], B. Cole[39], A.P. Colijn[120], J. Collot[58], P. Conde Muiño[140a,f], E. Coniavitis[52], S.H. Connell[33c], I.A. Connelly[57], S. Constantinescu[27b], F. Conventi[70a,ay], A.M. Cooper-Sarkar[135], F. Cormier[175], K.J.R. Cormier[167], L.D. Corpe[95], M. Corradi[73a,73b], E.E. Corrigan[97], F. Corriveau[104,af], M.J. Costa[174], F. Costanza[5], D. Costanzo[149], G. Cowan[94], J.W. Cowley[32], J. Crane[101], K. Cranmer[125], S.J. Crawley[57], R.A. Creager[137], S. Crépé-Renaudin[58], F. Crescioli[136], M. Cristinziani[24], V. Croft[120], G. Crosetti[41b,41a], A. Cueto[5], T. Cuhadar Donszelmann[149], A.R. Cukierman[153], S. Czekierda[85], P. Czodrowski[36], M.J. Da Cunha Sargedas De Sousa[60b], J.V. Da Fonseca Pinto[81b], C. Da Via[101], W. Dabrowski[84a], T. Dado[28a], S. Dahbi[35e], T. Dai[106], C. Dallapiccola[103], M. Dam[40], G. D'amen[29], V. D'Amico[75a,75b], J. Damp[100], J.R. Dandoy[137], M.F. Daneri[30], N.P. Dang[181,j], N.S. Dann[101], M. Danninger[175], V. Dao[36], G. Darbo[55b], O. Dartsi[5], A. Dattagupta[132], T. Daubney[46], S. D'Auria[69a,69b], W. Davey[24], C. David[46], T. Davidek[143], D.R. Davis[49], I. Dawson[149], K. De[8], R. De Asmundis[70a], M. De Beurs[120], S. De Castro[23b,23a], S. De Cecco[73a,73b], N. De Groot[119], P. de Jong[120], H. De la Torre[107], A. De Maria[15c], D. De Pedis[73a], A. De Salvo[73a], U. De Sanctis[74a,74b], M. De Santis[74a,74b], A. De Santo[156], K. De Vasconcelos Corga[102], J.B. De Vivie De Regie[65], C. Debenedetti[146], D.V. Dedovich[80], A.M. Deiana[42], M. Del Gaudio[41b,41a], J. Del Peso[99], Y. Delabat Diaz[46], D. Delgove[65], F. Deliot[145,r], C.M. Delitzsch[7], M. Della Pietra[70a,70b], D. Della Volpe[54], A. Dell'Acqua[36], L. Dell'Asta[74a,74b], M. Delmastro[5], C. Delporte[65], P.A. Delsart[58], D.A. DeMarco[167], S. Demers[183], M. Demichev[80], G. Demontigny[110], S.P. Denisov[123], D. Denysiuk[120], L. D'Eramo[136], D. Derendarz[85], J.E. Derkaoui[35d], F. Derue[136], P. Dervan[91], K. Desch[24], C. Deterre[46], K. Dette[167], C. Deutsch[24], M.R. Devesa[30], P.O. Deviveiros[36], A. Dewhurst[144], F.A. Di Bello[54], A. Di Ciaccio[74a,74b], L. Di Ciaccio[5], W.K. Di Clemente[137], C. Di Donato[70a,70b], A. Di Girolamo[36], G. Di Gregorio[72a,72b], B. Di Micco[75a,75b], R. Di Nardo[103], K.F. Di Petrillo[59], R. Di Sipio[167], D. Di Valentino[34], C. Diaconu[102], F.A. Dias[40], T. Dias Do Vale[140a], M.A. Diaz[147a], J. Dickinson[18], E.B. Diehl[106], J. Dietrich[19], S. Díez Cornell[46], A. Dimitrievska[18], W. Ding[15b], J. Dingfelder[24], F. Dittus[36], F. Djama[102], T. Djobava[159b], J.I. Djuvsland[17], M.A.B. Do Vale[81c], M. Dobre[27b], D. Dodsworth[26], C. Doglioni[97], J. Dolejsi[143], Z. Dolezal[143], M. Donadelli[81d], B. Dong[60c], J. Donini[38], A. D'onofrio[93], M. D'Onofrio[91], J. Dopke[144], A. Doria[70a], M.T. Dova[89], A.T. Doyle[57], E. Drechsler[152], E. Dreyer[152], T. Dreyer[53], A.S. Drobac[170], Y. Duan[60b], F. Dubinin[111], M. Dubovsky[28a], A. Dubreuil[54], E. Duchovni[180], G. Duckeck[114], A. Ducourthial[136], O.A. Ducu[110], D. Duda[115], A. Dudarev[36], A.C. Dudder[100], E.M. Duffield[18], L. Duflot[65], M. Dührssen[36], C. Dülsen[182], M. Dumancic[180], A.E. Dumitriu[27b], A.K. Duncan[57], M. Dunford[61a], A. Duperrin[102], H. Duran Yildiz[4a], M. Düren[56], A. Durglishvili[159b], D. Duschinger[48], B. Dutta[46], D. Duvnjak[1], G.I. Dyckes[137], M. Dyndal[36], S. Dysch[101], B.S. Dziedzic[85], K.M. Ecker[115], R.C. Edgar[106], M.G. Eggleston[49], T. Eifert[36], G. Eigen[17], K. Einsweiler[18], T. Ekelof[172], H. El Jarrari[35e], M. El Kacimi[35c], R. El Kosseifi[102], V. Ellajosyula[172], M. Ellert[172], F. Ellinghaus[182], A.A. Elliot[93], N. Ellis[36], J. Elmsheuser[29], M. Elsing[36], D. Emeliyanov[144], A. Emerman[39], Y. Enari[163], M.B. Epland[49], J. Erdmann[47], A. Ereditato[20], M. Errenst[36], M. Escalier[65], C. Escobar[174], O. Estrada Pastor[174], E. Etzion[161], H. Evans[66], A. Ezhilov[138], F. Fabbri[57], L. Fabbri[23b,23a], V. Fabiani[119], G. Facini[95], R.M. Faisca Rodrigues Pereira[140a], R.M. Fakhrutdinov[123], S. Falciano[73a], P.J. Falke[5], S. Falke[5], J. Faltova[143], Y. Fang[15a], Y. Fang[15a], G. Fanourakis[44], M. Fanti[69a,69b], M. Faraj[67a,67c,u], A. Farbin[8], A. Farilla[75a], E.M. Farina[71a,71b], T. Farooque[107], S. Farrell[18], S.M. Farrington[50], P. Farthouat[36], F. Fassi[35e], P. Fassnacht[36], D. Fassouliotis[9], M. Faucci Giannelli[50], W.J. Fawcett[32], L. Fayard[65], O.L. Fedin[138,p], W. Fedorko[175], M. Feickert[42], L. Feligioni[102], A. Fell[149], C. Feng[60b], E.J. Feng[36], M. Feng[49], M.J. Fenton[57], A.B. Fenyuk[123], J. Ferrando[46], A. Ferrante[173], A. Ferrari[172], P. Ferrari[120], R. Ferrari[71a], D.E. Ferreira de Lima[61b], A. Ferrer[174], D. Ferrere[54], C. Ferretti[106],

JHEP10(2020)005

F. Fiedler[100], A. Filipčič[92], F. Filthaut[119], K.D. Finelli[25], M.C.N. Fiolhais[140a,140c,a], L. Fiorini[174], F. Fischer[114], W.C. Fisher[107], I. Fleck[151], P. Fleischmann[106], R.R.M. Fletcher[137], T. Flick[182], B.M. Flierl[114], L. Flores[137], L.R. Flores Castillo[63a], F.M. Follega[76a,76b], N. Fomin[17], J.H. Foo[167], G.T. Forcolin[76a,76b], A. Formica[145], F.A. Förster[14], A.C. Forti[101], A.G. Foster[21], M.G. Foti[135], D. Fournier[65], H. Fox[90], P. Francavilla[72a,72b], S. Francescato[73a,73b], M. Franchini[23b,23a], S. Franchino[61a], D. Francis[36], L. Franconi[20], M. Franklin[59], A.N. Fray[93], P.M. Freeman[21], B. Freund[110], W.S. Freund[81b], E.M. Freundlich[47], D.C. Frizzell[129], D. Froidevaux[36], J.A. Frost[135], C. Fukunaga[164], E. Fullana Torregrosa[174], E. Fumagalli[55b,55a], T. Fusayasu[116], J. Fuster[174], A. Gabrielli[23b,23a], A. Gabrielli[18], G.P. Gach[84a], S. Gadatsch[54], P. Gadow[115], G. Gagliardi[55b,55a], L.G. Gagnon[110], C. Galea[27b], B. Galhardo[140a], G.E. Gallardo[135], E.J. Gallas[135], B.J. Gallop[144], G. Galster[40], R. Gamboa Goni[93], K.K. Gan[127], S. Ganguly[180], J. Gao[60a], Y. Gao[50], Y.S. Gao[31,m], C. García[174], J.E. García Navarro[174], J.A. García Pascual[15a], C. Garcia-Argos[52], M. Garcia-Sciveres[18], R.W. Gardner[37], N. Garelli[153], S. Gargiulo[52], V. Garonne[134], A. Gaudiello[55b,55a], G. Gaudio[71a], I.L. Gavrilenko[111], A. Gavrilyuk[124], C. Gay[175], G. Gaycken[46], E.N. Gazis[10], A.A. Geanta[27b], C.M. Gee[146], C.N.P. Gee[144], J. Geisen[53], M. Geisen[100], M.P. Geisler[61a], C. Gemme[55b], M.H. Genest[58], C. Geng[106], S. Gentile[73a,73b], S. George[94], T. Geralis[44], L.O. Gerlach[53], P. Gessinger-Befurt[100], G. Gessner[47], S. Ghasemi[151], M. Ghasemi Bostanabad[176], A. Ghosh[65], A. Ghosh[78], B. Giacobbe[23b], S. Giagu[73a,73b], N. Giangiacomi[23b,23a], P. Giannetti[72a], A. Giannini[70a,70b], G. Giannini[14], S.M. Gibson[94], M. Gignac[146], D. Gillberg[34], G. Gilles[182], D.M. Gingrich[3,ax], M.P. Giordani[67a,67c], F.M. Giorgi[23b], P.F. Giraud[145], G. Giugliarelli[67a,67c], D. Giugni[69a], F. Giuli[74a,74b], S. Gkaitatzis[162], I. Gkialas[9,h], E.L. Gkougkousis[14], P. Gkountoumis[10], L.K. Gladilin[113], C. Glasman[99], J. Glatzer[14], P.C.F. Glaysher[46], A. Glazov[46], G.R. Gledhill[132], M. Goblirsch-Kolb[26], D. Godin[110], S. Goldfarb[105], T. Golling[54], D. Golubkov[123], A. Gomes[140a,140b], R. Goncalves Gama[53], R. Gonçalo[140a], G. Gonella[52], L. Gonella[21], A. Gongadze[80], F. Gonnella[21], J.L. Gonski[59], S. González de la Hoz[174], S. Gonzalez-Sevilla[54], G.R. Gonzalvo Rodriguez[174], L. Goossens[36], P.A. Gorbounov[124], H.A. Gordon[29], B. Gorini[36], E. Gorini[68a,68b], A. Gorišek[92], A.T. Goshaw[49], M.I. Gostkin[80], C.A. Gottardo[119], M. Gouighri[35b], D. Goujdami[35c], A.G. Goussiou[148], N. Govender[33c], C. Goy[5], E. Gozani[160], I. Grabowska-Bold[84a], E.C. Graham[91], J. Gramling[171], E. Gramstad[134], S. Grancagnolo[19], M. Grandi[156], V. Gratchev[138], P.M. Gravila[27f], F.G. Gravili[68a,68b], C. Gray[57], H.M. Gray[18], C. Grefe[24], K. Gregersen[97], I.M. Gregor[46], P. Grenier[153], K. Grevtsov[46], C. Grieco[14], N.A. Grieser[129], J. Griffiths[8], A.A. Grillo[146], K. Grimm[31,l], S. Grinstein[14,aa], J.-F. Grivaz[65], S. Groh[100], E. Gross[180], J. Grosse-Knetter[53], Z.J. Grout[95], C. Grud[106], A. Grummer[118], L. Guan[106], W. Guan[181], J. Guenther[36], A. Guerguichon[65], J.G.R. Guerrero Rojas[174], F. Guescini[115], D. Guest[171], R. Gugel[52], T. Guillemin[5], S. Guindon[36], U. Gul[57], J. Guo[60c], W. Guo[106], Y. Guo[60a,t], Z. Guo[102], R. Gupta[46], S. Gurbuz[12c], G. Gustavino[129], M. Guth[52], P. Gutierrez[129], C. Gutschow[95], C. Guyot[145], C. Gwenlan[135], C.B. Gwilliam[91], A. Haas[125], C. Haber[18], H.K. Hadavand[8], N. Haddad[35e], A. Hadef[60a], S. Hageböck[36], M. Haleem[177], J. Haley[130], G. Halladjian[107], G.D. Hallewell[102], K. Hamacher[182], P. Hamal[131], K. Hamano[176], H. Hamdaoui[35e], G.N. Hamity[149], K. Han[60a,z], L. Han[60a], S. Han[15a], Y.F. Han[167], K. Hanagaki[82,x], M. Hance[146], D.M. Handl[114], B. Haney[137], R. Hankache[136], E. Hansen[97], J.B. Hansen[40], J.D. Hansen[40], M.C. Hansen[24], P.H. Hansen[40], E.C. Hanson[101], K. Hara[169], T. Harenberg[182], S. Harkusha[108], P.F. Harrison[178], N.M. Hartmann[114], Y. Hasegawa[150], A. Hasib[50], S. Hassani[145], S. Haug[20], R. Hauser[107], L.B. Havener[39], M. Havranek[142], C.M. Hawkes[21], R.J. Hawkings[36], D. Hayden[107], C. Hayes[155], R.L. Hayes[175], C.P. Hays[135], J.M. Hays[93], H.S. Hayward[91], S.J. Haywood[144], F. He[60a], M.P. Heath[50], V. Hedberg[97], L. Heelan[8], S. Heer[24], K.K. Heidegger[52], W.D. Heidorn[79], J. Heilman[34], S. Heim[46], T. Heim[18], B. Heinemann[46,at], J.J. Heinrich[132], L. Heinrich[36],

JHEP10(2020)005

C. Heinz[56], J. Hejbal[141], L. Helary[61b], A. Held[175], S. Hellesund[134], C.M. Helling[146], S. Hellman[45a,45b], C. Helsens[36], R.C.W. Henderson[90], Y. Heng[181], S. Henkelmann[175], A.M. Henriques Correia[36], G.H. Herbert[19], H. Herde[26], V. Herget[177], Y. Hernández Jiménez[33e], H. Herr[100], M.G. Herrmann[114], T. Herrmann[48], G. Herten[52], R. Hertenberger[114], L. Hervas[36], T.C. Herwig[137], G.G. Hesketh[95], N.P. Hessey[168a], A. Higashida[163], S. Higashino[82], E. Higón-Rodriguez[174], K. Hildebrand[37], E. Hill[176], J.C. Hill[32], K.K. Hill[29], K.H. Hiller[46], S.J. Hillier[21], M. Hils[48], I. Hinchliffe[18], F. Hinterkeuser[24], M. Hirose[133], S. Hirose[52], D. Hirschbuehl[182], B. Hiti[92], O. Hladik[141], D.R. Hlaluku[33e], X. Hoad[50], J. Hobbs[155], N. Hod[180], M.C. Hodgkinson[149], A. Hoecker[36], F. Hoenig[114], D. Hohn[52], D. Hohov[65], T.R. Holmes[37], M. Holzbock[114], L.B.A.H. Hommels[32], S. Honda[169], T.M. Hong[139], A. Hönle[115], B.H. Hooberman[173], W.H. Hopkins[6], Y. Horii[117], P. Horn[48], L.A. Horyn[37], S. Hou[158], A. Hoummada[35a], J. Howarth[101], J. Hoya[89], M. Hrabovsky[131], J. Hrdinka[77], I. Hristova[19], J. Hrivnac[65], A. Hrynevich[109], T. Hryn'ova[5], P.J. Hsu[64], S.-C. Hsu[148], Q. Hu[29], S. Hu[60c], D.P. Huang[95], Y. Huang[60a], Y. Huang[15a], Z. Hubacek[142], F. Hubaut[102], M. Huebner[24], F. Huegging[24], T.B. Huffman[135], M. Huhtinen[36], R.F.H. Hunter[34], P. Huo[155], A.M. Hupe[34], N. Huseynov[80,ah], J. Huston[107], J. Huth[59], R. Hyneman[106], S. Hyrych[28a], G. Iacobucci[54], G. Iakovidis[29], I. Ibragimov[151], L. Iconomidou-Fayard[65], Z. Idrissi[35e], P. Iengo[36], R. Ignazzi[40], O. Igonkina[120,ac,*], R. Iguchi[163], T. Iizawa[54], Y. Ikegami[82], M. Ikeno[82], D. Iliadis[162], N. Ilic[119,167,af], F. Iltzsche[48], G. Introzzi[71a,71b], M. Iodice[75a], K. Iordanidou[168a], V. Ippolito[73a,73b], M.F. Isacson[172], M. Ishino[163], W. Islam[130], C. Issever[135], S. Istin[160], F. Ito[169], J.M. Iturbe Ponce[63a], R. Iuppa[76a,76b], A. Ivina[180], H. Iwasaki[82], J.M. Izen[43], V. Izzo[70a], P. Jacka[141], P. Jackson[1], R.M. Jacobs[24], B.P. Jaeger[152], V. Jain[2], G. Jäkel[182], K.B. Jakobi[100], K. Jakobs[52], S. Jakobsen[77], T. Jakoubek[141], J. Jamieson[57], K.W. Janas[84a], R. Jansky[54], J. Janssen[24], M. Janus[53], P.A. Janus[84a], G. Jarlskog[97], N. Javadov[80,ah], T. Javůrek[36], M. Javurkova[52], F. Jeanneau[145], L. Jeanty[132], J. Jejelava[159a,ai], A. Jelinskas[178], P. Jenni[52,b], J. Jeong[46], N. Jeong[46], S. Jézéquel[5], H. Ji[181], J. Jia[155], H. Jiang[79], Y. Jiang[60a], Z. Jiang[153,q], S. Jiggins[52], F.A. Jimenez Morales[38], J. Jimenez Pena[115], S. Jin[15c], A. Jinaru[27b], O. Jinnouchi[165], H. Jivan[33e], P. Johansson[149], K.A. Johns[7], C.A. Johnson[66], K. Jon-And[45a,45b], R.W.L. Jones[90], S.D. Jones[156], S. Jones[7], T.J. Jones[91], J. Jongmanns[61a], P.M. Jorge[140a], J. Jovicevic[36], X. Ju[18], J.J. Junggeburth[115], A. Juste Rozas[14,aa], A. Kaczmarska[85], M. Kado[73a,73b], H. Kagan[127], M. Kagan[153], C. Kahra[100], T. Kaji[179], E. Kajomovitz[160], C.W. Kalderon[97], A. Kaluza[100], A. Kamenshchikov[123], M. Kaneda[163], L. Kanjir[92], Y. Kano[163], V.A. Kantserov[112], J. Kanzaki[82], L.S. Kaplan[181], D. Kar[33e], K. Karava[135], M.J. Kareem[168b], S.N. Karpov[80], Z.M. Karpova[80], V. Kartvelishvili[90], A.N. Karyukhin[123], L. Kashif[181], R.D. Kass[127], A. Kastanas[45a,45b], C. Kato[60d,60c], J. Katzy[46], K. Kawade[150], K. Kawagoe[88], T. Kawaguchi[117], T. Kawamoto[163], G. Kawamura[53], E.F. Kay[176], V.F. Kazanin[122b,122a], R. Keeler[176], R. Kehoe[42], J.S. Keller[34], E. Kellermann[97], D. Kelsey[156], J.J. Kempster[21], J. Kendrick[21], O. Kepka[141], S. Kersten[182], B.P. Kerševan[92], S. Ketabchi Haghighat[167], M. Khader[173], F. Khalil-Zada[13], M. Khandoga[145], A. Khanov[130], A.G. Kharlamov[122b,122a], T. Kharlamova[122b,122a], E.E. Khoda[175], A. Khodinov[166], T.J. Khoo[54], E. Khramov[80], J. Khubua[159b], S. Kido[83], M. Kiehn[54], C.R. Kilby[94], Y.K. Kim[37], N. Kimura[95], O.M. Kind[19], B.T. King[91,*], D. Kirchmeier[48], J. Kirk[144], A.E. Kiryunin[115], T. Kishimoto[163], D.P. Kisliuk[167], V. Kitali[46], O. Kivernyk[5], T. Klapdor-Kleingrothaus[52], M. Klassen[61a], M.H. Klein[106], M. Klein[91], U. Klein[91], K. Kleinknecht[100], P. Klimek[121], A. Klimentov[29], T. Klingl[24], T. Klioutchnikova[36], F.F. Klitzner[114], P. Kluit[120], S. Kluth[115], E. Kneringer[77], E.B.F.G. Knoops[102], A. Knue[52], D. Kobayashi[88], T. Kobayashi[163], M. Kobel[48], M. Kocian[153], P. Kodys[143], P.T. Koenig[24], T. Koffas[34], N.M. Köhler[36], T. Koi[153], M. Kolb[61b], I. Koletsou[5], T. Komarek[131], T. Kondo[82], N. Kondrashova[60c], K. Köneke[52], A.C. König[119], T. Kono[126], R. Konoplich[125,ao], V. Konstantinides[95], N. Konstantinidis[95], B. Konya[97],

JHEP10(2020)005

R. Kopeliansky[66], S. Koperny[84a], K. Korcyl[85], K. Kordas[162], G. Koren[161], A. Korn[95], I. Korolkov[14], E.V. Korolkova[149], N. Korotkova[113], O. Kortner[115], S. Kortner[115], T. Kosek[143], V.V. Kostyukhin[166], A. Kotwal[49], A. Koulouris[10], A. Kourkoumeli-Charalampidi[71a,71b], C. Kourkoumelis[9], E. Kourlitis[149], V. Kouskoura[29], A.B. Kowalewska[85], R. Kowalewski[176], C. Kozakai[163], W. Kozanecki[145], A.S. Kozhin[123], V.A. Kramarenko[113], G. Kramberger[92], D. Krasnopevtsev[60a], M.W. Krasny[136], A. Krasznahorkay[36], D. Krauss[115], J.A. Kremer[84a], J. Kretzschmar[91], P. Krieger[167], F. Krieter[114], A. Krishnan[61b], K. Krizka[18], K. Kroeninger[47], H. Kroha[115], J. Kroll[141], J. Kroll[137], J. Krstic[16], U. Kruchonak[80], H. Krüger[24], N. Krumnack[79], M.C. Kruse[49], J.A. Krzysiak[85], T. Kubota[105], O. Kuchinskaia[166], S. Kuday[4b], J.T. Kuechler[46], S. Kuehn[36], A. Kugel[61a], T. Kuhl[46], V. Kukhtin[80], R. Kukla[102], Y. Kulchitsky[108,al], S. Kuleshov[147d], Y.P. Kulinich[173], M. Kuna[58], T. Kunigo[86], A. Kupco[141], T. Kupfer[47], O. Kuprash[52], H. Kurashige[83], L.L. Kurchaninov[168a], Y.A. Kurochkin[108], A. Kurova[112], M.G. Kurth[15a,15d], E.S. Kuwertz[36], M. Kuze[165], A.K. Kvam[148], J. Kvita[131], T. Kwan[104], A. La Rosa[115], L. La Rotonda[41b,41a], F. La Ruffa[41b,41a], C. Lacasta[174], F. Lacava[73a,73b], D.P.J. Lack[101], H. Lacker[19], D. Lacour[136], E. Ladygin[80], R. Lafaye[5], B. Laforge[136], T. Lagouri[33e], S. Lai[53], S. Lammers[66], W. Lampl[7], C. Lampoudis[162], E. Lançon[29], U. Landgraf[52], M.P.J. Landon[93], M.C. Lanfermann[54], V.S. Lang[46], J.C. Lange[53], R.J. Langenberg[36], A.J. Lankford[171], F. Lanni[29], K. Lantzsch[24], A. Lanza[71a], A. Lapertosa[55b,55a], S. Laplace[136], J.F. Laporte[145], T. Lari[69a], F. Lasagni Manghi[23b,23a], M. Lassnig[36], T.S. Lau[63a], A. Laudrain[65], A. Laurier[34], M. Lavorgna[70a,70b], S.D. Lawlor[94], M. Lazzaroni[69a,69b], B. Le[105], E. Le Guirriec[102], M. LeBlanc[7], T. LeCompte[6], F. Ledroit-Guillon[58], A.C.A. Lee[95], C.A. Lee[29], G.R. Lee[17], L. Lee[59], S.C. Lee[158], S.J. Lee[34], B. Lefebvre[168a], M. Lefebvre[176], F. Legger[114], C. Leggett[18], K. Lehmann[152], N. Lehmann[182], G. Lehmann Miotto[36], W.A. Leight[46], A. Leisos[162,y], M.A.L. Leite[81d], C.E. Leitgeb[114], R. Leitner[143], D. Lellouch[180,*], K.J.C. Leney[42], T. Lenz[24], B. Lenzi[36], R. Leone[7], S. Leone[72a], C. Leonidopoulos[50], A. Leopold[136], G. Lerner[156], C. Leroy[110], R. Les[167], C.G. Lester[32], M. Levchenko[138], J. Levêque[5], D. Levin[106], L.J. Levinson[180], D.J. Lewis[21], B. Li[15b], B. Li[106], C-Q. Li[60a], F. Li[60c], H. Li[60a], H. Li[60b], J. Li[60c], K. Li[153], L. Li[60c], M. Li[15a,15d], Q. Li[15a,15d], Q.Y. Li[60a], S. Li[60d,60c], X. Li[46], Y. Li[46], Z. Li[60b], Z. Liang[15a], B. Liberti[74a], A. Liblong[167], K. Lie[63c], C.Y. Lin[32], K. Lin[107], T.H. Lin[100], R.A. Linck[66], J.H. Lindon[21], A.L. Lionti[54], E. Lipeles[137], A. Lipniacka[17], M. Lisovyi[61b], T.M. Liss[173,av], A. Lister[175], A.M. Litke[146], J.D. Little[8], B. Liu[79], B.L. Liu[6], H.B. Liu[29], H. Liu[106], J.B. Liu[60a], J.K.K. Liu[135], K. Liu[136], M. Liu[60a], P. Liu[18], Y. Liu[15a,15d], Y.L. Liu[106], Y.W. Liu[60a], M. Livan[71a,71b], A. Lleres[58], J. Llorente Merino[152], S.L. Lloyd[93], C.Y. Lo[63b], F. Lo Sterzo[42], E.M. Lobodzinska[46], P. Loch[7], S. Loffredo[74a,74b], T. Lohse[19], K. Lohwasser[149], M. Lokajicek[141], J.D. Long[173], R.E. Long[90], L. Longo[36], K.A. Looper[127], J.A. Lopez[147d], I. Lopez Paz[101], A. Lopez Solis[149], J. Lorenz[114], N. Lorenzo Martinez[5], M. Losada[22a], P.J. Lösel[114], A. Lösle[52], X. Lou[46], X. Lou[15a], A. Lounis[65], J. Love[6], P.A. Love[90], J.J. Lozano Bahilo[174], M. Lu[60a], Y.J. Lu[64], H.J. Lubatti[148], C. Luci[73a,73b], A. Lucotte[58], C. Luedtke[52], F. Luehring[66], I. Luise[136], L. Luminari[73a], B. Lund-Jensen[154], M.S. Lutz[103], D. Lynn[29], R. Lysak[141], E. Lytken[97], F. Lyu[15a], V. Lyubushkin[80], T. Lyubushkina[80], H. Ma[29], L.L. Ma[60b], Y. Ma[60b], G. Maccarrone[51], A. Macchiolo[115], C.M. Macdonald[149], J. Machado Miguens[137], D. Madaffari[174], R. Madar[38], W.F. Mader[48], N. Madysa[48], J. Maeda[83], S. Maeland[17], T. Maeno[29], M. Maerker[48], A.S. Maevskiy[113], V. Magerl[52], N. Magini[79], D.J. Mahon[39], C. Maidantchik[81b], T. Maier[114], A. Maio[140a,140b,140d], K. Maj[84a], O. Majersky[28a], S. Majewski[132], Y. Makida[82], N. Makovec[65], B. Malaescu[136], Pa. Malecki[85], V.P. Maleev[138], F. Malek[58], U. Mallik[78], D. Malon[6], C. Malone[32], S. Maltezos[10], S. Malyukov[80], J. Mamuzic[174], G. Mancini[51], I. Mandić[92], L. Manhaes de Andrade Filho[81a], I.M. Maniatis[162], J. Manjarres Ramos[48], K.H. Mankinen[97], A. Mann[114], A. Manousos[77], B. Mansoulie[145], I. Manthos[162], S. Manzoni[120], A. Marantis[162],

JHEP10(2020)005

G. Marceca[30], L. Marchese[135], G. Marchiori[136], M. Marcisovsky[141], C. Marcon[97], C.A. Marin Tobon[36], M. Marjanovic[129], Z. Marshall[18], M.U.F. Martensson[172], S. Marti-Garcia[174], C.B. Martin[127], T.A. Martin[178], V.J. Martin[50], B. Martin dit Latour[17], L. Martinelli[75a,75b], M. Martinez[14,aa], V.I. Martinez Outschoorn[103], S. Martin-Haugh[144], V.S. Martoiu[27b], A.C. Martyniuk[95], A. Marzin[36], S.R. Maschek[115], L. Masetti[100], T. Mashimo[163], R. Mashinistov[111], J. Masik[101], A.L. Maslennikov[122b,122a], L. Massa[74a,74b], P. Massarotti[70a,70b], P. Mastrandrea[72a,72b], A. Mastroberardino[41b,41a], T. Masubuchi[163], D. Matakias[10], A. Matic[114], P. Mättig[24], J. Maurer[27b], B. Maček[92], D.A. Maximov[122b,122a], R. Mazini[158], I. Maznas[162], S.M. Mazza[146], S.P. Mc Kee[106], T.G. McCarthy[115], W.P. McCormack[18], E.F. McDonald[105], J.A. Mcfayden[36], G. Mchedlidze[159b], M.A. McKay[42], K.D. McLean[176], S.J. McMahon[144], P.C. McNamara[105], C.J. McNicol[178], R.A. McPherson[176,af], J.E. Mdhluli[33e], Z.A. Meadows[103], S. Meehan[36], T. Megy[52], S. Mehlhase[114], A. Mehta[91], T. Meideck[58], B. Meirose[43], D. Melini[174], B.R. Mellado Garcia[33e], J.D. Mellenthin[53], M. Melo[28a], F. Meloni[46], A. Melzer[24], S.B. Menary[101], E.D. Mendes Gouveia[140a,140e], L. Meng[36], X.T. Meng[106], S. Menke[115], E. Meoni[41b,41a], S. Mergelmeyer[19], S.A.M. Merkt[139], C. Merlassino[20], P. Mermod[54], L. Merola[70a,70b], C. Meroni[69a], O. Meshkov[113,111], J.K.R. Meshreki[151], A. Messina[73a,73b], J. Metcalfe[6], A.S. Mete[171], C. Meyer[66], J. Meyer[160], J-P. Meyer[145], H. Meyer Zu Theenhausen[61a], F. Miano[156], M. Michetti[19], R.P. Middleton[144], L. Mijović[50], G. Mikenberg[180], M. Mikestikova[141], M. Mikuž[92], H. Mildner[149], M. Milesi[105], A. Milic[167], D.A. Millar[93], D.W. Miller[37], A. Milov[180], D.A. Milstead[45a,45b], R.A. Mina[153,q], A.A. Minaenko[123], M. Miñano Moya[174], I.A. Minashvili[159b], A.I. Mincer[125], B. Mindur[84a], M. Mineev[80], Y. Minegishi[163], L.M. Mir[14], A. Mirto[68a,68b], K.P. Mistry[137], T. Mitani[179], J. Mitrevski[114], V.A. Mitsou[174], M. Mittal[60c], O. Miu[167], A. Miucci[20], P.S. Miyagawa[149], A. Mizukami[82], J.U. Mjörnmark[97], T. Mkrtchyan[184], M. Mlynarikova[143], T. Moa[45a,45b], K. Mochizuki[110], P. Mogg[52], S. Mohapatra[39], R. Moles-Valls[24], M.C. Mondragon[107], K. Mönig[46], J. Monk[40], E. Monnier[102], A. Montalbano[152], J. Montejo Berlingen[36], M. Montella[95], F. Monticelli[89], S. Monzani[69a], N. Morange[65], D. Moreno[22a], M. Moreno Llácer[36], C. Moreno Martinez[14], P. Morettini[55b], M. Morgenstern[120], S. Morgenstern[48], D. Mori[152], M. Morii[59], M. Morinaga[179], V. Morisbak[134], A.K. Morley[36], G. Mornacchi[36], A.P. Morris[95], L. Morvaj[155], P. Moschovakos[36], B. Moser[120], M. Mosidze[159b], T. Moskalets[145], H.J. Moss[149], J. Moss[31,n], E.J.W. Moyse[103], S. Muanza[102], J. Mueller[139], R.S.P. Mueller[114], D. Muenstermann[90], G.A. Mullier[97], J.L. Munoz Martinez[14], F.J. Munoz Sanchez[101], P. Murin[28b], W.J. Murray[178,144], A. Murrone[69a,69b], M. Muškinja[18], C. Mwewa[33a], A.G. Myagkov[123,ap], J. Myers[132], M. Myska[142], B.P. Nachman[18], O. Nackenhorst[47], A.Nag Nag[48], K. Nagai[135], K. Nagano[82], Y. Nagasaka[62], M. Nagel[52], J.L. Nagle[29], E. Nagy[102], A.M. Nairz[36], Y. Nakahama[117], K. Nakamura[82], T. Nakamura[163], I. Nakano[128], H. Nanjo[133], F. Napolitano[61a], R.F. Naranjo Garcia[46], R. Narayan[42], I. Naryshkin[138], T. Naumann[46], G. Navarro[22a], H.A. Neal[106,*], P.Y. Nechaeva[111], F. Nechansky[46], T.J. Neep[21], A. Negri[71a,71b], M. Negrini[23b], C. Nellist[53], M.E. Nelson[135], S. Nemecek[141], P. Nemethy[125], M. Nessi[36,d], M.S. Neubauer[173], M. Neumann[182], P.R. Newman[21], Y.S. Ng[19], Y.W.Y. Ng[171], B. Ngair[35e], H.D.N. Nguyen[102], T. Nguyen Manh[110], E. Nibigira[38], R.B. Nickerson[135], R. Nicolaidou[145], D.S. Nielsen[40], J. Nielsen[146], N. Nikiforou[11], V. Nikolaenko[123,ap], I. Nikolic-Audit[136], K. Nikolopoulos[21], P. Nilsson[29], H.R. Nindhito[54], Y. Ninomiya[82], A. Nisati[73a], N. Nishu[60c], R. Nisius[115], I. Nitsche[47], T. Nitta[179], T. Nobe[163], Y. Noguchi[86], I. Nomidis[136], M.A. Nomura[29], M. Nordberg[36], N. Norjoharuddeen[135], T. Novak[92], O. Novgorodova[48], R. Novotny[142], L. Nozka[131], K. Ntekas[171], E. Nurse[95], F.G. Oakham[34,ax], H. Oberlack[115], J. Ocariz[136], A. Ochi[83], I. Ochoa[39], J.P. Ochoa-Ricoux[147a], K. O'Connor[26], S. Oda[88], S. Odaka[82], S. Oerdek[53], A. Ogrodnik[84a], A. Oh[101], S.H. Oh[49], C.C. Ohm[154], H. Oide[165], M.L. Ojeda[167], H. Okawa[169], Y. Okazaki[86], Y. Okumura[163], T. Okuyama[82], A. Olariu[27b], L.F. Oleiro Seabra[140a],

JHEP10(2020)005

S.A. Olivares Pino[147a], D. Oliveira Damazio[29], J.L. Oliver[1], M.J.R. Olsson[171], A. Olszewski[85], J. Olszowska[85], D.C. O'Neil[152], A.P. O'neill[135], A. Onofre[140a,140e], P.U.E. Onyisi[11], H. Oppen[134], M.J. Oreglia[37], G.E. Orellana[89], D. Orestano[75a,75b], N. Orlando[14], R.S. Orr[167], V. O'Shea[57], R. Ospanov[60a], G. Otero y Garzon[30], H. Otono[88], P.S. Ott[61a], M. Ouchrif[35d], J. Ouellette[29], F. Ould-Saada[134], A. Ouraou[145], Q. Ouyang[15a], M. Owen[57], R.E. Owen[21], V.E. Ozcan[12c], N. Ozturk[8], J. Pacalt[131], H.A. Pacey[32], K. Pachal[49], A. Pacheco Pages[14], C. Padilla Aranda[14], S. Pagan Griso[18], M. Paganini[183], G. Palacino[66], S. Palazzo[50], S. Palestini[36], M. Palka[84b], D. Pallin[38], I. Panagoulias[10], C.E. Pandini[36], J.G. Panduro Vazquez[94], P. Pani[46], G. Panizzo[67a,67c], L. Paolozzi[54], C. Papadatos[110], K. Papageorgiou[9,h], S. Parajuli[43], A. Paramonov[6], D. Paredes Hernandez[63b], S.R. Paredes Saenz[135], B. Parida[166], T.H. Park[167], A.J. Parker[31], M.A. Parker[32], F. Parodi[55b,55a], E.W. Parrish[121], J.A. Parsons[39], U. Parzefall[52], L. Pascual Dominguez[136], V.R. Pascuzzi[167], J.M.P. Pasner[146], E. Pasqualucci[73a], S. Passaggio[55b], F. Pastore[94], P. Pasuwan[45a,45b], S. Pataraia[100], J.R. Pater[101], A. Pathak[181,j], T. Pauly[36], B. Pearson[115], M. Pedersen[134], L. Pedraza Diaz[119], R. Pedro[140a], T. Peiffer[53], S.V. Peleganchuk[122b,122a], O. Penc[141], H. Peng[60a], B.S. Peralva[81a], M.M. Perego[65], A.P. Pereira Peixoto[140a], D.V. Perepelitsa[29], F. Peri[19], L. Perini[69a,69b], H. Pernegger[36], S. Perrella[70a,70b], K. Peters[46], R.F.Y. Peters[101], B.A. Petersen[36], T.C. Petersen[40], E. Petit[102], A. Petridis[1], C. Petridou[162], P. Petroff[65], M. Petrov[135], F. Petrucci[75a,75b], M. Pettee[183], N.E. Pettersson[103], K. Petukhova[143], A. Peyaud[145], R. Pezoa[147d], L. Pezzotti[71a,71b], T. Pham[105], F.H. Phillips[107], P.W. Phillips[144], M.W. Phipps[173], G. Piacquadio[155], E. Pianori[18], A. Picazio[103], R.H. Pickles[101], R. Piegaia[30], D. Pietreanu[27b], J.E. Pilcher[37], A.D. Pilkington[101], M. Pinamonti[74a,74b], J.L. Pinfold[3], M. Pitt[161], L. Pizzimento[74a,74b], M.-A. Pleier[29], V. Pleskot[143], E. Plotnikova[80], P. Podberezko[122b,122a], R. Poettgen[97], R. Poggi[54], L. Poggioli[65], I. Pogrebnyak[107], D. Pohl[24], I. Pokharel[53], G. Polesello[71a], A. Poley[18], A. Policicchio[73a,73b], R. Polifka[143], A. Polini[23b], C.S. Pollard[46], V. Polychronakos[29], D. Ponomarenko[112], L. Pontecorvo[36], S. Popa[27a], G.A. Popeneciu[27d], L. Portales[5], D.M. Portillo Quintero[58], S. Pospisil[142], K. Potamianos[46], I.N. Potrap[80], C.J. Potter[32], H. Potti[11], T. Poulsen[97], J. Poveda[36], T.D. Powell[149], G. Pownall[46], M.E. Pozo Astigarraga[36], P. Pralavorio[102], S. Prell[79], D. Price[101], M. Primavera[68a], S. Prince[104], M.L. Proffitt[148], N. Proklova[112], K. Prokofiev[63c], F. Prokoshin[80], S. Protopopescu[29], J. Proudfoot[6], M. Przybycien[84a], D. Pudzha[138], A. Puri[173], P. Puzo[65], J. Qian[106], Y. Qin[101], A. Quadt[53], M. Queitsch-Maitland[46], A. Qureshi[1], M. Racko[28a], P. Rados[105], F. Ragusa[69a,69b], G. Rahal[98], J.A. Raine[54], S. Rajagopalan[29], A. Ramirez Morales[93], K. Ran[15a,15d], T. Rashid[65], S. Raspopov[5], D.M. Rauch[46], F. Rauscher[114], S. Rave[100], B. Ravina[149], I. Ravinovich[180], J.H. Rawling[101], M. Raymond[36], A.L. Read[134], N.P. Readioff[58], M. Reale[68a,68b], D.M. Rebuzzi[71a,71b], A. Redelbach[177], G. Redlinger[29], K. Reeves[43], L. Rehnisch[19], J. Reichert[137], D. Reikher[161], A. Reiss[100], A. Rej[151], C. Rembser[36], M. Renda[27b], M. Rescigno[73a], S. Resconi[69a], E.D. Resseguie[137], S. Rettie[175], E. Reynolds[21], O.L. Rezanova[122b,122a], P. Reznicek[143], E. Ricci[76a,76b], R. Richter[115], S. Richter[46], E. Richter-Was[84b], O. Ricken[24], M. Ridel[136], P. Rieck[115], C.J. Riegel[182], O. Rifki[46], M. Rijssenbeek[155], A. Rimoldi[71a,71b], M. Rimoldi[46], L. Rinaldi[23b], G. Ripellino[154], I. Riu[14], J.C. Rivera Vergara[176], F. Rizatdinova[130], E. Rizvi[93], C. Rizzi[36], R.T. Roberts[101], S.H. Robertson[104,af], M. Robin[46], D. Robinson[32], J.E.M. Robinson[46], C.M. Robles Gajardo[147d], A. Robson[57], A. Rocchi[74a,74b], E. Rocco[100], C. Roda[72a,72b], S. Rodriguez Bosca[174], A. Rodriguez Perez[14], D. Rodriguez Rodriguez[174], A.M. Rodríguez Vera[168b], S. Roe[36], O. Røhne[134], R. Röhrig[115], C.P.A. Roland[66], J. Roloff[59], A. Romaniouk[112], M. Romano[23b,23a], N. Rompotis[91], M. Ronzani[125], L. Roos[136], S. Rosati[73a], K. Rosbach[52], G. Rosin[103], B.J. Rosser[137], E. Rossi[46], E. Rossi[75a,75b], E. Rossi[70a,70b], L.P. Rossi[55b], L. Rossini[69a,69b], R. Rosten[14], M. Rotaru[27b], J. Rothberg[148], D. Rousseau[65], G. Rovelli[71a,71b], A. Roy[11], D. Roy[33e],

JHEP10(2020)005

A. Rozanov[102], Y. Rozen[160], X. Ruan[33e], F. Rubbo[153], F. Rühr[52], A. Ruiz-Martinez[174], A. Rummler[36], Z. Rurikova[52], N.A. Rusakovich[80], H.L. Russell[104], L. Rustige[38,47], J.P. Rutherfoord[7], E.M. Rüttinger[149], M. Rybar[39], G. Rybkin[65], E.B. Rye[134], A. Ryzhov[123], P. Sabatini[53], G. Sabato[120], S. Sacerdoti[65], H.F-W. Sadrozinski[146], R. Sadykov[80], F. Safai Tehrani[73a], B. Safarzadeh Samani[156], P. Saha[121], S. Saha[104], M. Sahinsoy[61a], A. Sahu[182], M. Saimpert[46], M. Saito[163], T. Saito[163], H. Sakamoto[163], A. Sakharov[125,ao], D. Salamani[54], G. Salamanna[75a,75b], J.E. Salazar Loyola[147d], P.H. Sales De Bruin[172], A. Salnikov[153], J. Salt[174], D. Salvatore[41b,41a], F. Salvatore[156], A. Salvucci[63a,63b,63c], A. Salzburger[36], J. Samarati[36], D. Sammel[52], D. Sampsonidis[162], D. Sampsonidou[162], J. Sánchez[174], A. Sanchez Pineda[67a,67c], H. Sandaker[134], C.O. Sander[46], I.G. Sanderswood[90], M. Sandhoff[182], C. Sandoval[22a], D.P.C. Sankey[144], M. Sannino[55b,55a], Y. Sano[117], A. Sansoni[51], C. Santoni[38], H. Santos[140a,140b], S.N. Santpur[18], A. Santra[174], A. Sapronov[80], J.G. Saraiva[140a,140d], O. Sasaki[82], K. Sato[169], F. Sauerburger[52], E. Sauvan[5], P. Savard[167,ax], N. Savic[115], R. Sawada[163], C. Sawyer[144], L. Sawyer[96,am], C. Sbarra[23b], A. Sbrizzi[23a], T. Scanlon[95], J. Schaarschmidt[148], P. Schacht[115], B.M. Schachtner[114], D. Schaefer[37], L. Schaefer[137], J. Schaeffer[100], S. Schaepe[36], U. Schäfer[100], A.C. Schaffer[65], D. Schaile[114], R.D. Schamberger[155], N. Scharmberg[101], V.A. Schegelsky[138], D. Scheirich[143], F. Schenck[19], M. Schernau[171], C. Schiavi[55b,55a], S. Schier[146], L.K. Schildgen[24], Z.M. Schillaci[26], E.J. Schioppa[36], M. Schioppa[41b,41a], K.E. Schleicher[52], S. Schlenker[36], K.R. Schmidt-Sommerfeld[115], K. Schmieden[36], C. Schmitt[100], S. Schmitt[46], S. Schmitz[100], J.C. Schmoeckel[46], U. Schnoor[52], L. Schoeffel[145], A. Schoening[61b], P.G. Scholer[52], E. Schopf[135], M. Schott[100], J.F.P. Schouwenberg[119], J. Schovancova[36], S. Schramm[54], F. Schroeder[182], A. Schulte[100], H-C. Schultz-Coulon[61a], M. Schumacher[52], B.A. Schumm[146], Ph. Schune[145], A. Schwartzman[153], T.A. Schwarz[106], Ph. Schwemling[145], R. Schwienhorst[107], A. Sciandra[146], G. Sciolla[26], M. Scodeggio[46], M. Scornajenghi[41b,41a], F. Scuri[72a], F. Scutti[105], L.M. Scyboz[115], C.D. Sebastiani[73a,73b], P. Seema[19], S.C. Seidel[118], A. Seiden[146], B.D. Seidlitz[29], T. Seiss[37], J.M. Seixas[81b], G. Sekhniaidze[70a], K. Sekhon[106], S.J. Sekula[42], N. Semprini-Cesari[23b,23a], S. Sen[49], S. Senkin[38], C. Serfon[77], L. Serin[65], L. Serkin[67a,67b], M. Sessa[60a], H. Severini[129], T. Šfiligoj[92], F. Sforza[55b,55a], A. Sfyrla[54], E. Shabalina[53], J.D. Shahinian[146], N.W. Shaikh[45a,45b], D. Shaked Renous[180], L.Y. Shan[15a], R. Shang[173], J.T. Shank[25], M. Shapiro[18], A. Sharma[135], A.S. Sharma[1], P.B. Shatalov[124], K. Shaw[156], S.M. Shaw[101], A. Shcherbakova[138], M. Shehade[180], Y. Shen[129], N. Sherafati[34], A.D. Sherman[25], P. Sherwood[95], L. Shi[158,au], S. Shimizu[82], C.O. Shimmin[183], Y. Shimogama[179], M. Shimojima[116], I.P.J. Shipsey[135], S. Shirabe[88], M. Shiyakova[80,ad], J. Shlomi[180], A. Shmeleva[111], M.J. Shochet[37], J. Shojaii[105], D.R. Shope[129], S. Shrestha[127], E.M. Shrif[33e], E. Shulga[180], P. Sicho[141], A.M. Sickles[173], P.E. Sidebo[154], E. Sideras Haddad[33e], O. Sidiropoulou[36], A. Sidoti[23b,23a], F. Siegert[48], Dj. Sijacki[16], M.Jr. Silva[181], M.V. Silva Oliveira[81a], S.B. Silverstein[45a], S. Simion[65], E. Simioni[100], R. Simoniello[100], S. Simsek[12b], P. Sinervo[167], V. Sinetckii[113,111], N.B. Sinev[132], M. Sioli[23b,23a], I. Siral[106], S.Yu. Sivoklokov[113], J. Sjölin[45a,45b], E. Skorda[97], P. Skubic[129], M. Slawinska[85], K. Sliwa[170], R. Slovak[143], V. Smakhtin[180], B.H. Smart[144], J. Smiesko[28a], N. Smirnov[112], S.Yu. Smirnov[112], Y. Smirnov[112], L.N. Smirnova[113,v], O. Smirnova[97], J.W. Smith[53], M. Smizanska[90], K. Smolek[142], A. Smykiewicz[85], A.A. Snesarev[111], H.L. Snoek[120], I.M. Snyder[132], S. Snyder[29], R. Sobie[176,af], A. Soffer[161], A. Søgaard[50], F. Sohns[53], C.A. Solans Sanchez[36], E.Yu. Soldatov[112], U. Soldevila[174], A.A. Solodkov[123], A. Soloshenko[80], O.V. Solovyanov[123], V. Solovyev[138], P. Sommer[149], H. Son[170], W. Song[144], W.Y. Song[168b], A. Sopczak[142], F. Sopkova[28b], C.L. Sotiropoulou[72a,72b], S. Sottocornola[71a,71b], R. Soualah[67a,67c,g], A.M. Soukharev[122b,122a], D. South[46], S. Spagnolo[68a,68b], M. Spalla[115], M. Spangenberg[178], F. Spanò[94], D. Sperlich[52], T.M. Spieker[61a], R. Spighi[23b], G. Spigo[36], M. Spina[156], D.P. Spiteri[57], M. Spousta[143], A. Stabile[69a,69b], B.L. Stamas[121], R. Stamen[61a], M. Stamenkovic[120],

JHEP10(2020)005

E. Stanecka[85], B. Stanislaus[135], M.M. Stanitzki[46], M. Stankaityte[135], B. Stapf[120], E.A. Starchenko[123], G.H. Stark[146], J. Stark[58], S.H. Stark[40], P. Staroba[141], P. Starovoitov[61a], S. Stärz[104], R. Staszewski[85], G. Stavropoulos[44], M. Stegler[46], P. Steinberg[29], A.L. Steinhebel[132], B. Stelzer[152], H.J. Stelzer[139], O. Stelzer-Chilton[168a], H. Stenzel[56], T.J. Stevenson[156], G.A. Stewart[36], M.C. Stockton[36], G. Stoicea[27b], M. Stolarski[140a], S. Stonjek[115], A. Straessner[48], J. Strandberg[154], S. Strandberg[45a,45b], M. Strauss[129], P. Strizenec[28b], R. Ströhmer[177], D.M. Strom[132], R. Stroynowski[42], A. Strubig[50], S.A. Stucci[29], B. Stugu[17], J. Stupak[129], N.A. Styles[46], D. Su[153], S. Suchek[61a], V.V. Sulin[111], M.J. Sullivan[91], D.M.S. Sultan[54], S. Sultansoy[4c], T. Sumida[86], S. Sun[106], X. Sun[3], K. Suruliz[156], C.J.E. Suster[157], M.R. Sutton[156], S. Suzuki[82], M. Svatos[141], M. Swiatlowski[37], S.P. Swift[2], T. Swirski[177], A. Sydorenko[100], I. Sykora[28a], M. Sykora[143], T. Sykora[143], D. Ta[100], K. Tackmann[46,ab], J. Taenzer[161], A. Taffard[171], R. Tafirout[168a], H. Takai[29], R. Takashima[87], K. Takeda[83], T. Takeshita[150], E.P. Takeva[50], Y. Takubo[82], M. Talby[102], A.A. Talyshev[122b,122a], N.M. Tamir[161], J. Tanaka[163], M. Tanaka[165], R. Tanaka[65], S. Tapia Araya[173], S. Tapprogge[100], A. Tarek Abouelfadl Mohamed[136], S. Tarem[160], K. Tariq[60b], G. Tarna[27b,c], G.F. Tartarelli[69a], P. Tas[143], M. Tasevsky[141], T. Tashiro[86], E. Tassi[41b,41a], A. Tavares Delgado[140a,140b], Y. Tayalati[35e], A.J. Taylor[50], G.N. Taylor[105], W. Taylor[168b], A.S. Tee[90], R. Teixeira De Lima[153], P. Teixeira-Dias[94], H. Ten Kate[36], J.J. Teoh[120], S. Terada[82], K. Terashi[163], J. Terron[99], S. Terzo[14], M. Testa[51], R.J. Teuscher[167,af], S.J. Thais[183], T. Theveneaux-Pelzer[46], F. Thiele[40], D.W. Thomas[94], J.O. Thomas[42], J.P. Thomas[21], A.S. Thompson[57], P.D. Thompson[21], L.A. Thomsen[183], E. Thomson[137], E.J. Thorpe[93], Y. Tian[39], R.E. Ticse Torres[53], V.O. Tikhomirov[111,aq], Yu.A. Tikhonov[122b,122a], S. Timoshenko[112], P. Tipton[183], S. Tisserant[102], K. Todome[23b,23a], S. Todorova-Nova[5], S. Todt[48], J. Tojo[88], S. Tokár[28a], K. Tokushuku[82], E. Tolley[127], K.G. Tomiwa[33e], M. Tomoto[117], L. Tompkins[153,q], B. Tong[59], P. Tornambe[103], E. Torrence[132], H. Torres[48], E. Torró Pastor[148], C. Tosciri[135], J. Toth[102,ae], D.R. Tovey[149], A. Traeet[17], C.J. Treado[125], T. Trefzger[177], F. Tresoldi[156], A. Tricoli[29], I.M. Trigger[168a], S. Trincaz-Duvoid[136], W. Trischuk[167], B. Trocmé[58], A. Trofymov[145], C. Troncon[69a], M. Trovatelli[176], F. Trovato[156], L. Truong[33c], M. Trzebinski[85], A. Trzupek[85], F. Tsai[46], J.C-L. Tseng[135], P.V. Tsiareshka[108,al], A. Tsirigotis[162], N. Tsirintanis[9], V. Tsiskaridze[155], E.G. Tskhadadze[159a], M. Tsopoulou[162], I.I. Tsukerman[124], V. Tsulaia[18], S. Tsuno[82], D. Tsybychev[155], Y. Tu[63b], A. Tudorache[27b], V. Tudorache[27b], T.T. Tulbure[27a], A.N. Tuna[59], S. Turchikhin[80], D. Turgeman[180], I. Turk Cakir[4b,w], R.J. Turner[21], R. Turra[69a], P.M. Tuts[39], S. Tzamarias[162], E. Tzovara[100], G. Ucchielli[47], K. Uchida[163], I. Ueda[82], M. Ughetto[45a,45b], F. Ukegawa[169], G. Unal[36], A. Undrus[29], G. Unel[171], F.C. Ungaro[105], Y. Unno[82], K. Uno[163], J. Urban[28b], P. Urquijo[105], G. Usai[8], Z. Uysal[12d], L. Vacavant[102], V. Vacek[142], B. Vachon[104], K.O.H. Vadla[134], A. Vaidya[95], C. Valderanis[114], E. Valdes Santurio[45a,45b], M. Valente[54], S. Valentinetti[23b,23a], A. Valero[174], L. Valéry[46], R.A. Vallance[21], A. Vallier[36], J.A. Valls Ferrer[174], T.R. Van Daalen[14], P. Van Gemmeren[6], I. Van Vulpen[120], M. Vanadia[74a,74b], W. Vandelli[36], A. Vaniachine[166], D. Vannicola[73a,73b], R. Vari[73a], E.W. Varnes[7], C. Varni[55b,55a], T. Varol[158], D. Varouchas[65], K.E. Varvell[157], M.E. Vasile[27b], G.A. Vasquez[176], J.G. Vasquez[183], F. Vazeille[38], D. Vazquez Furelos[14], T. Vazquez Schroeder[36], J. Veatch[53], V. Vecchio[75a,75b], M.J. Veen[120], L.M. Veloce[167], F. Veloso[140a,140c], S. Veneziano[73a], A. Ventura[68a,68b], N. Venturi[36], A. Verbytskyi[115], V. Vercesi[71a], M. Verducci[72a,72b], C.M. Vergel Infante[79], C. Vergis[24], W. Verkerke[120], A.T. Vermeulen[120], J.C. Vermeulen[120], M.C. Vetterli[152,ax], N. Viaux Maira[147d], M. Vicente Barreto Pinto[54], T. Vickey[149], O.E. Vickey Boeriu[149], G.H.A. Viehhauser[135], L. Vigani[61b], M. Villa[23b,23a], M. Villaplana Perez[69a,69b], E. Vilucchi[51], M.G. Vincter[34], G.S. Virdee[21], A. Vishwakarma[46], C. Vittori[23b,23a], I. Vivarelli[156], M. Vogel[182], P. Vokac[142], S.E. von Buddenbrock[33e], E. Von Toerne[24], V. Vorobel[143], K. Vorobev[112], M. Vos[174],

JHEP10(2020)005

J.H. Vossebeld[91], M. Vozak[101], N. Vranjes[16], M. Vranjes Milosavljevic[16], V. Vrba[142], M. Vreeswijk[120], R. Vuillermet[36], I. Vukotic[37], P. Wagner[24], W. Wagner[182], J. Wagner-Kuhr[114], S. Wahdan[182], H. Wahlberg[89], V.M. Walbrecht[115], J. Walder[90], R. Walker[114], S.D. Walker[94], W. Walkowiak[151], V. Wallangen[45a,45b], A.M. Wang[59], C. Wang[60c], C. Wang[60b], F. Wang[181], H. Wang[18], H. Wang[3], J. Wang[63a], J. Wang[157], J. Wang[61b], P. Wang[42], Q. Wang[129], R.-J. Wang[100], R. Wang[60a], R. Wang[6], S.M. Wang[158], W.T. Wang[60a], W. Wang[15c,ag], W.X. Wang[60a,ag], Y. Wang[60a,an], Z. Wang[60c], C. Wanotayaroj[46], A. Warburton[104], C.P. Ward[32], D.R. Wardrope[95], N. Warrack[57], A. Washbrook[50], A.T. Watson[21], M.F. Watson[21], G. Watts[148], B.M. Waugh[95], A.F. Webb[11], S. Webb[100], C. Weber[183], M.S. Weber[20], S.A. Weber[34], S.M. Weber[61a], A.R. Weidberg[135], J. Weingarten[47], M. Weirich[100], C. Weiser[52], P.S. Wells[36], T. Wenaus[29], T. Wengler[36], S. Wenig[36], N. Wermes[24], M.D. Werner[79], M. Wessels[61a], T.D. Weston[20], K. Whalen[132], N.L. Whallon[148], A.M. Wharton[90], A.S. White[106], A. White[8], M.J. White[1], D. Whiteson[171], B.W. Whitmore[90], W. Wiedenmann[181], M. Wielers[144], N. Wieseotte[100], C. Wiglesworth[40], L.A.M. Wiik-Fuchs[52], F. Wilk[101], H.G. Wilkens[36], L.J. Wilkins[94], H.H. Williams[137], S. Williams[32], C. Willis[107], S. Willocq[103], J.A. Wilson[21], I. Wingerter-Seez[5], E. Winkels[156], F. Winklmeier[132], O.J. Winston[156], B.T. Winter[52], M. Wittgen[153], M. Wobisch[96], A. Wolf[100], T.M.H. Wolf[120], R. Wolff[102], R. Wölker[135], J. Wollrath[52], M.W. Wolter[85], H. Wolters[140a,140c], V.W.S. Wong[175], N.L. Woods[146], S.D. Worm[21], B.K. Wosiek[85], K.W. Woźniak[85], K. Wraight[57], S.L. Wu[181], X. Wu[54], Y. Wu[60a], T.R. Wyatt[101], B.M. Wynne[50], S. Xella[40], Z. Xi[106], L. Xia[178], X. Xiao[106], I. Xiotidis[156], D. Xu[15a], H. Xu[60a,c], L. Xu[29], T. Xu[145], W. Xu[106], Z. Xu[60b], Z. Xu[153], B. Yabsley[157], S. Yacoob[33a], K. Yajima[133], D.P. Yallup[95], D. Yamaguchi[165], Y. Yamaguchi[165], A. Yamamoto[82], M. Yamatani[163], T. Yamazaki[163], Y. Yamazaki[83], Z. Yan[25], H.J. Yang[60c,60d], H.T. Yang[18], S. Yang[78], X. Yang[60b,58], Y. Yang[163], W-M. Yao[18], Y.C. Yap[46], Y. Yasu[82], E. Yatsenko[60c,60d], J. Ye[42], S. Ye[29], I. Yeletskikh[80], M.R. Yexley[90], E. Yigitbasi[25], K. Yorita[179], K. Yoshihara[137], C.J.S. Young[36], C. Young[153], J. Yu[79], R. Yuan[60b,i], X. Yue[61a], S.P.Y. Yuen[24], M. Zaazoua[35e], B. Zabinski[85], G. Zacharis[10], E. Zaffaroni[54], J. Zahreddine[136], A.M. Zaitsev[123,ap], T. Zakareishvili[159b], N. Zakharchuk[34], S. Zambito[59], D. Zanzi[36], D.R. Zaripovas[57], S.V. Zeißner[47], C. Zeitnitz[182], G. Zemaityte[135], J.C. Zeng[173], O. Zenin[123], T. Ženiš[28a], D. Zerwas[65], M. Zgubič[135], D.F. Zhang[15b], G. Zhang[15b], H. Zhang[15c], J. Zhang[6], L. Zhang[15c], L. Zhang[60a], M. Zhang[173], R. Zhang[24], X. Zhang[60b], Y. Zhang[15a,15d], Z. Zhang[63a], Z. Zhang[65], P. Zhao[49], Y. Zhao[60b], Z. Zhao[60a], A. Zhemchugov[80], Z. Zheng[106], D. Zhong[173], B. Zhou[106], C. Zhou[181], M.S. Zhou[15a,15d], M. Zhou[155], N. Zhou[60c], Y. Zhou[7], C.G. Zhu[60b], H.L. Zhu[60a], H. Zhu[15a], J. Zhu[106], Y. Zhu[60a], X. Zhuang[15a], K. Zhukov[111], V. Zhulanov[122b,122a], D. Zieminska[66], N.I. Zimine[80], S. Zimmermann[52], Z. Zinonos[115], M. Ziolkowski[151], L. Živković[16], G. Zobernig[181], A. Zoccoli[23b,23a], K. Zoch[53], T.G. Zorbas[149], R. Zou[37], L. Zwalinski[36]

[1] *Department of Physics, University of Adelaide, Adelaide, Australia*
[2] *Physics Department, SUNY Albany, Albany NY, United States of America*
[3] *Department of Physics, University of Alberta, Edmonton AB, Canada*
[4] [(a)] *Department of Physics, Ankara University, Ankara;* [(b)] *Istanbul Aydin University, Application and Research Center for Advanced Studies, Istanbul;* [(c)] *Division of Physics, TOBB University of Economics and Technology, Ankara, Turkey*
[5] *LAPP, Université Grenoble Alpes, Université Savoie Mont Blanc, CNRS/IN2P3, Annecy, France*
[6] *High Energy Physics Division, Argonne National Laboratory, Argonne IL, United States of America*
[7] *Department of Physics, University of Arizona, Tucson AZ, United States of America*
[8] *Department of Physics, University of Texas at Arlington, Arlington TX, United States of America*
[9] *Physics Department, National and Kapodistrian University of Athens, Athens, Greece*
[10] *Physics Department, National Technical University of Athens, Zografou, Greece*

JHEP10(2020)005

[11] Department of Physics, University of Texas at Austin, Austin TX, United States of America
[12] [(a)] Bahcesehir University, Faculty of Engineering and Natural Sciences, Istanbul; [(b)] Istanbul Bilgi University, Faculty of Engineering and Natural Sciences, Istanbul; [(c)] Department of Physics, Bogazici University, Istanbul; [(d)] Department of Physics Engineering, Gaziantep University, Gaziantep, Turkey
[13] Institute of Physics, Azerbaijan Academy of Sciences, Baku, Azerbaijan
[14] Institut de Física d'Altes Energies (IFAE), Barcelona Institute of Science and Technology, Barcelona, Spain
[15] [(a)] Institute of High Energy Physics, Chinese Academy of Sciences, Beijing; [(b)] Physics Department, Tsinghua University, Beijing; [(c)] Department of Physics, Nanjing University, Nanjing; [(d)] University of Chinese Academy of Science (UCAS), Beijing, China
[16] Institute of Physics, University of Belgrade, Belgrade, Serbia
[17] Department for Physics and Technology, University of Bergen, Bergen, Norway
[18] Physics Division, Lawrence Berkeley National Laboratory and University of California, Berkeley CA, United States of America
[19] Institut für Physik, Humboldt Universität zu Berlin, Berlin, Germany
[20] Albert Einstein Center for Fundamental Physics and Laboratory for High Energy Physics, University of Bern, Bern, Switzerland
[21] School of Physics and Astronomy, University of Birmingham, Birmingham, United Kingdom
[22] [(a)] Facultad de Ciencias y Centro de Investigaciónes, Universidad Antonio Nariño, Bogotá; [(b)] Departamento de Física, Universidad Nacional de Colombia, Bogotá, Colombia, Colombia
[23] [(a)] INFN Bologna and Universita' di Bologna, Dipartimento di Fisica; [(b)] INFN Sezione di Bologna, Italy
[24] Physikalisches Institut, Universität Bonn, Bonn, Germany
[25] Department of Physics, Boston University, Boston MA, United States of America
[26] Department of Physics, Brandeis University, Waltham MA, United States of America
[27] [(a)] Transilvania University of Brasov, Brasov; [(b)] Horia Hulubei National Institute of Physics and Nuclear Engineering, Bucharest; [(c)] Department of Physics, Alexandru Ioan Cuza University of Iasi, Iasi; [(d)] National Institute for Research and Development of Isotopic and Molecular Technologies, Physics Department, Cluj-Napoca; [(e)] University Politehnica Bucharest, Bucharest; [(f)] West University in Timisoara, Timisoara, Romania
[28] [(a)] Faculty of Mathematics, Physics and Informatics, Comenius University, Bratislava; [(b)] Department of Subnuclear Physics, Institute of Experimental Physics of the Slovak Academy of Sciences, Kosice, Slovak Republic
[29] Physics Department, Brookhaven National Laboratory, Upton NY, United States of America
[30] Departamento de Física, Universidad de Buenos Aires, Buenos Aires, Argentina
[31] California State University, CA, United States of America
[32] Cavendish Laboratory, University of Cambridge, Cambridge, United Kingdom
[33] [(a)] Department of Physics, University of Cape Town, Cape Town; [(b)] iThemba Labs, Western Cape; [(c)] Department of Mechanical Engineering Science, University of Johannesburg, Johannesburg; [(d)] University of South Africa, Department of Physics, Pretoria; [(e)] School of Physics, University of the Witwatersrand, Johannesburg, South Africa
[34] Department of Physics, Carleton University, Ottawa ON, Canada
[35] [(a)] Faculté des Sciences Ain Chock, Réseau Universitaire de Physique des Hautes Energies — Université Hassan II, Casablanca; [(b)] Faculté des Sciences, Université Ibn-Tofail, Kénitra; [(c)] Faculté des Sciences Semlalia, Université Cadi Ayyad, LPHEA-Marrakech; [(d)] Faculté des Sciences, Université Mohamed Premier and LPTPM, Oujda; [(e)] Faculté des sciences, Université Mohammed V, Rabat, Morocco
[36] CERN, Geneva, Switzerland
[37] Enrico Fermi Institute, University of Chicago, Chicago IL, United States of America
[38] LPC, Université Clermont Auvergne, CNRS/IN2P3, Clermont-Ferrand, France
[39] Nevis Laboratory, Columbia University, Irvington NY, United States of America

JHEP10(2020)005

[40] Niels Bohr Institute, University of Copenhagen, Copenhagen, Denmark
[41] [(a)] Dipartimento di Fisica, Università della Calabria, Rende; [(b)] INFN Gruppo Collegato di Cosenza, Laboratori Nazionali di Frascati, Italy
[42] Physics Department, Southern Methodist University, Dallas TX, United States of America
[43] Physics Department, University of Texas at Dallas, Richardson TX, United States of America
[44] National Centre for Scientific Research "Demokritos", Agia Paraskevi, Greece
[45] [(a)] Department of Physics, Stockholm University; [(b)] Oskar Klein Centre, Stockholm, Sweden
[46] Deutsches Elektronen-Synchrotron DESY, Hamburg and Zeuthen, Germany
[47] Lehrstuhl für Experimentelle Physik IV, Technische Universität Dortmund, Dortmund, Germany
[48] Institut für Kern und Teilchenphysik, Technische Universität Dresden, Dresden, Germany
[49] Department of Physics, Duke University, Durham NC, United States of America
[50] SUPA — School of Physics and Astronomy, University of Edinburgh, Edinburgh, United Kingdom
[51] INFN e Laboratori Nazionali di Frascati, Frascati, Italy
[52] Physikalisches Institut, Albert-Ludwigs-Universität Freiburg, Freiburg, Germany
[53] II. Physikalisches Institut, Georg-August-Universität Göttingen, Göttingen, Germany
[54] Département de Physique Nucléaire et Corpusculaire, Université de Genève, Genève, Switzerland
[55] [(a)] Dipartimento di Fisica, Università di Genova, Genova; [(b)] INFN Sezione di Genova, Italy
[56] II. Physikalisches Institut, Justus-Liebig-Universität Giessen, Giessen, Germany
[57] SUPA — School of Physics and Astronomy, University of Glasgow, Glasgow, United Kingdom
[58] LPSC, Université Grenoble Alpes, CNRS/IN2P3, Grenoble INP, Grenoble, France
[59] Laboratory for Particle Physics and Cosmology, Harvard University, Cambridge MA, United States of America
[60] [(a)] Department of Modern Physics and State Key Laboratory of Particle Detection and Electronics, University of Science and Technology of China, Hefei; [(b)] Institute of Frontier and Interdisciplinary Science and Key Laboratory of Particle Physics and Particle Irradiation (MOE), Shandong University, Qingdao; [(c)] School of Physics and Astronomy, Shanghai Jiao Tong University, KLPPAC-MoE, SKLPPC, Shanghai; [(d)] Tsung-Dao Lee Institute, Shanghai, China
[61] [(a)] Kirchhoff-Institut für Physik, Ruprecht-Karls-Universität Heidelberg, Heidelberg; [(b)] Physikalisches Institut, Ruprecht-Karls-Universität Heidelberg, Heidelberg, Germany
[62] Faculty of Applied Information Science, Hiroshima Institute of Technology, Hiroshima, Japan
[63] [(a)] Department of Physics, Chinese University of Hong Kong, Shatin, N.T., Hong Kong; [(b)] Department of Physics, University of Hong Kong, Hong Kong; [(c)] Department of Physics and Institute for Advanced Study, Hong Kong University of Science and Technology, Clear Water Bay, Kowloon, Hong Kong, China
[64] Department of Physics, National Tsing Hua University, Hsinchu, Taiwan
[65] IJCLab, Université Paris-Saclay, CNRS/IN2P3, 91405, Orsay, France
[66] Department of Physics, Indiana University, Bloomington IN, United States of America
[67] [(a)] INFN Gruppo Collegato di Udine, Sezione di Trieste, Udine; [(b)] ICTP, Trieste; [(c)] Dipartimento Politecnico di Ingegneria e Architettura, Università di Udine, Udine, Italy
[68] [(a)] INFN Sezione di Lecce; [(b)] Dipartimento di Matematica e Fisica, Università del Salento, Lecce, Italy
[69] [(a)] INFN Sezione di Milano; [(b)] Dipartimento di Fisica, Università di Milano, Milano, Italy
[70] [(a)] INFN Sezione di Napoli; [(b)] Dipartimento di Fisica, Università di Napoli, Napoli, Italy
[71] [(a)] INFN Sezione di Pavia; [(b)] Dipartimento di Fisica, Università di Pavia, Pavia, Italy
[72] [(a)] INFN Sezione di Pisa; [(b)] Dipartimento di Fisica E. Fermi, Università di Pisa, Pisa, Italy
[73] [(a)] INFN Sezione di Roma; [(b)] Dipartimento di Fisica, Sapienza Università di Roma, Roma, Italy
[74] [(a)] INFN Sezione di Roma Tor Vergata; [(b)] Dipartimento di Fisica, Università di Roma Tor Vergata, Roma, Italy
[75] [(a)] INFN Sezione di Roma Tre; [(b)] Dipartimento di Matematica e Fisica, Università Roma Tre, Roma, Italy
[76] [(a)] INFN-TIFPA; [(b)] Università degli Studi di Trento, Trento, Italy
[77] Institut für Astro und Teilchenphysik, Leopold-Franzens-Universität, Innsbruck, Austria

JHEP10(2020)005

[78] University of Iowa, Iowa City IA, United States of America
[79] Department of Physics and Astronomy, Iowa State University, Ames IA, United States of America
[80] Joint Institute for Nuclear Research, Dubna, Russia
[81] [(a)] Departamento de Engenharia Elétrica, Universidade Federal de Juiz de Fora (UFJF), Juiz de Fora; [(b)] Universidade Federal do Rio De Janeiro COPPE/EE/IF, Rio de Janeiro; [(c)] Universidade Federal de São João del Rei (UFSJ), São João del Rei; [(d)] Instituto de Física, Universidade de São Paulo, São Paulo, Brazil
[82] KEK, High Energy Accelerator Research Organization, Tsukuba, Japan
[83] Graduate School of Science, Kobe University, Kobe, Japan
[84] [(a)] AGH University of Science and Technology, Faculty of Physics and Applied Computer Science, Krakow; [(b)] Marian Smoluchowski Institute of Physics, Jagiellonian University, Krakow, Poland
[85] Institute of Nuclear Physics Polish Academy of Sciences, Krakow, Poland
[86] Faculty of Science, Kyoto University, Kyoto, Japan
[87] Kyoto University of Education, Kyoto, Japan
[88] Research Center for Advanced Particle Physics and Department of Physics, Kyushu University, Fukuoka , Japan
[89] Instituto de Física La Plata, Universidad Nacional de La Plata and CONICET, La Plata, Argentina
[90] Physics Department, Lancaster University, Lancaster, United Kingdom
[91] Oliver Lodge Laboratory, University of Liverpool, Liverpool, United Kingdom
[92] Department of Experimental Particle Physics, Jožef Stefan Institute and Department of Physics, University of Ljubljana, Ljubljana, Slovenia
[93] School of Physics and Astronomy, Queen Mary University of London, London, United Kingdom
[94] Department of Physics, Royal Holloway University of London, Egham, United Kingdom
[95] Department of Physics and Astronomy, University College London, London, United Kingdom
[96] Louisiana Tech University, Ruston LA, United States of America
[97] Fysiska institutionen, Lunds universitet, Lund, Sweden
[98] Centre de Calcul de l'Institut National de Physique Nucléaire et de Physique des Particules (IN2P3), Villeurbanne, France
[99] Departamento de Física Teorica C-15 and CIAFF, Universidad Autónoma de Madrid, Madrid, Spain
[100] Institut für Physik, Universität Mainz, Mainz, Germany
[101] School of Physics and Astronomy, University of Manchester, Manchester, United Kingdom
[102] CPPM, Aix-Marseille Université, CNRS/IN2P3, Marseille, France
[103] Department of Physics, University of Massachusetts, Amherst MA, United States of America
[104] Department of Physics, McGill University, Montreal QC, Canada
[105] School of Physics, University of Melbourne, Victoria, Australia
[106] Department of Physics, University of Michigan, Ann Arbor MI, United States of America
[107] Department of Physics and Astronomy, Michigan State University, East Lansing MI, United States of America
[108] B.I. Stepanov Institute of Physics, National Academy of Sciences of Belarus, Minsk, Belarus
[109] Research Institute for Nuclear Problems of Byelorussian State University, Minsk, Belarus
[110] Group of Particle Physics, University of Montreal, Montreal QC, Canada
[111] P.N. Lebedev Physical Institute of the Russian Academy of Sciences, Moscow, Russia
[112] National Research Nuclear University MEPhI, Moscow, Russia
[113] D.V. Skobeltsyn Institute of Nuclear Physics, M.V. Lomonosov Moscow State University, Moscow, Russia
[114] Fakultät für Physik, Ludwig-Maximilians-Universität München, München, Germany
[115] Max-Planck-Institut für Physik (Werner-Heisenberg-Institut), München, Germany
[116] Nagasaki Institute of Applied Science, Nagasaki, Japan
[117] Graduate School of Science and Kobayashi-Maskawa Institute, Nagoya University, Nagoya, Japan
[118] Department of Physics and Astronomy, University of New Mexico, Albuquerque NM, United States of America

JHEP10(2020)005

[119] Institute for Mathematics, Astrophysics and Particle Physics, Radboud University Nijmegen/Nikhef, Nijmegen, Netherlands
[120] Nikhef National Institute for Subatomic Physics and University of Amsterdam, Amsterdam, Netherlands
[121] Department of Physics, Northern Illinois University, DeKalb IL, United States of America
[122] [(a)] Budker Institute of Nuclear Physics and NSU, SB RAS, Novosibirsk; [(b)] Novosibirsk State University Novosibirsk, Russia
[123] Institute for High Energy Physics of the National Research Centre Kurchatov Institute, Protvino, Russia
[124] Institute for Theoretical and Experimental Physics named by A.I. Alikhanov of National Research Centre "Kurchatov Institute", Moscow, Russia
[125] Department of Physics, New York University, New York NY, United States of America
[126] Ochanomizu University, Otsuka, Bunkyo-ku, Tokyo, Japan
[127] Ohio State University, Columbus OH, United States of America
[128] Faculty of Science, Okayama University, Okayama, Japan
[129] Homer L. Dodge Department of Physics and Astronomy, University of Oklahoma, Norman OK, United States of America
[130] Department of Physics, Oklahoma State University, Stillwater OK, United States of America
[131] Palacký University, RCPTM, Joint Laboratory of Optics, Olomouc, Czech Republic
[132] Institute for Fundamental Science, University of Oregon, Eugene, OR, United States of America
[133] Graduate School of Science, Osaka University, Osaka, Japan
[134] Department of Physics, University of Oslo, Oslo, Norway
[135] Department of Physics, Oxford University, Oxford, United Kingdom
[136] LPNHE, Sorbonne Université, Université de Paris, CNRS/IN2P3, Paris, France
[137] Department of Physics, University of Pennsylvania, Philadelphia PA, United States of America
[138] Konstantinov Nuclear Physics Institute of National Research Centre "Kurchatov Institute", PNPI, St. Petersburg, Russia
[139] Department of Physics and Astronomy, University of Pittsburgh, Pittsburgh PA, United States of America
[140] [(a)] Laboratório de Instrumentação e Física Experimental de Partículas — LIP, Lisboa; [(b)] Departamento de Física, Faculdade de Ciências, Universidade de Lisboa, Lisboa; [(c)] Departamento de Física, Universidade de Coimbra, Coimbra; [(d)] Centro de Física Nuclear da Universidade de Lisboa, Lisboa; [(e)] Departamento de Física, Universidade do Minho, Braga; [(f)] Departamento de Física Teórica y del Cosmos, Universidad de Granada, Granada (Spain); [(g)] Departamento de Física and CEFITEC of Faculdade de Ciências e Tecnologia, Universidade Nova de Lisboa, Caparica; [(h)] Instituto Superior Técnico, Universidade de Lisboa, Lisboa, Portugal
[141] Institute of Physics of the Czech Academy of Sciences, Prague, Czech Republic
[142] Czech Technical University in Prague, Prague, Czech Republic
[143] Charles University, Faculty of Mathematics and Physics, Prague, Czech Republic
[144] Particle Physics Department, Rutherford Appleton Laboratory, Didcot, United Kingdom
[145] IRFU, CEA, Université Paris-Saclay, Gif-sur-Yvette, France
[146] Santa Cruz Institute for Particle Physics, University of California Santa Cruz, Santa Cruz CA, United States of America
[147] [(a)] Departamento de Física, Pontificia Universidad Católica de Chile, Santiago; [(b)] Universidad Andres Bello, Department of Physics, Santiago; [(c)] Instituto de Alta Investigación, Universidad de Tarapacá; [(d)] Departamento de Física, Universidad Técnica Federico Santa María, Valparaíso, Chile
[148] Department of Physics, University of Washington, Seattle WA, United States of America
[149] Department of Physics and Astronomy, University of Sheffield, Sheffield, United Kingdom
[150] Department of Physics, Shinshu University, Nagano, Japan
[151] Department Physik, Universität Siegen, Siegen, Germany
[152] Department of Physics, Simon Fraser University, Burnaby BC, Canada
[153] SLAC National Accelerator Laboratory, Stanford CA, United States of America

JHEP10(2020)005

[154] Physics Department, Royal Institute of Technology, Stockholm, Sweden
[155] Departments of Physics and Astronomy, Stony Brook University, Stony Brook NY, United States of America
[156] Department of Physics and Astronomy, University of Sussex, Brighton, United Kingdom
[157] School of Physics, University of Sydney, Sydney, Australia
[158] Institute of Physics, Academia Sinica, Taipei, Taiwan
[159] [(a)] E. Andronikashvili Institute of Physics, Iv. Javakhishvili Tbilisi State University, Tbilisi; [(b)] High Energy Physics Institute, Tbilisi State University, Tbilisi, Georgia
[160] Department of Physics, Technion, Israel Institute of Technology, Haifa, Israel
[161] Raymond and Beverly Sackler School of Physics and Astronomy, Tel Aviv University, Tel Aviv, Israel
[162] Department of Physics, Aristotle University of Thessaloniki, Thessaloniki, Greece
[163] International Center for Elementary Particle Physics and Department of Physics, University of Tokyo, Tokyo, Japan
[164] Graduate School of Science and Technology, Tokyo Metropolitan University, Tokyo, Japan
[165] Department of Physics, Tokyo Institute of Technology, Tokyo, Japan
[166] Tomsk State University, Tomsk, Russia
[167] Department of Physics, University of Toronto, Toronto ON, Canada
[168] [(a)] TRIUMF, Vancouver BC; [(b)] Department of Physics and Astronomy, York University, Toronto ON, Canada
[169] Division of Physics and Tomonaga Center for the History of the Universe, Faculty of Pure and Applied Sciences, University of Tsukuba, Tsukuba, Japan
[170] Department of Physics and Astronomy, Tufts University, Medford MA, United States of America
[171] Department of Physics and Astronomy, University of California Irvine, Irvine CA, United States of America
[172] Department of Physics and Astronomy, University of Uppsala, Uppsala, Sweden
[173] Department of Physics, University of Illinois, Urbana IL, United States of America
[174] Instituto de Física Corpuscular (IFIC), Centro Mixto Universidad de Valencia — CSIC, Valencia, Spain
[175] Department of Physics, University of British Columbia, Vancouver BC, Canada
[176] Department of Physics and Astronomy, University of Victoria, Victoria BC, Canada
[177] Fakultät für Physik und Astronomie, Julius-Maximilians-Universität Würzburg, Würzburg, Germany
[178] Department of Physics, University of Warwick, Coventry, United Kingdom
[179] Waseda University, Tokyo, Japan
[180] Department of Particle Physics, Weizmann Institute of Science, Rehovot, Israel
[181] Department of Physics, University of Wisconsin, Madison WI, United States of America
[182] Fakultät für Mathematik und Naturwissenschaften, Fachgruppe Physik, Bergische Universität Wuppertal, Wuppertal, Germany
[183] Department of Physics, Yale University, New Haven CT, United States of America
[184] Yerevan Physics Institute, Yerevan, Armenia

[a] Also at Borough of Manhattan Community College, City University of New York, New York NY, United States of America
[b] Also at CERN, Geneva, Switzerland
[c] Also at CPPM, Aix-Marseille Université, CNRS/IN2P3, Marseille, France
[d] Also at Département de Physique Nucléaire et Corpusculaire, Université de Genève, Genève, Switzerland
[e] Also at Departament de Fisica de la Universitat Autonoma de Barcelona, Barcelona, Spain
[f] Also at Departamento de Física, Instituto Superior Técnico, Universidade de Lisboa, Lisboa, Portugal
[g] Also at Department of Applied Physics and Astronomy, University of Sharjah, Sharjah, United Arab Emirates

JHEP10(2020)005

[h] Also at Department of Financial and Management Engineering, University of the Aegean, Chios, Greece
[i] Also at Department of Physics and Astronomy, Michigan State University, East Lansing MI, United States of America
[j] Also at Department of Physics and Astronomy, University of Louisville, Louisville, KY, United States of America
[k] Also at Department of Physics, Ben Gurion University of the Negev, Beer Sheva, Israel
[l] Also at Department of Physics, California State University, East Bay, United States of America
[m] Also at Department of Physics, California State University, Fresno, United States of America
[n] Also at Department of Physics, California State University, Sacramento, United States of America
[o] Also at Department of Physics, King's College London, London, United Kingdom
[p] Also at Department of Physics, St. Petersburg State Polytechnical University, St. Petersburg, Russia
[q] Also at Department of Physics, Stanford University, Stanford CA, United States of America
[r] Also at Department of Physics, University of Adelaide, Adelaide, Australia
[s] Also at Department of Physics, University of Fribourg, Fribourg, Switzerland
[t] Also at Department of Physics, University of Michigan, Ann Arbor MI, United States of America
[u] Also at Dipartimento di Matematica, Informatica e Fisica, Università di Udine, Udine, Italy
[v] Also at Faculty of Physics, M.V. Lomonosov Moscow State University, Moscow, Russia
[w] Also at Giresun University, Faculty of Engineering, Giresun, Turkey
[x] Also at Graduate School of Science, Osaka University, Osaka, Japan
[y] Also at Hellenic Open University, Patras, Greece
[z] Also at IJCLab, Université Paris-Saclay, CNRS/IN2P3, 91405, Orsay, France
[aa] Also at Institucio Catalana de Recerca i Estudis Avancats, ICREA, Barcelona, Spain
[ab] Also at Institut für Experimentalphysik, Universität Hamburg, Hamburg, Germany
[ac] Also at Institute for Mathematics, Astrophysics and Particle Physics, Radboud University Nijmegen/Nikhef, Nijmegen, Netherlands
[ad] Also at Institute for Nuclear Research and Nuclear Energy (INRNE) of the Bulgarian Academy of Sciences, Sofia, Bulgaria
[ae] Also at Institute for Particle and Nuclear Physics, Wigner Research Centre for Physics, Budapest, Hungary
[af] Also at Institute of Particle Physics (IPP), Vancouver, Canada
[ag] Also at Institute of Physics, Academia Sinica, Taipei, Taiwan
[ah] Also at Institute of Physics, Azerbaijan Academy of Sciences, Baku, Azerbaijan
[ai] Also at Institute of Theoretical Physics, Ilia State University, Tbilisi, Georgia
[aj] Also at Instituto de Fisica Teorica, IFT-UAM/CSIC, Madrid, Spain
[ak] Also at Istanbul University, Department of Physics, Istanbul, Turkey
[al] Also at Joint Institute for Nuclear Research, Dubna, Russia
[am] Also at Louisiana Tech University, Ruston LA, United States of America
[an] Also at LPNHE, Sorbonne Université, Université de Paris, CNRS/IN2P3, Paris, France
[ao] Also at Manhattan College, New York NY, United States of America
[ap] Also at Moscow Institute of Physics and Technology State University, Dolgoprudny, Russia
[aq] Also at National Research Nuclear University MEPhI, Moscow, Russia
[ar] Also at Physics Department, An-Najah National University, Nablus, Palestine
[as] Also at Physics Dept, University of South Africa, Pretoria, South Africa
[at] Also at Physikalisches Institut, Albert-Ludwigs-Universität Freiburg, Freiburg, Germany
[au] Also at School of Physics, Sun Yat-sen University, Guangzhou, China
[av] Also at The City College of New York, New York NY, United States of America
[aw] Also at The Collaborative Innovation Center of Quantum Matter (CICQM), Beijing, China
[ax] Also at TRIUMF, Vancouver BC, Canada
[ay] Also at Universita di Napoli Parthenope, Napoli, Italy
[*] Deceased

JHEP10(2020)005